

# **The Performance of Viscous and Friction Dampers in Steel Frame Structures**

**Maroan Mohamed M Elgallal**

Submitted to the  
Institute of Graduate Studies and Research  
in partial fulfillment of the requirements for the degree of

Master of Science  
in  
Civil Engineering

Eastern Mediterranean University  
September 2019  
Gazimağusa, North Cyprus

Approval of the Institute of Graduate Studies and Research

---

Prof. Dr. Ali Hakan Ulusoy  
Acting Director

I certify that this thesis satisfies all the requirements as a thesis for the degree of Master of Science in Civil Engineering.

---

Assoc. Prof. Dr. Serhan Şensoy  
Chair, Department of Civil Engineering

We certify that we have read this thesis and that in our opinion it is fully adequate in scope and quality as a thesis for the degree of Master of Science in Civil Engineering.

---

Assoc. Prof. Dr. Giray Özyay  
Supervisor

---

Examining Committee

1. Assoc. Prof. Dr. Mahmood Hosseini

2. Assoc. Prof. Dr. Giray Özyay

3. Assoc. Prof. Dr. Rifat Reşatoğlu

## ABSTRACT

It is common concern for structural engineer to design building that can withstand high seismic activity in order to maintain both lives and building integrity. For this purpose, energy dissipating devices are invented in order to absorb the energy delivered to the building. The seismic behavior of steel structural building equipped with two types of energy dissipating devices including both viscos and friction dampers for 5, 10, and 20 story steel buildings is investigated in this study. The performance is assessed by means of story drift, base shear, roof displacement, structure ductility, yield strength, energy and building performance. These parameters are evaluated through nonlinear pushover and time history analysis conducted using ETABS2017 in accordance with TBDY2018. Results indicate that viscous damper placed at the outer corner of the structure yielded the best performance among the other locations and damping devices where it reduced the base shear by 69% and 64% in average for both directions X and Y respectively compared to the results of moment resisting frames. Also, the roof displacement reduced by 85% and 81% in average for both directions X and Y respectively compared to the results of moment resisting frames.

**Keyword:** dampers, viscous, friction, pushover, time history, nonlinear, analysis, TBDY2018.

## ÖZ

Yüksek sismik riske sahip bölgelerde can güvenliği ve yapı bütünlüğünü koruyacak bir tasarım yapmak inşaat mühendislerinin ortak arzusudur. Bu amaçla, deprem esnasındaki enerjinin bir kısmını azaltmak için günümüzde birtakım araçlar geliştirilmiştir. Bu çalışmada, 5, 10 ve 20 katlı viskoz ve sürtünme sönümleyicili çelik binaların sismik davranışı incelenmiştir. Yapılan analizlerde kat ötelemeleri, taban kesme kuvvetleri, yapı sünekliği, akma dayanımı, çatı deplasmanları, enerji ve bina performansları incelenmiştir. Bu parametreler TBDY2018 uyarınca, ETABS2017 programı kullanılarak yapılan doğrusal olmayan pushover ve zaman tanım alanında analiz yöntemleriyle değerlendirilmiştir. Sonuçlar, yapının dış köşesine yerleştirilmiş viskoz sönümleyicinin, diğer konumlar arasında en iyi performansı sağladığını ve sönümleme cihazlarının moment dirençli çerçevelere kıyasla taban kesme kuvvetlerini x ve y yönlerinde sırasıyla % 69 ve % 64 oranında azalttığı gözlenmiştir. Ayrıca, çatı deplasmanları, moment dirençli çerçevelerin sonuçlarına kıyasla X ve Y yönlerinde sırasıyla % 85 ve % 81 oranlarında azalmıştır.

**Anahtar Kelimeler:** Sönümleyici, viskoz, sürtünme, statik itme, zaman tanım alanında hesap, doğrusal olmayan, analiz, TBDY2018.

## **ACKNOWLEDGMENT**

I would first like to thank my supervisor Assoc. Prof. Dr. Giray Özay for the continuous support, motivation, patience and immense knowledge. His office door was always open at any time I ran into a trouble spot or had a question about my research or writing. I could not have imagined having a better supervisor and mentor for my study.

I would like to express my very deep gratitude to my parents and to my friends for providing me with unfailing support and nonstop help all the way through my years of study and during the process of researching and writing my thesis. This achievement would not have been possible without them. Thank you!

# TABLE OF CONTENT

ABSTRACT .....	iii
ÖZ .....	iv
ACKNOWLEDGMENT .....	v
LIST OF TABLES .....	ix
LIST OF FIGURES .....	x
1 INTRODUCTION .....	1
1.1 General.....	1
1.2 Previous Work Done .....	2
1.3 Aim and Scope.....	7
1.4 Organization of the Thesis.....	8
2 ANALYSIS METHODS AND MATERIALS.....	9
2.1 Introduction.....	9
2.2 Nonlinear Analysis Methods.....	9
2.2.1 Static Pushover Analysis .....	9
2.2.1.1 Target Displacement .....	11
2.2.1.2 Capacity Curve (Pushover Curve) .....	11
2.2.1.3 Base Shear .....	13
2.2.1.4 Performance Level.....	13
2.2.1.5 Pushover Analysis Results .....	13
2.2.2 Nonlinear Time History Analysis .....	14
2.2.2.1 Scaling methods of ground motion .....	15
2.2.3 Modal Analysis .....	16
2.2.3.1 Ritz-Vector Analysis Method.....	16

2.2.3.2 Eigen-Vector Analysis Method .....	17
2.3 Types of Energy Dissipating Devices .....	17
2.3.1 Viscous Dampers .....	18
2.3.2 Friction Dampers .....	19
2.4 Steel Structures.....	21
2.5 Ductility .....	22
2.6 Displacement and Drift.....	22
3 METHODOLOGY .....	24
3.1 Introduction.....	24
3.2 Strategy of Analysis .....	24
3.3 Location of the Case Study .....	24
3.4 Modelling of Steel Structures .....	26
3.4.1 Column Cross-Section .....	28
3.4.2 Beam Cross-Section.....	28
3.4.3 Slab Type.....	29
3.5 Energy Dissipation Devices Properties and Locations.....	30
3.6 Design Assumptions.....	34
3.6.1 Gravity Loads .....	35
3.6.2 Earthquake Parameters.....	35
3.6.3 Load Combinations .....	36
3.7 Nonlinear Analysis .....	36
3.7.1 Pushover Analysis.....	36
3.7.2 Time History Analysis .....	39
4 RESULTS AND DISCUSSIONS.....	41
4.1 Introduction.....	41

4.2 Nonlinear Pushover Analysis.....	41
4.2.1 Elastic Lateral Stiffness.....	41
4.2.2 Structure Yield Strength.....	43
4.2.5 Pushover Capacity Curves.....	46
4.3 Time History Analysis Results .....	50
4.3.1 Base Shear .....	50
4.3.2 Top Story Displacement.....	53
4.3.3 Story Drift.....	56
4.3.4 Performance Level .....	59
4.3.5 Energy Component .....	63
5 CONCLUSION AND RECOMMENDATIONS FOR FUTURE STUDIES .....	66
5.1 Conclusion .....	66
5.2 Recommendations for Future Studies .....	67
REFERENCES .....	68
APPENDICES .....	74
Appendix A: Properties of Slab Deck and Materials .....	75
Appendix B: Properties of Response Spectrum.....	76
Appendix C: Ground Motion Records and Spectral Matching .....	79



## LIST OF TABLES

Table 1: Characteristics of the structural system.....	28
Table 2: Material properties .....	28
Table 3: Viscous damper properties (Taylor Device Company) .....	32
Table 4: Friction damper properties (Taylor Device Company) .....	33
Table 5: Earthquake Parameters .....	35
Table 6: Load Combinations for Design (ETABS 2017) .....	36
Table 7: Details of ground motion records (PEER).....	39
Table 8: Target displacements obtained and number of hinges of 5-story structure..	48
Table 9: Target displacements obtained and number of hinges of 10-story structure. .....	49
Table 10: Target displacements obtained and number of hinges of 20-story structure. .....	49
Table 11: Reduction percentage of base shear force compared to the resisting moment frame. ....	53
Table 12: Reduction percentage of roof displacement compared to the resisting moment frame.....	55
Table 13: Performance level of all modals (ETABS 2017) .....	63

# LIST OF FIGURES

Figure 1: Multi degree of freedom system and Single degree of freedom system.....	11
Figure 2: Capacity Curve (FEMA-356).....	12
Figure 3: Performance Level Stages (Inel et al. 2006). ....	12
Figure 4: EI Centro Earthquake Record (Zahrai. S. M-2009).....	15
Figure 5: Components of mode shapes (CSI,2014).....	17
Figure 6: Viscous Damper Device ( Lee & Taylor-2001) .....	19
Figure 7: Friction Damper Device (Becker et al. 2007) .....	20
Figure 8: Steel building with columns, beams and bracing .....	22
Figure 9: Roof displacement and inter-story displacement (Jabeen et al. 2014).....	23
Figure 10: Flow chart of the analysis strategy .....	25
Figure 11: Assumed Location of the Steel structure models (Google map 2019) .....	26
Figure 12: Plan layout of the steel buildings .....	27
Figure 13: 3D view of 5-story steel building without dampers.....	27
Figure 14: Schematic view of the HEB cross-section (EN1993-1-1:2005).....	29
Figure 15: Schematic view of the IPE cross-section (EN1993-1-1:2005).....	29
Figure 16: Schematic view of the Aldeck 70/915 cross-section (EN1993-1-1:2005)	30
Figure 17: Dampers located in outer mid-frame for 10-story steel building .....	31
Figure 18: Dampers located in outer corner frames for 10-story steel building .....	31
Figure 19: Dampers located between outer corner and mid-frame for 10-story steel building .....	32
Figure 20: Nonlinear Properties of Friction Dampers .....	33
Figure 21: Nonlinear Properties of Viscous Dampers .....	34
Figure 22: Plastic Hinges of beams .....	37

Figure 23: Plastic Hinges of Columns .....	38
Figure 24: Load Cases Including (Push down, Push X and Push Y) .....	38
Figure 25: Response Spectrum with 2% exceedance probability at 50 years .....	40
Figure 26: Ground motion Records (PEER) .....	40
Figure 27: Initial lateral stiffness for 5-story steel building.....	42
Figure 28: Initial lateral stiffness for 10-story steel building.....	42
Figure 29: Initial lateral stiffness for 20-story steel building.....	43
Figure 30: Yield strength for 5-story steel building .....	43
Figure 31: Yield strength for 10-story steel building .....	44
Figure 32: Yield strength for 20-story steel building .....	44
Figure 33: Ductility demand factor for 5-story steel building.....	45
Figure 34: Ductility demand factor for 10-story steel building.....	46
Figure 35: Ductility demand factor for 20-story steel building.....	46
Figure 36: Capacity curves for 5-story steel building.....	48
Figure 37: Capacity curves for 10-story steel building.....	48
Figure 38: Capacity curves for 20-story steel building.....	49
Figure 39: Base shear in X and Y directions for 5-story steel building.....	51
Figure 40: Base shear in X and Y directions for 10-story steel building.....	51
Figure 41: Base shear in X and Y directions for 20-story steel building.....	52
Figure 42: Base shear in X directions for 5-story steel building (FD.L2) .....	52
Figure 43: Base shear in Y directions for 5-story steel building (FD.L2) .....	52
Figure 44: Roof displacement in X and Y directions for 5-story steel building .....	54
Figure 45: Roof displacement in X and Y directions for 10-story steel building .....	54
Figure 46: Roof displacement in X and Y directions for 20-story s steel building .....	54
Figure 47: Displacement in X direction for 5-story steel building (VD.L2) .....	55

Figure 48: Displacement in Y direction for 5-story steel building (VD.L2) .....	55
Figure 49: Story drift in X direction for 5-story steel building .....	56
Figure 50: Story drift in Y direction for 5-story steel building .....	57
Figure 51: Story drift in X direction for 10-story steel building .....	57
Figure 52: Story drift in Y direction for 10-story steel building .....	58
Figure 53: Story drift in X direction for 20-story steel building .....	58
Figure 54: Story drift in Y direction for 20-story steel building .....	59
Figure 55: Performance check of MRF for 5-story steel building .....	60
Figure 56: Performance check of VD.L2 for 5-story steel building .....	60
Figure 57: Performance check of VD.L3 for 5-story steel building .....	61
Figure 58: Performance check of FD.L1 for 5-story steel building .....	61
Figure 59: Collapse stage of plastic hinges of MRF 5-story steel building .....	62
Figure 60: immediate occupancy stage of plastic hinges of FD.L1 5-story steel building .....	62
Figure 61: Energy component for 5-story steel building .....	64
Figure 62: Energy component for 10-story steel building .....	64
Figure 63: Energy component for 20-story steel building .....	65

## LIST OF SYMBOLS

$A_0$	Effective ground acceleration coefficient
$C$	Coefficient of damping
$d_{max}$	Maximum displacement
$d_y$	Yield displacement
$F$	Force of damping
$F_E$	Restoring force
$F_t$	The total absorbed energy by the damper
$g$	The gravitational acceleration
$I$	Importance factor
$K$	Stiffness matrix
$M$	Diagonal matrix of mass
$R$	Structure behavior factor
$r$	The applied load
$t$	Time
$T_e$	The effective period of the structure
$u$	Displacement
$\dot{u}$	Velocity
$\ddot{u}$	Acceleration
$X$	Damper displacement
$\Phi$	Eigen vector's matrix
$\Omega$	Eigen value's matrix
$\delta$	Target displacement
$\mu$	Ductility

## LIST OF ABBREVIATIONS

CP	Collapse prevention
DL	Dead load
EDR	The energy dissipating restraint
EX	Earthquake force on X-direction
EY	Earthquake force on Y-direction
FD	Friction damper
FD.L1	Friction damper at the frame between the outer corner and middle frames
FD.L2	Friction damper at the outer corner frame
FD.L3	Friction damper at the outer mid-frame
FEMA	Federal Emergency Management Agency
G+19	20-story steel structure
G+4	5-story steel structure
G+9	10-story steel structure
IO	Immediate occupancy
LL	Live load
LS	Live safety
NTHA	Non-linear time history analysis
NVD	Non-linear Viscous Damping
NHD	Non-linear Hysteretic Damping
PEER	Pacific Earthquake Engineering Research
PGA	Peak Ground Acceleration
PGV	Peak Ground Velocity

$S_1$	Spectral acceleration for one second
$S_a$	Spectral acceleration
SDOF	Single Degree of Freedom
$S_s$	Spectral acceleration at short period
TBDY-2018	Turkish stander for earthquake resistant structure
VD	Viscous damper
VD.L1	Viscous damper at the frame between the outer corner and middle frames
VD.L2	Viscous damper at the outer corner frame
VD.L3	Viscous damper at the outer mid-frame

# Chapter 1

## INTRODUCTION

### 1.1 General

Several countries are suffering from strong earthquakes that could destroy the infrastructure and lead to the economic loss. Therefore, designing and strengthening of existing buildings in a way that resist earthquakes is a vital necessity. For this purpose, many techniques are implemented to counter the seismic actions, depending on the condition and type of the building. To increase the strength and stiffness of a building shear wall, moment frame or bracing can be added to the structural system. Nevertheless, during earthquakes structural elements may exceeds the yielding stresses which can led to the plastic hinges formation which may cause the complete failure of the building. There are many methods to encounter this issue such as the implementation of the following devices;

- Bracing system
- Damping devices
- Base isolation devices

However, energy dissipating devices can be designated as the best alternative since it absorbs most of the energy delivered by the earthquake. In addition, it can be installed and maintained in an easy manner. The most common type of these devices are viscous and friction dampers and they consider as passive energy control system.



Not to mention the fact that these devices can enhance the ability of construction tall buildings with relatively small structural element cross-sections.

## **1.2 Previous Work Done**

A brief audit of earlier studies on the effectiveness of viscous and friction dampers in steel frame structures is discussed below. This literature review focuses on studies that have been done years ago and progressively important to the present investigations.

10 and 16 story steel buildings are investigated by Goel and Booker (2001), in order to check their performance when viscous dampers are used. The amount of energy absorbed by dampers have been tested in different positions. Hysteretic diagram is considered in this study to get more accurate results. However, the steel building with dampers performed a considerable dissipation of energy compared to free dampers building.

Investigation of the performance of the building with the addition of fluid viscous dampers to resist the earthquake forces have been studied in Nepal (Gosain. 2013). Although these devices are not commonly used in this country. The analysis is performed by 3D linear and non-linear time history. Also, ETABS V2015 is used to achieve the analysis. The viscous dampers were distributed in uniform way while the damping force is equal in the first six floors and for the 4 sides of the structure. As a results of this study and after comparing the modeled steel building with the other one without dampers the base shear is reduced by 55% in average while the inter story drift is reduced by 50 to 80%. On the other hand, the internal stresses were minimized by roughly 40%. Also, the top most story displacement and floor acceleration of the high raised building are highly reduced upon the addition of the damping devices.

performance of steel buildings with the addition of energy dissipating device such as viscous dampers have been studied by Peer. 2009 where the viscous damper is modeled as dashpot with elastic bracing elements. The seismic performance of the modeled building is simulated using Opensees software by conducting time history analysis using the ground motion record of Kobe earthquake Japan which took place in 1994. The outcomes of analysis indicate that dampers enhanced the performance of the building by preventing formation of collapse prevention hinges under the seismic actions.

Esmailzadeh, et al. 2004 compared the capacity of energy dissipation when the friction dampers have different slipping surface. The nonlinear analysis is used to check the performance of 2 and 3 story steel buildings located in two different soil types S2 and S3. However, the aspect ratio that calculated from the friction dampers is good for energy dissipation which is in the maximum level when the device is located next to the main frame which increase the performance level of the building.

Mualla, et al. 2002 investigated the response of friction damper devices to the earthquake when it is applied to one story steel building. The reaction of the steel frame to the lateral forces and the damper unit performance are tested. However, the analysis is carried out by applying the nonlinear time history method to study the seismic behavior of the building. They found that, the earthquake resistance of the building has been enhanced when the model includes dampers.

Tokuda, et al. 2008 applied the viscous damper device to a tall steel building in Japan where the first story of the modeled building is designed as a soft story. Nevertheless, the steel building showed a good performance when it is subjected to the seismic

action. Displacement and base shear were reduced by 60% and 43% respectively compared to the building without dampers. Moreover, the effect of seismic forces on the upper floors are decreased significantly. Since dampers are placed affectively such that most of the seismic forces are absorbed at the first floor level.

Ras, et al. 2016 retrofitted 12 story steel frame by the addition of viscous dampers. Nonlinear time history is performed under the ground motion record of Algeria earthquake 2003. SAP2000 software is used to carry out the analysis. Also, the study compared braced, unbraced and damped building. The aim of the study is to investigate the response of buildings with and without dampers when it is subjected to lateral loads. However, the results showed that the building performance is improved without increasing the rigidity of the building. Finally, the demand of steel elements is reduced.

Saghafi, et al. 2016 evaluated the behavior of 4 and 8 story steel moment resisting frame structures subjected to seven different seismic forces in order to compare the response of each hazard level. Where viscous dampers are used to decrease the demand of the structural elements. The response is evaluated through nonlinear time history and Pushover analysis. Results illustrated that the behavior of rehabilitated frames have been improved. Also, the maximum floor acceleration, roof displacement and the shear forces are declined. In addition, these models achieved life safety level performance.

Whittle, et al. 2012 Studied the role of viscous damper on the seismic behavior using 20 different ground motion records. The location of the damper is altered in five different locations along the building plan. Both regular and irregular steel frame

structures are considered. Results show that the buildings achieved immediate occupancy performance regardless of the viscous damper locations.

Martínez, et al. 2013 studied the best location and size of the viscous dampers in steel building with different stiffness distribution along the elevation. The decision of placing these devices is taken by checking the story drift and base shear values. The building is tested many times to come up with the right location and size of the damper. However, the results illustrated that the most effective place for these devices is in the first stories since the stiffness eccentricity can be corrected and the torsional effect will be minimized.

Miyamoto et al. 2011 perform the innovative design of steel structural building equipped with viscous dampers in order to control the story drift ratio is investigated based on analytical approach in cooperation with experimental data. results showed that viscous damper enhanced the seismic performance of building. However, the enhanced performance objective of 1% drift resulted in an almost exclusive first-level soft-story mechanism.

Tzimas et al. 2016 evaluated the risk of collapse of steel structural building near faults using 91 earthquake records, where the records are scaled in a manner to cause failure within the structure. Results indicated that steel structural building equipped with Viscous dampers dramatically reduced the risk of collapse where it is reduced between 50-60% depending on the location of the building from the fault.

Dimopoulos et al. 2016 compared the post tensioning method with the viscous damper in steel structural system. results specify that viscous damper is the best in enhancing

the performance of buildings subjected to earthquake records equal in magnitude or even higher than the maximum considered earthquake, where viscous damper bypass the post tensioning method by roughly 50%.

Kim et al. 2016 Investigated a special truss moment frame (STMF) having viscous dampers by fragility analyses and the results are compared with the performance of special moment resisting frames. Then seismic retrofit scheme is proposed by installing a viscous damper in the special segment to meet enhanced seismic performance objective. The required amount of additional viscous damping is determined based on the nonlinear static procedure provided in the ASCE/SEI 41-10. The analysis results showed that the STMF showed larger stiffness and strength but smaller ductility compared with the moment frames, which resulted in similar seismic fragility in both structures. The seismic performance of STMF with viscous dampers in the special segments turned out to meet the desired target performance, and the effect of adding viscous dampers in the seismic fragility is most significant in the complete damage state.

Kang et al. 2016 Investigated the inelastic spectral displacement and the inelastic first mode vector for steel frame buildings with fluid viscous dampers. In this method, the inelastic spectral displacement is estimated using a single-degree-of-freedom (SDOF) system equivalent to a multi-story frame with an SEDS using FVDs, and the inelastic first mode vector is estimated using a pattern of floor displacements obtained from nonlinear static pushover analysis (NSPA) of a multi-story frame, which considers the behavior of velocity-dependent dampers. Nonlinear time history analysis (NTHA) is performed on series of three- and six-story steel moment-resisting frames with an SEDS using FVDs and a corresponding equivalent SDOF system model. Also, NSPA

is performed on an inelastic multi-story frame with an additional spring, which considers the viscous behavior of velocity-dependent dampers. Comparing the results of the peak inter-story drift ratio estimated by the proposed method with those computed via NTHA, the proposed method has sufficient accuracy for the evaluation of seismic demands.

Hamidia et al. 2014 studied a simple procedure to evaluate the seismic sidesway collapse capacity of frame building structures incorporating linear and nonlinear viscous dampers. The proposed procedure is based on a robust database of seismic peak displacement responses of viscously damped nonlinear single-degree-of-freedom systems for various seismic intensities and uses nonlinear static (pushover) analysis without the need for nonlinear time history dynamic analysis. The proposed procedure is assessed by comparing its collapse capacity predictions on 1,190 different building models with those obtained from incremental nonlinear dynamic analyses. A straightforward collapse capacity-based design procedure aimed at achieving a predetermined probability of collapse under maximum considered earthquake event is also introduced for viscously damped structures without extreme soft story irregularities.

### **1.3 Aim and Scope**

The role of energy dissipation devices in enhancing the behavior of steel buildings is extensively studied in the literature. However, until the moment of writing this research the behavior of viscous and friction damper in accordance with the new Turkish earthquake standard TBDY2018 is not discussed. For this purpose, this research is focusing on evaluating the behavior of steel framed buildings equipped with energy dissipating devices including both viscous and friction dampers in

accordance with TS2018. In order to meet this objective, both nonlinear static pushover analysis and nonlinear time history analysis are conducted. The effect of the dampers locations both along the plan and elevation is considered for multiple story heights including 5,10 and 20 floors. All obtained results are compared side by side with the ordinary moment resistant structure.

#### **1.4 Organization of the Thesis**

This research is mainly composed of five chapters.

The current chapter is providing a general introduction, previous works done related to the study also aims and scope of this research.

Second chapter demonstrates general information about the methods used to analyze the steel building models such as pushover analysis and nonlinear time history analysis methods. In addition to the present literature regarding the viscous and friction dampers.

Third chapter gives description of the plan geometry, the properties of the structural cross-sections, the energy dissipating devices properties and the analysis assumptions.

Fourth chapter presents the obtained results and discuss them in order to estimate the optimum type and location of the adopted dampers for 5, 10 and 20 story steel buildings.

Fifth chapter summarize the research and highlight the main research outcomes.

## **Chapter 2**

### **ANALYSIS METHODS AND MATERIALS**

#### **2.1 Introduction**

Around the globe natural disasters such as earthquake are responsible of large number of casualties and fatalities, not to mention the huge destruction of both superstructure and infrastructure. For this purpose, engineers are aiming to design buildings that can withstand the severe ground motions that might take place in a particular region. Buildings are designed such that the internal stresses within the structural elements does not exceeds the yielding stress of the building material. However, this is not always applicable since earthquake are rather random and hard to predict their frequencies and magnitudes. Hence, more sophisticated analysis that consider the nonlinear behavior of the structure are developed such as;

- 1- Static pushover analysis.
- 2- Nonlinear time history analysis.

This chapter presents the analysis methods which are adopted in this research. In addition, it gives a brief description of the adopted damper devices (Viscous and Friction).

#### **2.2 Nonlinear Analysis Methods**

##### **2.2.1 Static Pushover Analysis**

The static pushover analysis is based on the assumption that the first modal shape of the structure natural vibration modes is governing the seismic response of the structure during both elastic and inelastic behavior of the structure. The method basically



calculates the response of the multi degree of freedom system using an equivalent single degree of freedom system as shown in Figure 1. The mass of the structure is lumped at the top most floor level, and the lateral stiffness is assumed to be homogenous throughout the elevation of the building. The response of the equivalent system under the applied load patterns is calculated using the general equation of motion.

$$m\ddot{u} + c\dot{u} + ku = F(t) \quad (2.1)$$

where;

$m$ : The mass matrix of the structure.

$c$ : The damping matrix of the structure.

$k$ : The lateral stiffness matrix of the structure.

$\ddot{u}$ : The induced acceleration under the considered load.

$\dot{u}$ : The induced velocity under the considered load.

$u$ : The induced displacement under the considered load.

$F(t)$ : Is the applied lateral loads with respect to time.

At high loads the internal stresses within some of the structural elements exceeds the yielding stress of the structure material which leads to the formation of plastic hinges. For this reason, the lateral stiffness matrix is not constant. Hence, in order to predict accurately the response of the structure the load is applied in a number of steps till a target displacement is reached.

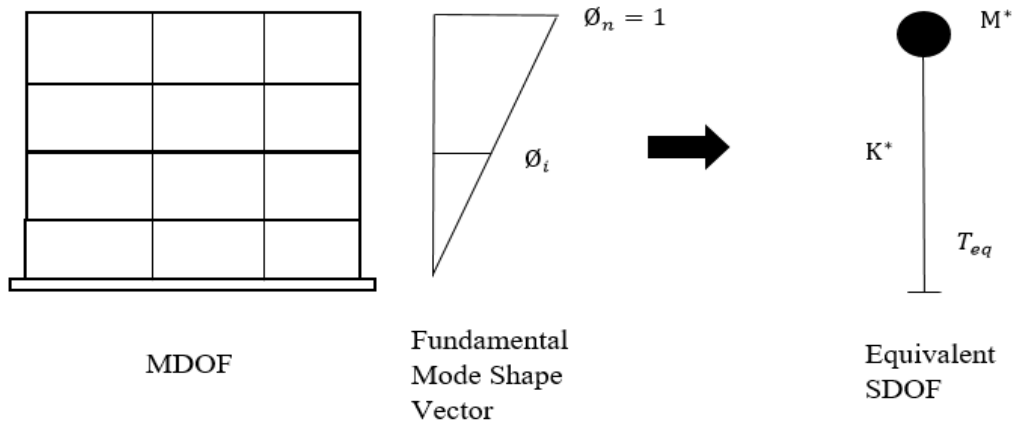


Figure 1: Multi degree of freedom system and Single degree of freedom system

### 2.2.1.1 Target Displacement

The pushover analysis should be carried till the complete failure of the structure is reached. For this reason, target displacement is calculated in order to predict the displacement at which the structure fails. The target displacement can be calculated as shown in Equation 2.2.

$$\delta = C_0 C_1 C_2 C_3 S_a \frac{T_e^2}{4\pi} g \quad (2.2)$$

where;

$C_0 C_1 C_2 C_3$ : Coefficients obtained from ATC40-1996.

$S_a$ : The spectral acceleration at the natural period of the structure in the considered direction.

$T_e$ : The effective period of the structure.

$g$ : The gravitational acceleration.

### 2.2.1.2 Capacity Curve (Pushover Curve)

The ability of the structure to resist the earthquake is calculated by this curve. It illustrates the graph which shows the total lateral force on a building, against the lateral deflection of the roof of the building. The location of hinges in any stage and the

performance point of the model can be obtained by capacity curve as shown in Figure 2. The area from A to B represents the elastic stage, B to IO shows the immediate occupancy stage, IO to LS shows the life safety stage and LS to CP is the collapse prevention stage as presented in Figure 3.

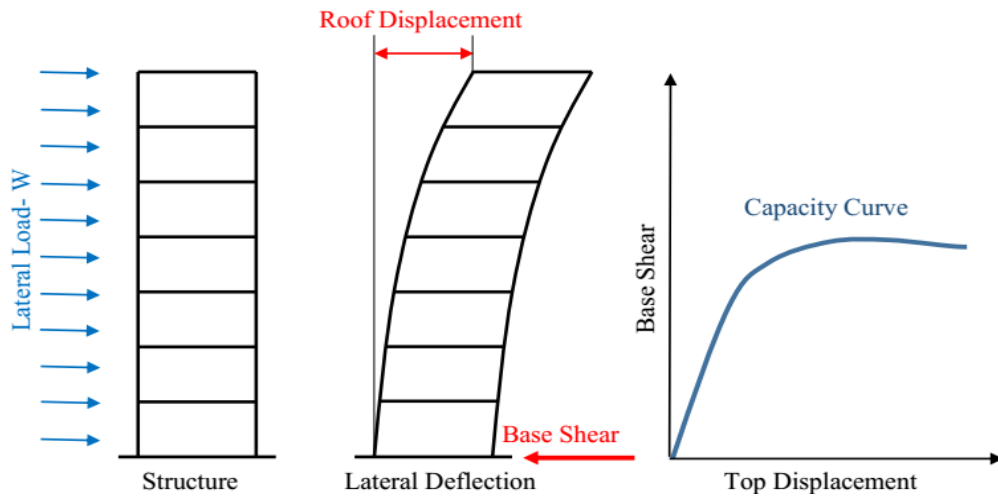


Figure 2: Capacity Curve (FEMA-356)

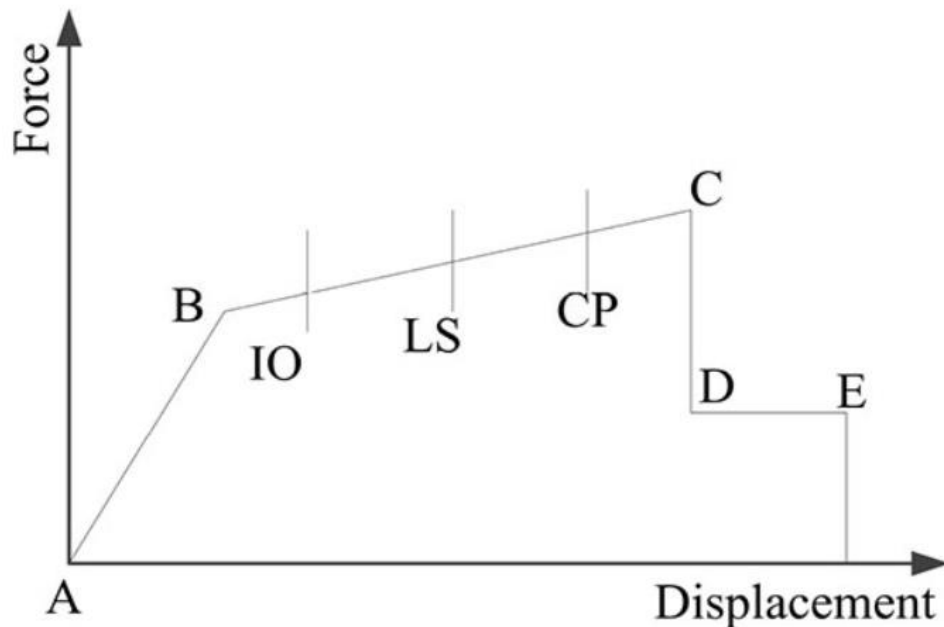


Figure 3: Performance Level Stages (Inel et al. 2006).

### **2.2.1.3 Base Shear**

Base shear is an approximation of the maximum predictable lateral force that will happen due to seismic ground motion at the base of a structure.

### **2.2.1.4 Performance Level**

The required level of performance when the structure exposed to a particular ground motion is defined as performance level. In addition, it provides a description of the permissible damage to the structural and non-structural elements. The level of performance is defined according to ATC-40 as the state at which the building will be after it is subjected to a certain ground motion. In another words, it is the maximum allowable damage to a building due to a certain level of seismic hazard. The three main category of performance level are listed as follow;

- 1- Immediate Occupancy Level (IO): Immediate Occupancy Structural Performance Level is defined as the post-earthquake damage state that remains safe, basically keeps the pre-earthquake design stiffness and strength.
- 2- Life Safety Level (LS): Life Safety Performance Level is defined as the post-earthquake damage state that contains damage to structural elements but retains a boundary against onset of partial or total failure.
- 3- Collapse Prevention Level (CP): Collapse Prevention Performance Level is defined as the post-earthquake damage state that contains damage to structural elements such that the structure remains to support gravity loads but retains no margin against failure.

### **2.2.1.5 Pushover Analysis Results**

Pushover analysis method is performed to determine the response parameters acting on the building to be almost the same with the results of nonlinear dynamic analysis. Pushover analysis method can be preferred since it shows the nonlinear behavior of

the building. Also, the elastic dynamic and static analysis methods cannot deliver many response features that pushover analysis can provide such as;

- Inter-story drift and the value of drift along the height of the structure.
- Deformation demand of some ductile elements.
- Strength discontinuity which can change the elastic range parameters in elevation and plan.
- Beam-columns joint moment demands and columns axial forces demands of the brittle elements.
- Weak points of the structure.

### **2.2.2 Nonlinear Time History Analysis**

Nonlinear time history analysis method is used to determine the response of the building to real ground motion records. When the structure is subjected to high level of seismic actions and the response of the structure is needed to be known, the nonlinear time history analysis method will be the most accurate way to do that (PInho, 2007). The nonlinear time history analysis is characterized by the frequency and magnitude of the ground motion records. It is a hard task to select the appropriate record to analyze the structure since every earthquake record have a unique nature that results in unpredicted response. For this purpose, analysis is conducted in analytical manner. Where a various number of records are used and the average or maximum response is selected in the design or assessment (Seneviratna, 1996). Figure 4 shows the graph a real earthquake record of EI Centro.

There are numerous methods to obtain solution for the nonlinear time history analysis such as;

- Modal and direct integration, which can be used to evaluate the equilibrium equation.
- Linear and non-linear time history analysis.
- Ritz and Eigen modal, both of these methods can be used to analyze the structural systems for non-linear modal.
- Periodic analysis and transient analysis, the periodic analysis is used for linear analysis by considering limitless cycles for the applied load. However, the transient analysis is acting as one-time event by considering the load with beginning and end.

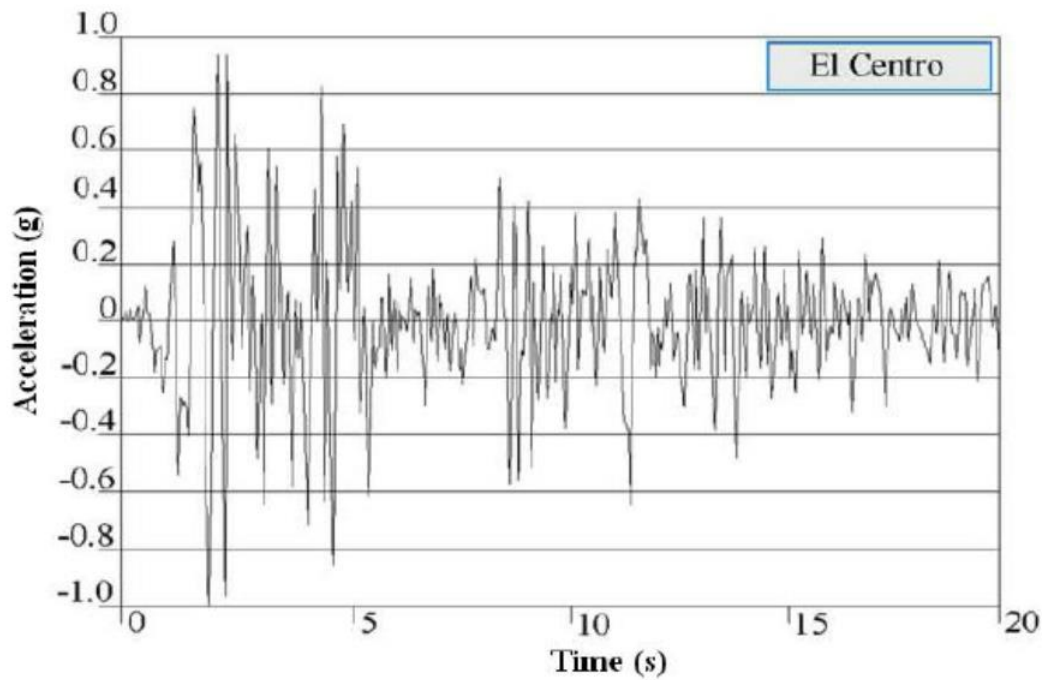


Figure 4: El Centro Earthquake Record (Zahrai. S. M-2009)

### 2.2.2.1 Scaling methods of ground motion

The records of ground motion are required to be matched with the design spectrum.

The main earthquake record scaling methods are listed below;

- Scaling in time domain method:

This method provides a matched function for the record with the used response spectrum without any change in the contents of frequency. Nevertheless, the acceleration of the ground motion record is adjusted in time domain by adding wavelets. These wavelets are functions that provide a limited period of wave-form which fluctuate up and down by passing from zero.

- Scaling in frequency domain method:

It depends on keeping the Fourier stage of motion constant when the aimed ratio of response spectrum to time series response spectrum is needed to be found. Although this method is simple, its convergence characteristics are not good. Also, increase in energy in ground motion can be occurred when this method is used, and it can lead to some changes in the time series properties.

### **2.2.3 Modal Analysis**

The natural vibration modes of the structures are determined by the modal analysis. These methods can be utilized like foundation for the modal superposition in the analysis of response spectrum and modal load cases for the time history analysis. In order to determine a modal load case there are two types of modal analysis Ritz and Eigen-vectors (Chopra 2001).

#### **2.2.3.1 Ritz-Vector Analysis Method**

When structures are subjected to dynamic loads, the value of natural free vibration modes is not great in terms of their superposition analysis. On the other hand, the results of Ritz-vector analysis are more accurate compared to the results of natural mode shapes since the free vibration modes are neglecting the spatial distribution of dynamic loading while this method is taken them into account.

### 2.2.3.2 Eigen-Vector Analysis Method

This method can determine the frequencies and undamped free vibration modes and of the modal which provide an acceptable view regarding to the structure's behavior. However, this method is applicable for all types of analysis. Equation 2.3 delivers the formula of generalized eigenvalue.

$$(K - \Omega^2 M)\phi = 0 \quad (2.3)$$

Where;

$\Omega$ : Matrix of eigenvalues

$\Phi$ : Matrix of Eigen vectors

The pair of eigenvector-eigenvalue is responsible to determine each shape of natural vibration modes. Figure 5 shows the components of mode shapes in order to determine the total response.

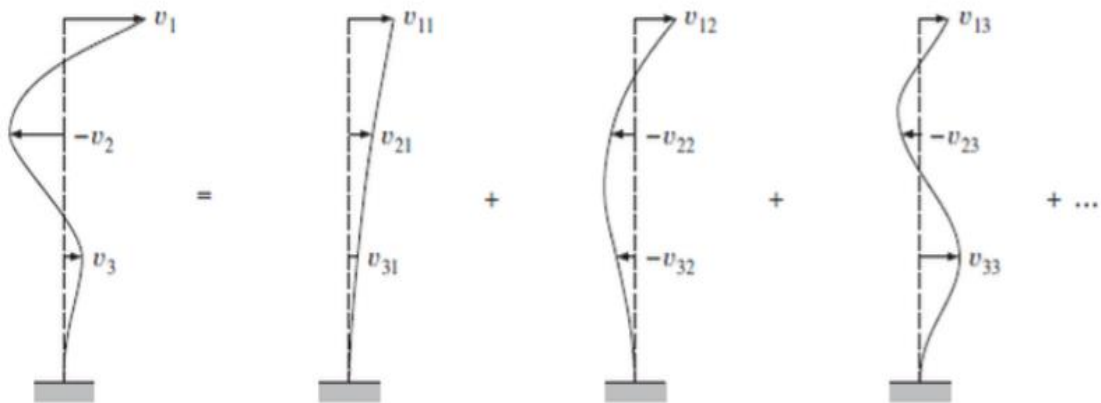


Figure 5: Components of mode shapes (CSI,2014)

## 2.3 Types of Energy Dissipating Devices

The types of energy dissipations systems can be subcategorized into three systems;

1- Passive systems: The main role of this system is to absorb a portion of the delivered excitement by the ground motion to the structure. Which will reduce by definition the



structural element demand and mitigate their collapse potential (Constantinou, et al. 1998).

2- Active systems: These systems are integrated with the structural system with real-time sensor. where their magnitude of dissipation is linked to the applied force (Chen, et al. 1999).

3- Semi active systems: These systems are combination of the both active and passive systems where they are consisted of stiff dissipater that is attached to an active joint (Ribakov. 2004).

This research will consider only viscous and friction dampers which are classified as passive energy dissipating devices.

### **2.3.1 Viscous Dampers**

viscous dampers were at first utilized within the aerospace and military industry then at the early 1990s they started to be used in the structural engineering field. They are generally comprising of head with holes contained in barrel filled with an exceedingly thick liquid, as a rule a compound of silicone or a comparative sort of oil. Energy is scattered in the damper by liquid slot when the piston head moves through the liquid. However, the liquid inside the barrel is almost incompressible, so when the damper is subjected to a compressive pressure the liquid volume interior the barrel is diminished as a result of the piston shaft area movement which caused to restore the force.

The linear behavior of damper is given by Equation 2.4. As recommended by Constantinou et al. 1992, Reinhorn et al. 1995, Seleemah et al. 1997 and seismic design guidelines such as FEMA 273 FEMA (1997).

$$F_t = CV + Kx = F_D + F_E \quad (2.4)$$

where;

$F_t$ : Is the total absorbed energy by the damper.

C: Is the damping coefficient.

V: Velocity of the damper.

K: The total stored stiffness.

x: Damper displacement.

The term CV is related to the damping force  $F_D$  and the term  $Kx$  is related to the restoring force  $F_E$ . However, dampers may exhibit nonlinear behavior due to the presence of internal configuration. Which is described using equation 2.5.

$$F_D = C|V|^n \text{sgn}(V) \quad (2.5)$$

Where n is an exponent of the damper velocity.

The setup of the viscous damper is presented in Figure 6.

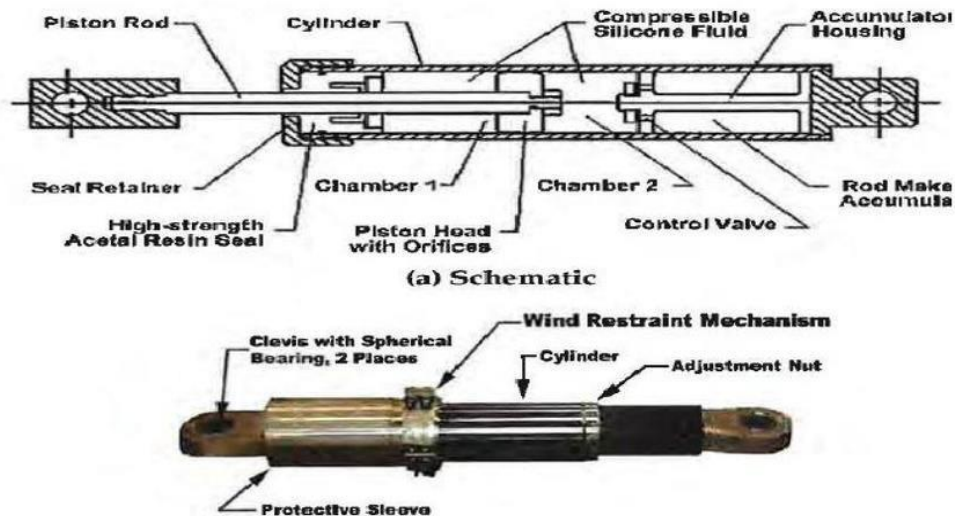


Figure 6: Viscous Damper Device ( Lee & Taylor-2001)

### 2.3.2 Friction Dampers

The usage of friction dampers in civil engineering starts at the early 1970's. Actually, friction device has been used successfully to control the movement of objects for a considerable length of time. Friction dampers utilize the component of strong grinding

that advances between two strong bodies sliding with respect to one another to empower to acquiring the ideal energy dissipation. Soong, 2002 has studied about some types of friction dampers to enhance the ability of the structure to resist seismic actions and also to improve the seismic response of the structure. Friction dampers slips at a predetermined load level in order to dissipate energy by friction mainly during intense earthquake movements. There are many types of Friction dampers have been considered and studied in construction area. Furthermore, they are industrially accessible and has been fabricated. These devices become distinctive with their mechanical property and utilized materials for the sliding parts from one another. The thermal fluctuation does not affect the friction dampers and their hysteretic behavior during the seismic actions.

There are several types of FDs as listed below:

- 1- Piezoelectric FDs.
- 2- Sumitomo passive energy dissipation devices.
- 3- Pall FDs.
- 4- Slotted-bolted connections.
- 5- The energy dissipating restraint (EDR).

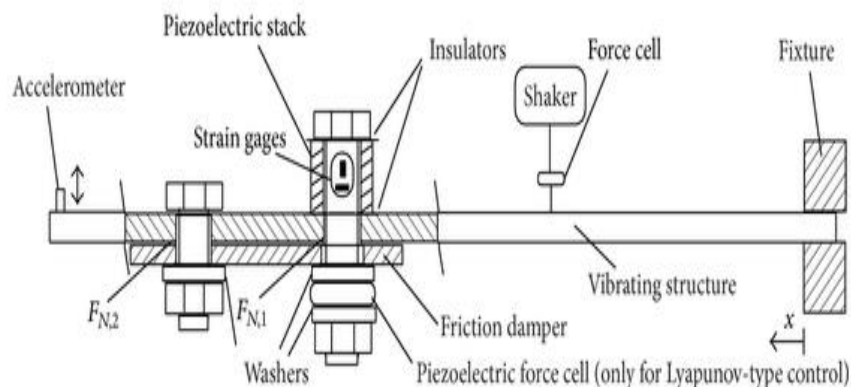


Figure 7: Friction Damper Device (Becker et al. 2007)

## 2.4 Steel Structures

Steel elements are used almost in every structures nowadays. It is also strong and have good quality control. At the nineteenth century steel started to be used as one of the main elements in the structure due to the low cost of manufacturing and design flexibility compared to other structural elements such as reinforced concrete (Tripeny, et al. 2011). However, steel has a great characteristic which is recyclability since steel can be recycle more than ones without any effect on its properties. So, it can be considered as natural friendly element in the construction area because it can reduce the waste of construction and save the natural resources. Also, it can reduce the pollution during the period of constructing.

Steel has some advantages when is used as a structural element as shown in the list below:

- Steel structures are taking less time to be constructed compared to other types of structures which leads the work to be more economic.
- The weight of steel structures is lower than reinforced concrete structure, because steel element has a big strength /weight ratio.
- It is quite simple to predict the properties of steel.
- The workers mistake and construction concerns are minimized during the process of constructing a steel structure. Also, the refabricated steel materials can be delivered safely to the construction site.
- Repairing steel elements is easy and getting access to any damaged member to be repaired does not take time.

- In the steel construction process the frame elements are transported in time for constructing which minimizes the zone needed for storage and therefore participating to an effective construction site.



Figure 8: Steel building with columns, beams and bracing

## 2.5 Ductility

The ability of the structure to withstand high magnitude of deformation without yielding (forming plastic hinges) is defined as ductility. And it is the ratio of the maximum displacement  $d_{max}$  obtained by the nonlinear time history analysis to the yield displacement  $d_y$  obtained by pushover analysis. As shown in equation 2.6.

$$\mu = \frac{d_{max}}{d_y} \quad (2.6)$$

## 2.6 Displacement and Drift

Displacement and Drift can be defined in many terms as shown below:

- 1- Global displacements, describe the displacement close to the base of an equivalent SDOF structure representing the system.
- 2- Roof displacement, shows the value of the lateral force on the roof of the structure with respect to the base.
- 3- Drift ratio, it can be calculated by dividing the inter story drift by the height of the story.
- 4- Inter story drift, it is usually described as a ratio of displacement of two consecutive story to height of that story.

Figure 9 shows the displacement of structure when it is subjected to earthquake ground motions.

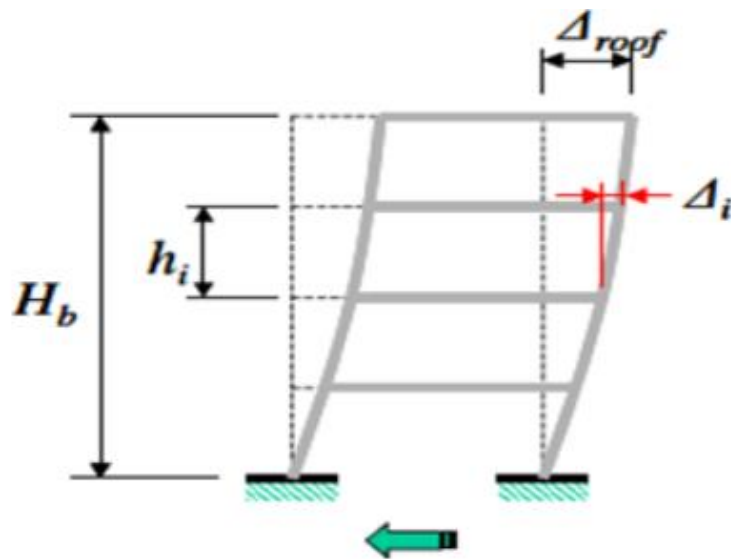


Figure 9: Roof displacement and inter-story displacement (Jabeen et al. 2014)

## **Chapter 3**

### **METHODOLOGY**

#### **3.1 Introduction**

This study mainly aspiring to investigate the influence of viscous and friction dampers on lateral force resistance of steel buildings at Duzce city, Turkey. For this purpose, 21 models of steel frame buildings with 5, 10 and 20 floors, with two different types of energy dissipation devices placed in three different locations were designed to accomplish the research aim. In addition, the nonlinear analysis methods such as pushover analysis and time history analysis are covered in this section.

#### **3.2 Strategy of Analysis**

In order to enhance the relatability of this study's results, three different methods of analyses are adapted which are listed as follow;

- 1- Equivalent lateral force method in accordance with TBDY-2018.
- 2- Pushover analysis method in accordance with FEMA-356.
- 3- Non-linear time history analysis method by using three different ground motion records.

Figure 10 is a flow chart representation the analysis strategy.

#### **3.3 Location of the Case Study**

The Location of the case study models have been assumed to be in Duzce region in Turkey as presented in Figure 11. The peak ground acceleration of this location is ranging between 0.552-0.933g for 10% and 2% exceedance within 50 years respectively. In addition, the location is characterized with soil type B.

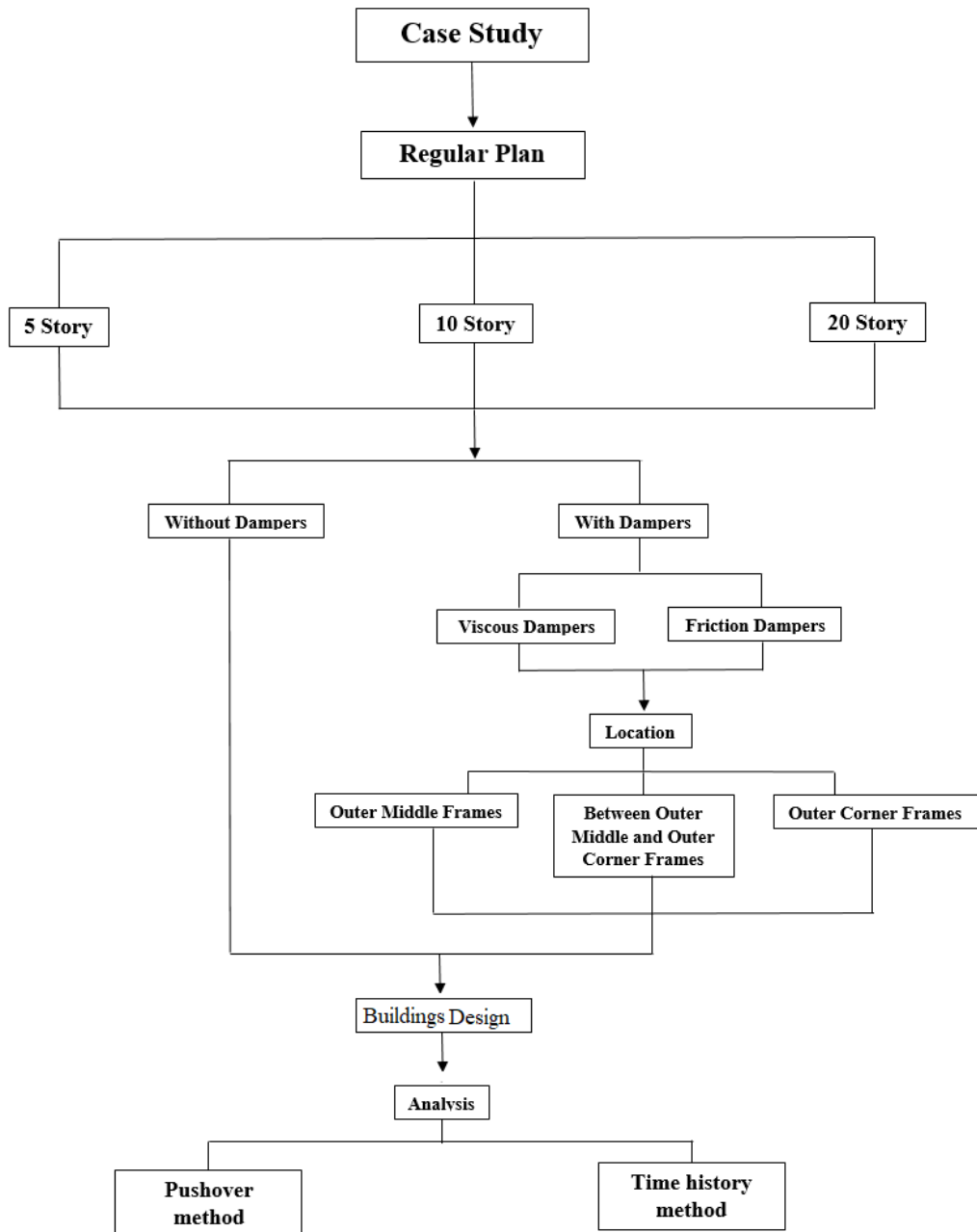


Figure 10: Flow chart of the analysis strategy



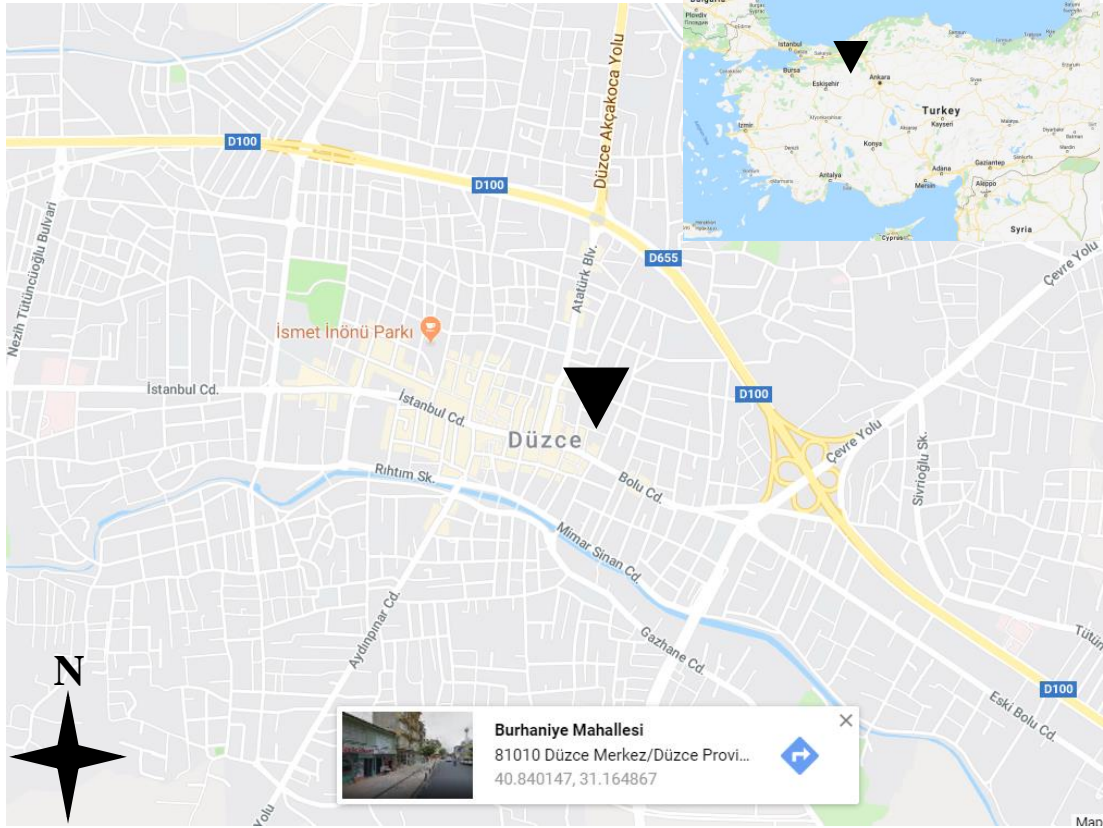


Figure 11: Assumed Location of the Steel structure models (Google map 2019)

### 3.4 Modelling of Steel Structures

ETABS2017 software was used to model, design and analyze all of the 21 steel frame models. The length of spans and arrangement of columns, beams and secondary beams are illustrated in Figure 12. All models are having ground floor of 3.25m from the ground level. However, the height of other floors is 3m. The 3D view of five story model is presented in Figure 13. Note that ten and twenty story models have the same geometry except the total height.

The characteristics of steel models are given in Table 1. However, Table 2 provides the properties of the materials that have been used in designing and analyzing the steel building models.

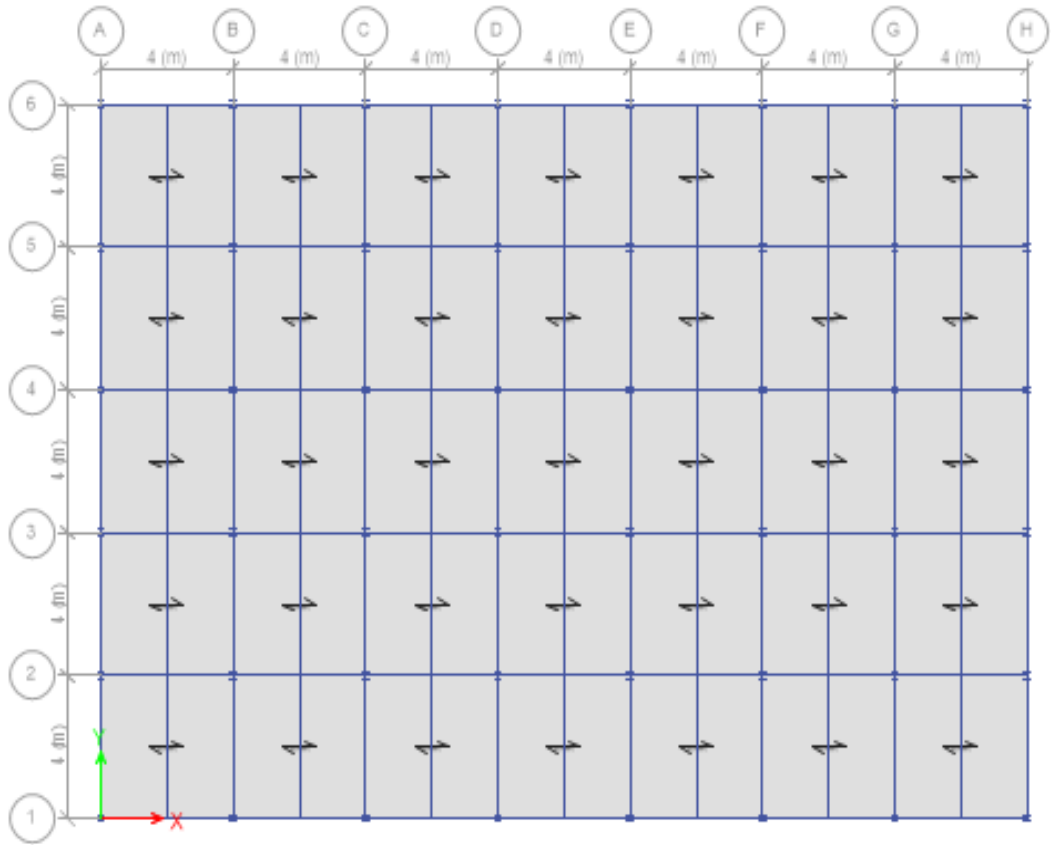


Figure 12: Plan layout of the steel buildings

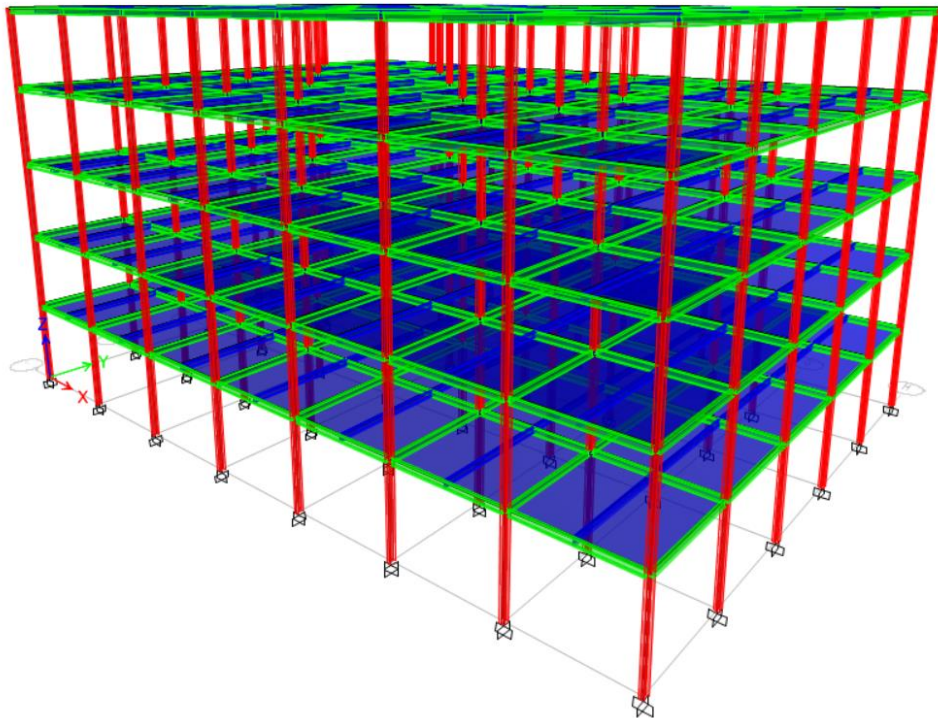


Figure 13: 3D view of 5-story steel building without dampers

Table 1: Characteristics of the structural system

Number of Bays (X-direction)	7
Number of Bays (Y-direction)	5
Width of Bays	4 m
Columns Section	HEB
Beam Section	IPE
Secondary Beam Section	IPE

Table 2: Material properties

Steel grade	S275
Characteristic Compressive strength of concrete	C30
Steel deck section	ALDECK70/915

### 3.4.1 Column Cross-Section

The cross-section of columns is selected as HEB which can give more ductility compared to HEA cross-section, because it has flange with higher thickness. Figure 13 presents the cross-section of the selected column of this research.

### 3.4.2 Beam Cross-Section

Steel beams are selected to resist the moment and shear of building along the element's major axis. Also, the additional resistance can be provided by the steel deck. Therefore, beams with cross-section of IPE have been selected for this study. Figure 15 illustrating the IPE cross-section overview.

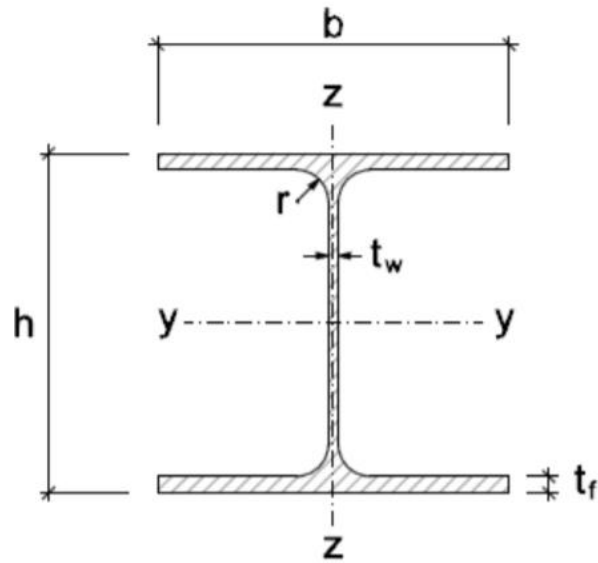


Figure 14: Schematic view of the HEB cross-section (EN1993-1-1:2005)

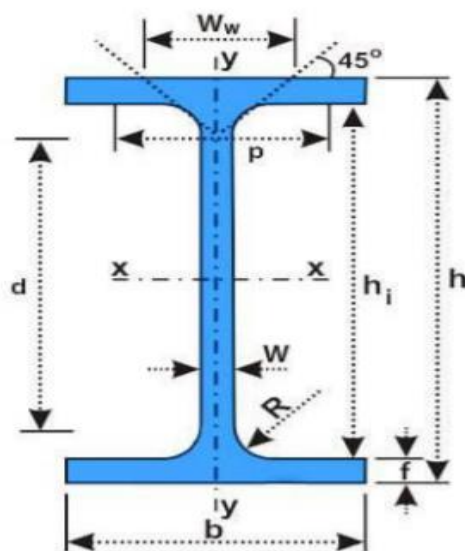


Figure 15: Schematic view of the IPE cross-section (EN1993-1-1:2005)

### 3.4.3 Slab Type

The slab type that have been selected to all models in this study is light metal gauge steel deck. The concrete that used to fill the steel deck is having compressive strength of 30 MPa. Aldeck 70/915 can give maximum span of 4m is selected for this research, and its cross-section overview is given in Figure 16.

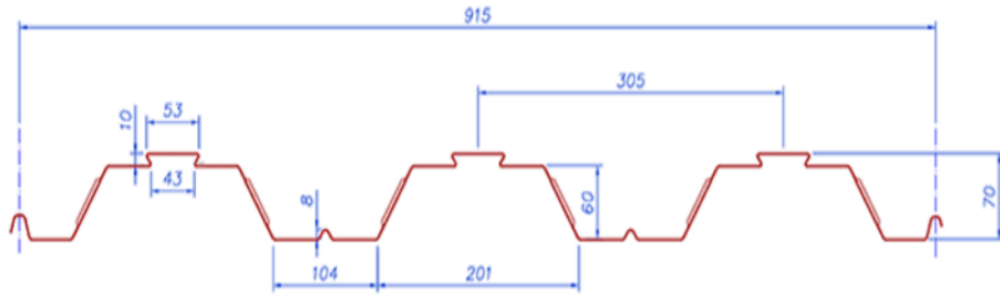


Figure 16: Schematic view of the Aldeck 70/915 cross-section (EN1993-1-1:2005)

### 3.5 Energy Dissipation Devices Properties and Locations

To investigate the effectiveness of energy dissipation devices in steel buildings, viscous and friction dampers are implemented in five, ten and twenty stories steel frame structures as diagonal bracing. However, these devices are placed in three different locations for each type of structure, first location is the outer mid-frame of the steel building, second location is the outer corner of the steel building and the last location of dampers is between the outer mid-frame and outer corner of the steel building as shown in Figure 17, 18 and 19 respectively. The previously mentioned figures correspond to the 10 story steel building. Models with 5 and 20 story have the same dampers distribution method as the 10 story model.

The dampers distribution method is applied for both viscous and friction dampers identically.

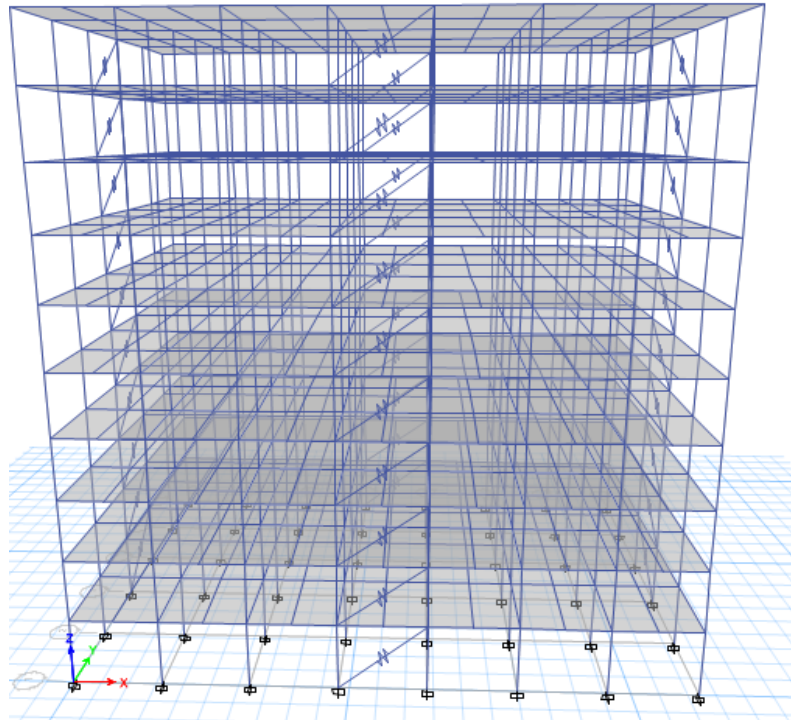


Figure 17: Dampers located in outer mid-frame for 10-story steel building

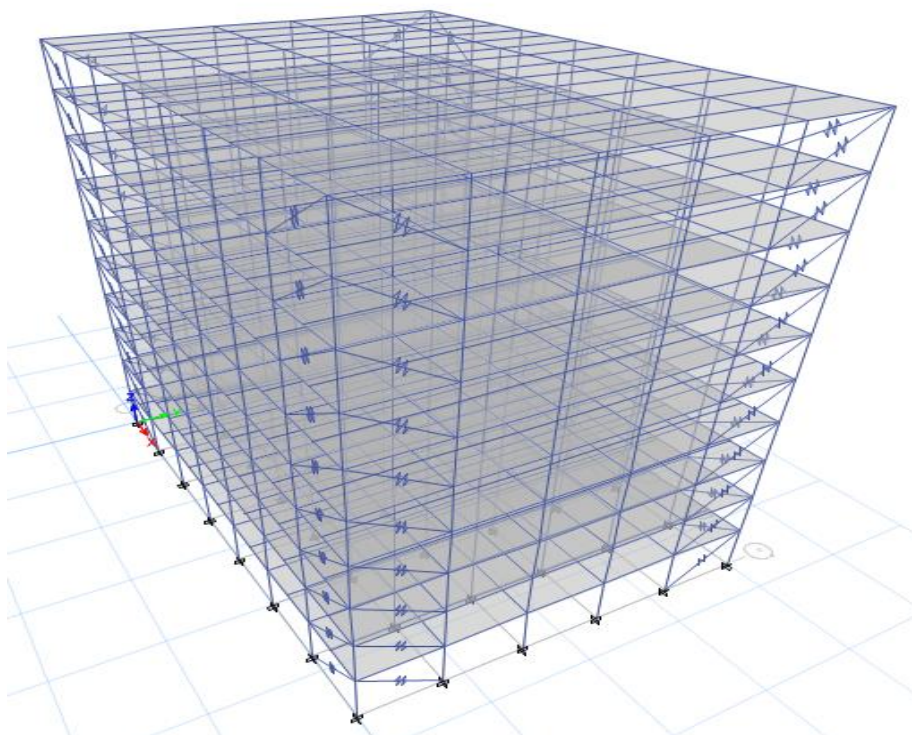


Figure 18: Dampers located in outer corner frames for 10-story steel building



Dampers properties are collected from Taylor Device Company. The properties of viscous dampers are given in Table 3. However, Table 4 provides the properties of friction dampers.

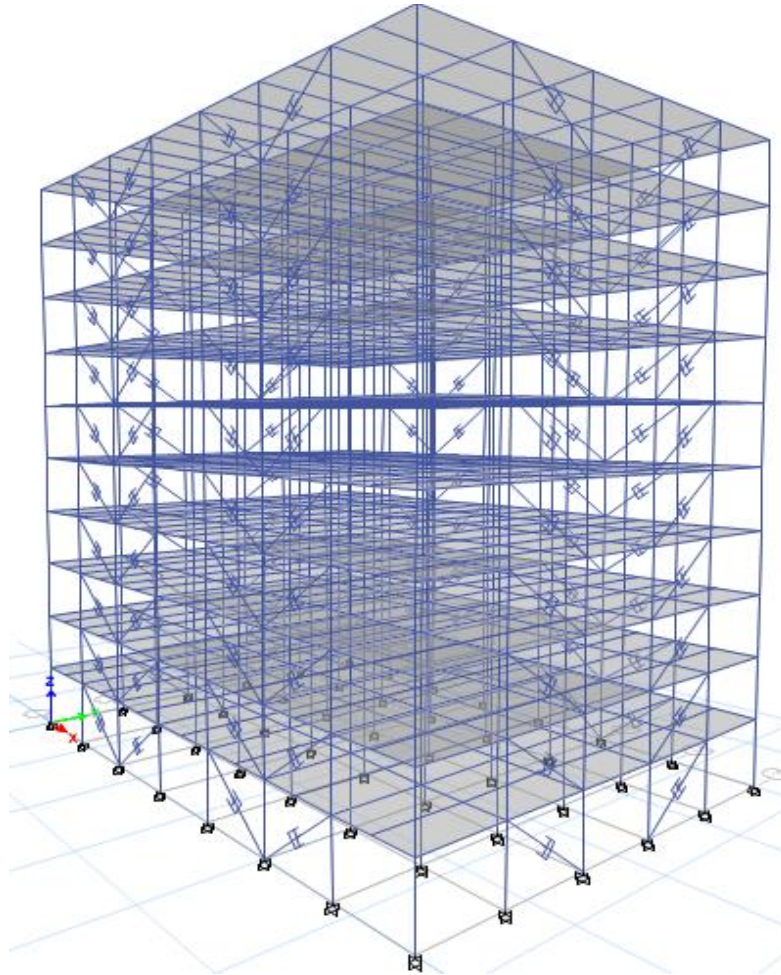


Figure 19: Dampers located between outer corner and mid-frame for 10-story steel building

Table 3: Viscous damper properties (Taylor Device Company)

Stiffness (kN/m)	Damping ( $\text{kN} \cdot (\text{s/m})^{C_{\text{exp}}}$ )	Damping Exponent
350254	17513	0.5

Table 4: Friction damper properties (Taylor Device Company)

Initial Stiffness (kN/m)	Slipping Stiffness (Loading) (kN/m)	Slipping Stiffness (Unloading) (kN/m)	Precompression Displacement (mm)
350254	262690	175127	-1.3

The properties mentioned in Tables 3 and 4 are selected as nonlinear properties by using Link element for both friction and viscous dampers in Etabs 2017 software as presented in Figure 20 and 21.

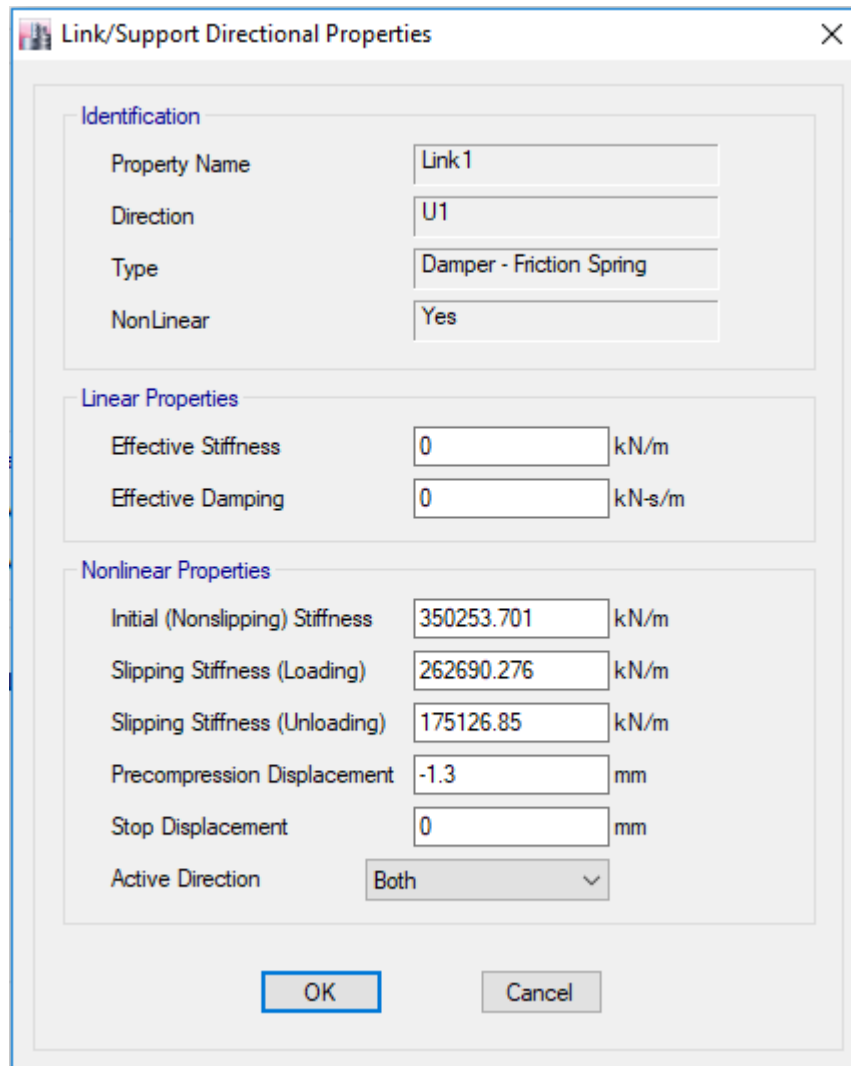


Figure 20: Nonlinear Properties of Friction Dampers



Identification	
Property Name	Link1
Direction	U1
Type	Damper - Exponential
NonLinear	Yes

Linear Properties	
Effective Stiffness	0 kN/m
Effective Damping	0 kN-s/m

Nonlinear Properties	
Stiffness	350253.581 kN/m
Damping	17512.679 kN*(s/m) <sup>Cexp</sup>
Damping Exponent	0.5

Figure 21: Nonlinear Properties of Viscous Dampers

### 3.6 Design Assumptions

Eurocode 3-2005 is used to select the most economic sections for both columns and beams to resist the applied loads that used to design the steel building models. All models are designed by using equivalent lateral force method which distribute part of the seismic force (base shear) to every floor, which are able to transfer lateral loads. Various types of loading are applied to the steel structure buildings as mentioned below:

### 3.6.1 Gravity Loads

The self-weight of the of slabs and structural elements is considered as gravity load. Also, the additional dead load is assumed to be  $1.5 \text{ kN/m}^2$ . Ultimately, live load is taken as  $2 \text{ kN/m}^2$  (TS-498 for residential buildings).

### 3.6.2 Earthquake Parameters

The 10% probability of exceedance for earthquake parameters is used to design all models as mentioned by (TBDY-2018). The 0.2 sec spectral acceleration ( $S_s$ ) is found as 1.344, while the 1 sec spectral acceleration ( $S_1$ ) is given as 0.365 for the selected region. However, the nonlinear analysis is carried according to 2% probability of exceedance. Where the 0.2 sec spectral acceleration ( $S_s$ ) is taken as 2.38, while the 1 sec spectral acceleration ( $S_1$ ) is taken as 0.645. Nevertheless, the site class is ZB.

Table 5 gives brief information on the Earthquake parameters.

Table 5: Earthquake Parameters

Case study location	Duzce city-Turkey
Site class	ZB
Earthquake seismic zone	Zone 1
Effective ground acceleration coefficient , ( $A_0$ ) for 10% exceedance (Design)	0.552
Effective ground acceleration coefficient , ( $A_0$ ) for 2% exceedance (Analyze)	0.933
Ground soil type	B
Live load reduction factor	0.3
Importance factor, (I)	1
Structural behavior factor $R$	5-8
Damping ratio	5%

ETABS2017 software is used to calculate the earthquake loads automatically and apply them to both directions. Furthermore, additional eccentricity is considered as  $\pm 0.05$  (TBDY-2018).

### 3.6.3 Load Combinations

Table 6 illustrates the load combinations that used to design all steel structure models.

Table 6: Load Combinations for Design

Gravity Load Combinations	Earthquake load	Combinations
DL + LL	LL + DL + EX + 0.3EY	$\pm 0.05$ eccentricity
1.4DL + 1.6 LL	LL + DL + EX - 0.3EY	$\pm 0.05$ eccentricity
	LL + DL - EX - 0.3EY	$\pm 0.05$ eccentricity
	LL + DL - EX + 0.3EY	$\pm 0.05$ eccentricity
	LL + DL + EY - 0.3EX	$\pm 0.05$ eccentricity
	LL + DL + EY + 0.3EX	$\pm 0.05$ eccentricity
	LL + DL - EY - 0.3EX	$\pm 0.05$ eccentricity
	LL + DL - EY + 0.3EX	$\pm 0.05$ eccentricity
	0.9GDL + EX - 0.3EY	$\pm 0.05$ eccentricity
	0.9DL + EX + 0.3EY	$\pm 0.05$ eccentricity
	0.9DL - EX + 0.3EY	$\pm 0.05$ eccentricity
	0.9DL - EX - 0.3EY	$\pm 0.05$ eccentricity
	0.9DL + EY - 0.3EX	$\pm 0.05$ eccentricity
	0.9D + EY + 0.3EX	$\pm 0.05$ eccentricity
	0.9DL - EY + 0.3EX	$\pm 0.05$ eccentricity
	0.9DL - EY - 0.3EX	$\pm 0.05$ eccentricity

## 3.7 Nonlinear Analysis

### 3.7.1 Pushover Analysis

The procedure of pushover analysis consists of applying vertical load to a structural model with progressively incremented lateral load. It continues till reaching the

collapse situation of structure. The main target of nonlinear pushover analysis is to find the coordinates of the performance point in terms of displacement and base shear. The performance of a building is calculated at the performance point. For example, the number of hinges is studied at the performance point or in an interval close to it. In this study, pushover analysis is conducted with accordance to FEMA 356 where the combinations are used for defining the value of vertical load and the definition of plastic hinges are reported from it. The definition of plastic hinges, vertical and lateral loads are illustrated in Figure 22, 23, 24. respectively.

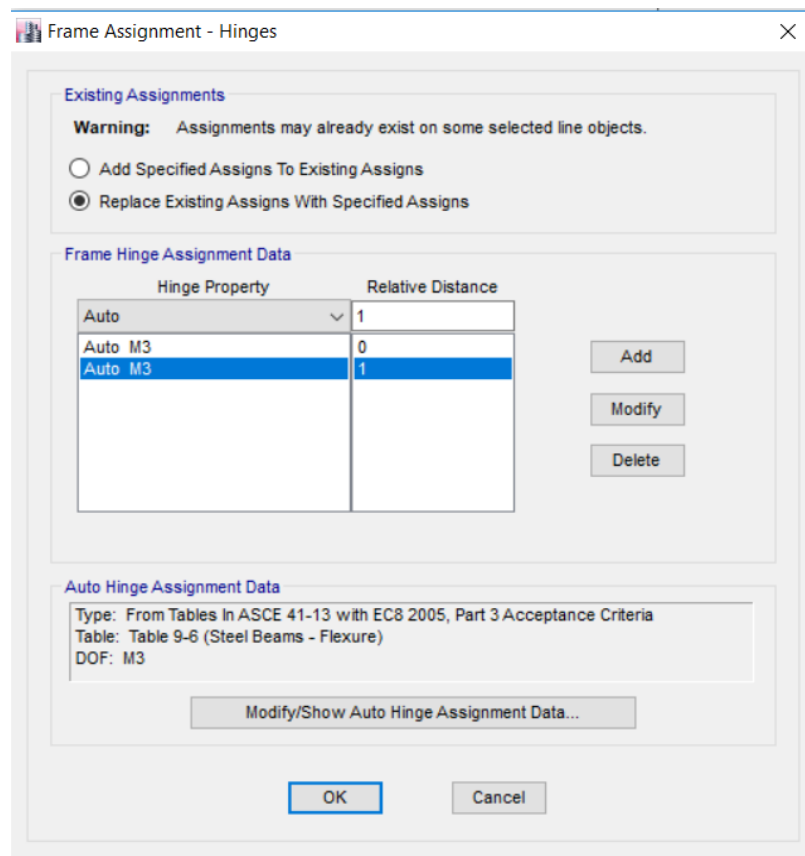


Figure 22: Plastic Hinges of beams

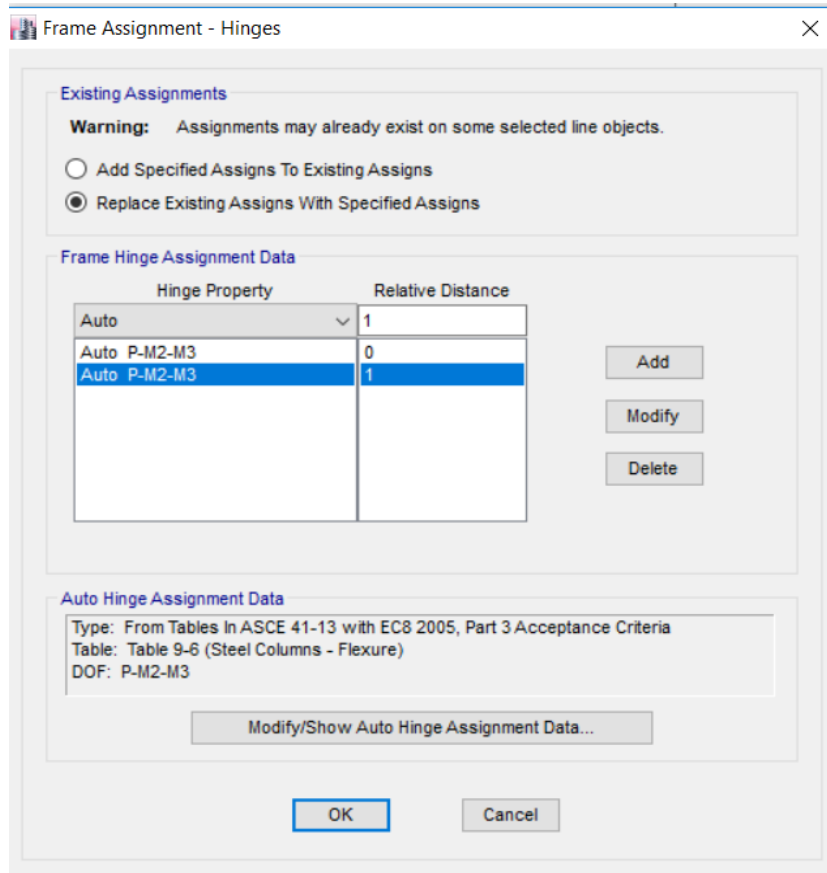


Figure 23: Plastic Hinges of Columns

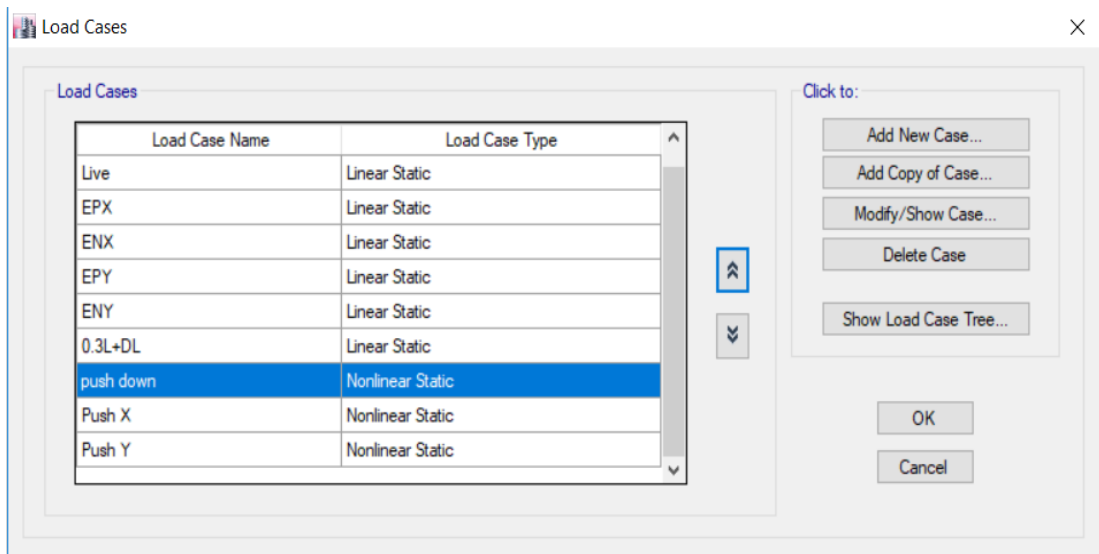


Figure 24: Load Cases Including (Push down, Push X and Push Y)

### 3.7.2 Time History Analysis

Time history analysis is used to determine the nonlinear behavior of structural models. This method is achieved when buildings are subjected to three records of real earthquakes to gather a large range of frequencies as mentioned by (TBDY-2018). Table 7 present the details of the ground motions records (APPENDIX C) that have been selected for this research. The first step in performing Time History Analysis is to import the characteristics of the earthquake records from the data base of ground motion by using Pacific Earthquake Engineering Research Centre (PEER), Ground motion records are taken from the data base without scaling, then they are scaled to the same earthquake spectrum which have 2% exceedance probability at 50 years. However, Plastic hinge properties to perform time history analysis are identical to the pushover analysis.

Table 7: Details of ground motion records (PEER)

Station Name	Duzce	Kocaeli	Izmir
Year	1999	1999	1977
Shear-wave velocity , Vs30 (m/sec)	414.91	281.86	535.24
Rrup (km)	45.16	15.37	3.21
Rjb (km)	45.16	13.6	0.74
Magnitude, Mw	7.51	7.14	5.3

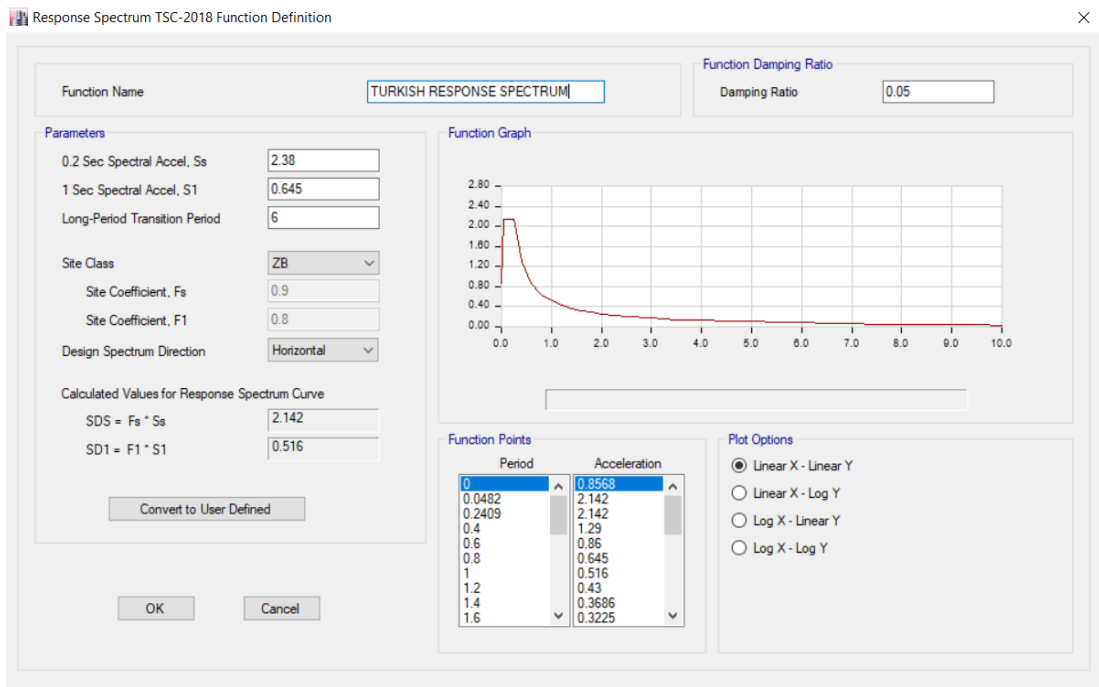


Figure 25: Response Spectrum with 2% exceedance probability at 50 years (ETABS 2017)

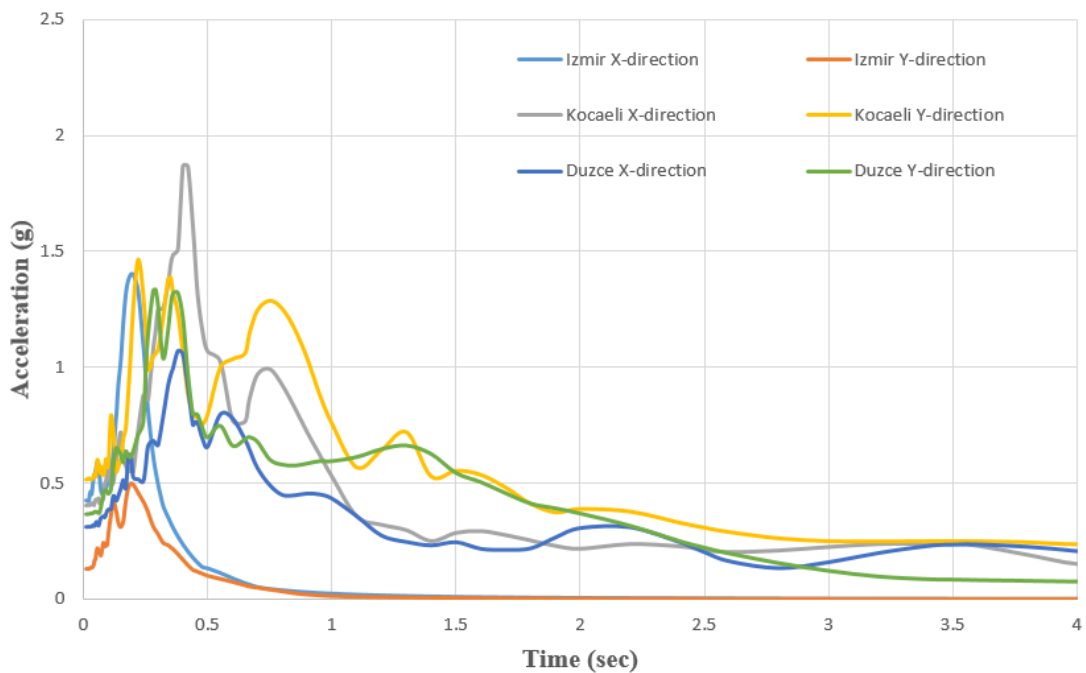


Figure 26: Ground motion Records (PEER)

## Chapter 4

### RESULTS AND DISCUSSIONS

#### 4.1 Introduction

The outcomes and discussions of the results will be presented in this chapter. Base shear, story drift, story displacement, stiffness, ductility, plastic hinges status, energy and performance level of the five, ten and twenty story steel buildings are taken into account to evaluate the effectiveness of viscous and friction dampers when the structures are subjected to earthquake forces.

#### 4.2 Nonlinear Pushover Analysis

This section of the thesis will discuss the seismic behavior of the steel buildings obtained through nonlinear pushover analysis.

##### 4.2.1 Elastic Lateral Stiffness

The elastic lateral stiffness is an important parameter in defining the seismic behavior of a building since it evaluates the amount of damages of the nonstructural elements. It is defined basically as the initial slope of the capacity curve obtained via nonlinear pushover analysis. Results indicate that models without damping devices have the least initial lateral stiffness since only the moment resistant frames are contributing in the resistant of the imposed lateral loads. On the other hand, buildings equipped with viscous dampers resulted in higher initial stiffness compared with the friction dampers at similar locations although both of which are having similar stiffness by definition. This variation in the lateral stiffness between the two devices can be related the fact that the mechanism of damping in the viscous dampers is higher than the friction



damping. Ultimately, it can clearly observed that the optimum location for the damping devices is at the outer corner frames (L2) which emphasize that dampers at the corners dissipate the lateral forces in better manners compared with the other locations. The results of the initial stiffness are shown in Figure 27, Figure 28 and Figure 29 for the 5-story, 10-story and 20-story respectively.

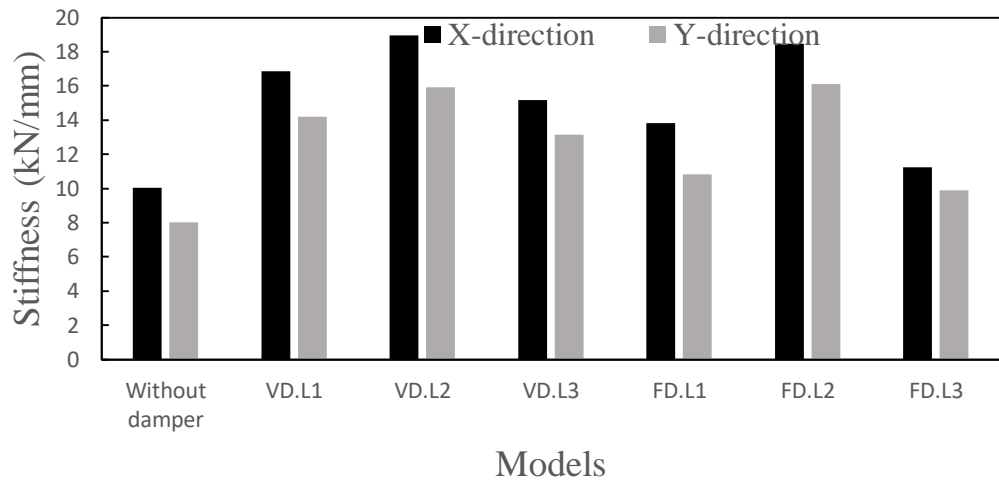


Figure 27: Initial lateral stiffness for 5-story steel building

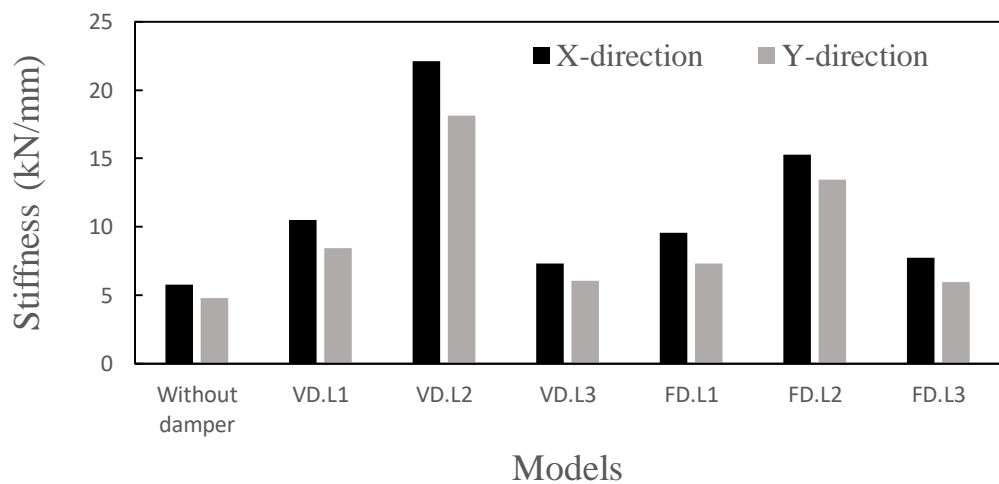


Figure 28: Initial lateral stiffness for 10-story steel building

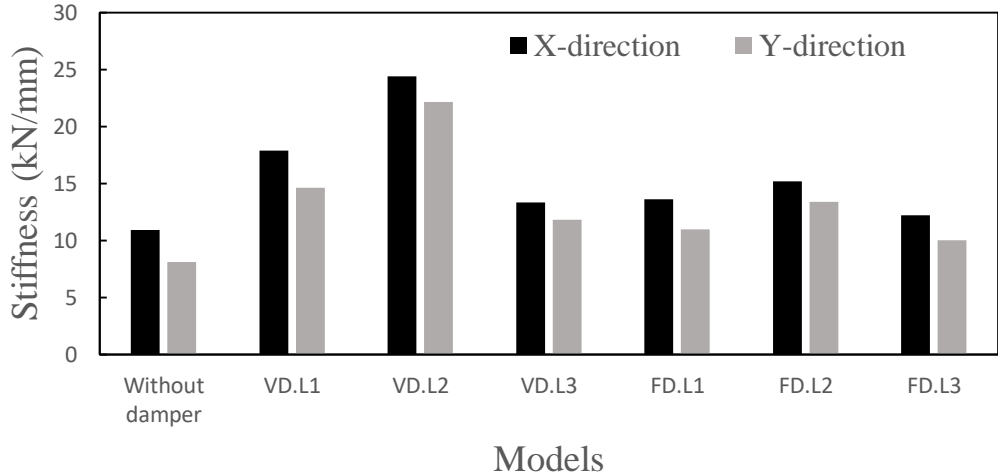


Figure 29: Initial lateral stiffness for 20-story steel building

#### 4.2.2 Structure Yield Strength

The yield strength of the structure is a main parameter in defining the seismic behavior of the buildings. The yield strength is defined as the lateral force required to the formation of the first plastic hinge through the nonlinear static pushover analysis. Results show that buildings equipped with viscous damper have higher strength compared with the other types of models. This can be link to the high lateral stiffness of the models equipped with the viscous dampers. This is valid for all the analyzed cases as shown in Figure 30, Figure 31 and Figure 32.

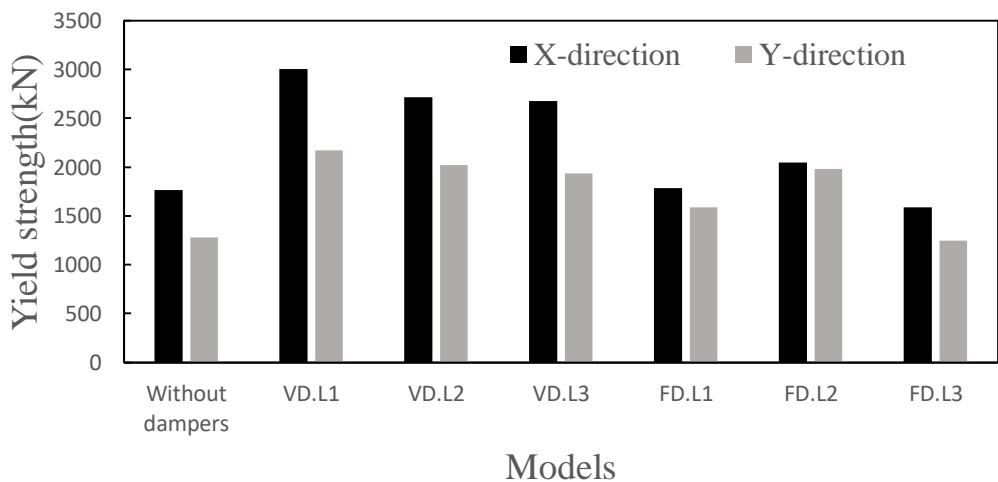


Figure 30: Yield strength for 5-story steel building

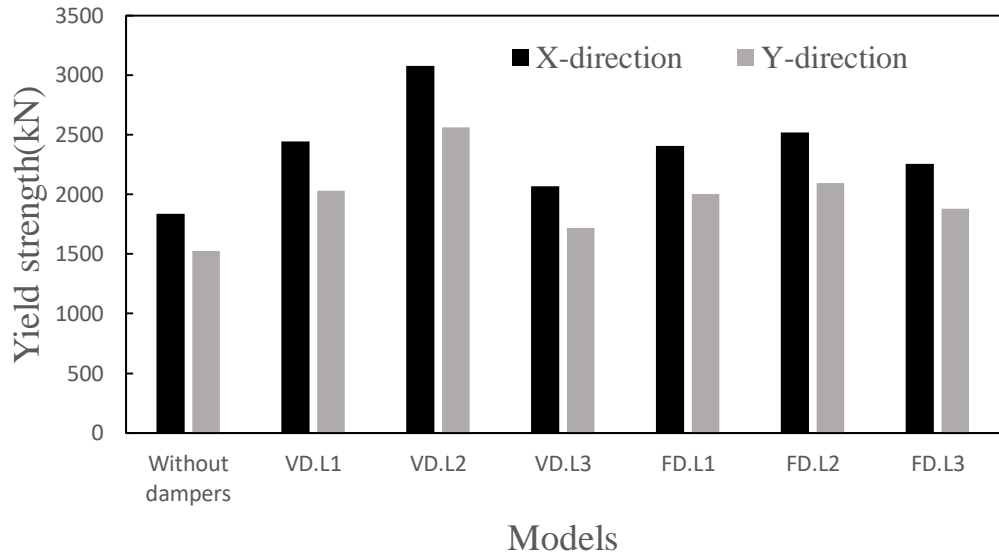


Figure 31: Yield strength for 10-story steel building

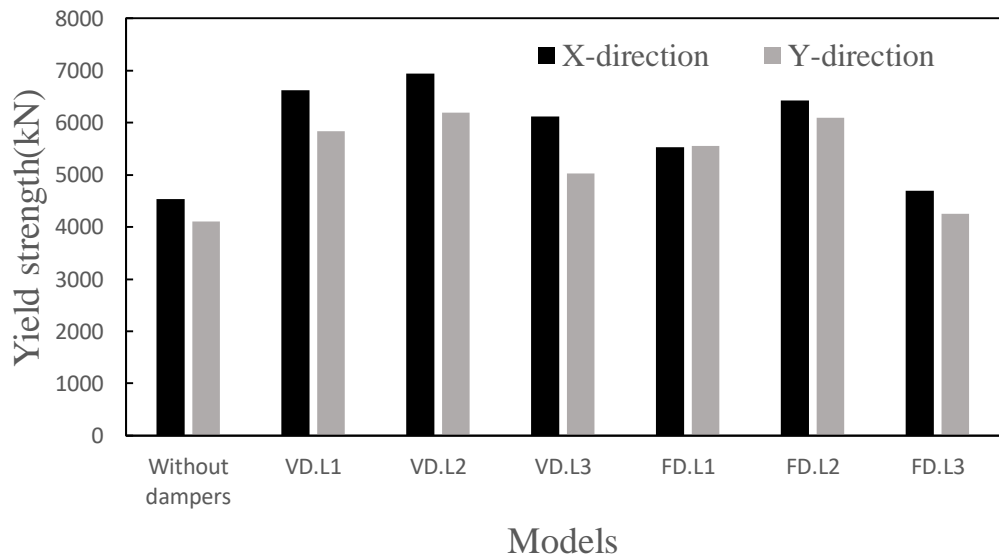


Figure 32: Yield strength for 20-story steel building

### 4.2.3 Ductility Demand Factor

The ability to absorb and dissipate the seismic excitation of a building through the inelastic behavior without any significant loss in the structure integrity is defined as ductility factor. Hence, it is a vital parameter for structural engineers since strong and flexible structure is more desirable. In order to evaluate this parameter, the maximum

absolute roof displacement obtained by the nonlinear time history analysis is divided by the yield displacement at which the first plastic hinge is formed. Results of all analyzed cases indicate that moment resistant frames unequipped with damping devices has the highest ductility which is extremely predictable since it is exposed to a relatively high displacement compared with the frames equipped with the damping devices. In addition, moment resistant frame buildings have very low yield displacement, where plastic hinges are formed at relatively small displacement. On the other hand, systems attached with viscous damping devices showed the least ductility for both the 5 story and 10 story buildings. This can be linked to the fact that viscous damped frames have lower displacement compared with the friction damped frames. However, the 20 story building showed insignificant variation among the viscous and friction damped frames. The result of the ductility demand factor is presented in Figure 33, Figure 34 and Figure 35 for 5 story, 10 story and 20 story buildings respectively.

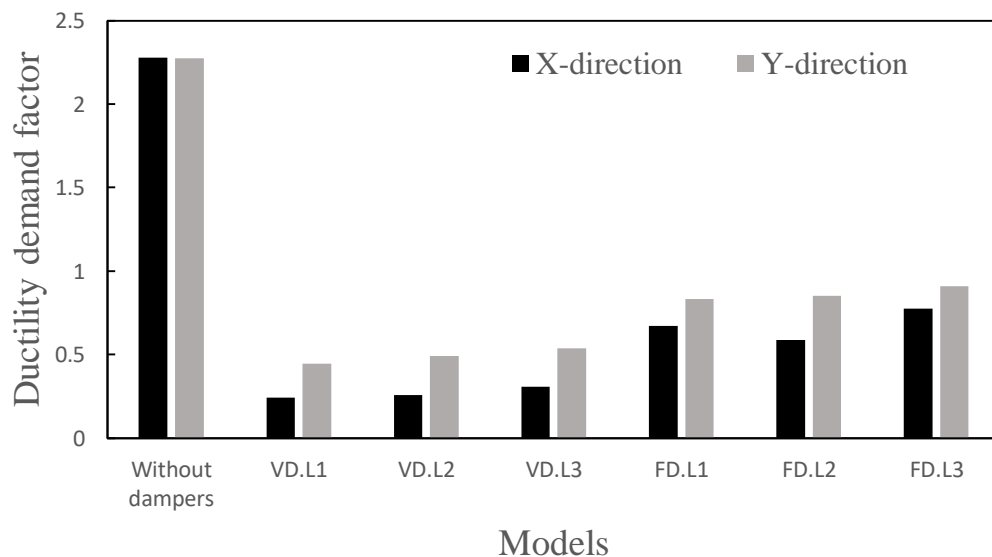


Figure 33: Ductility demand factor for 5-story steel building

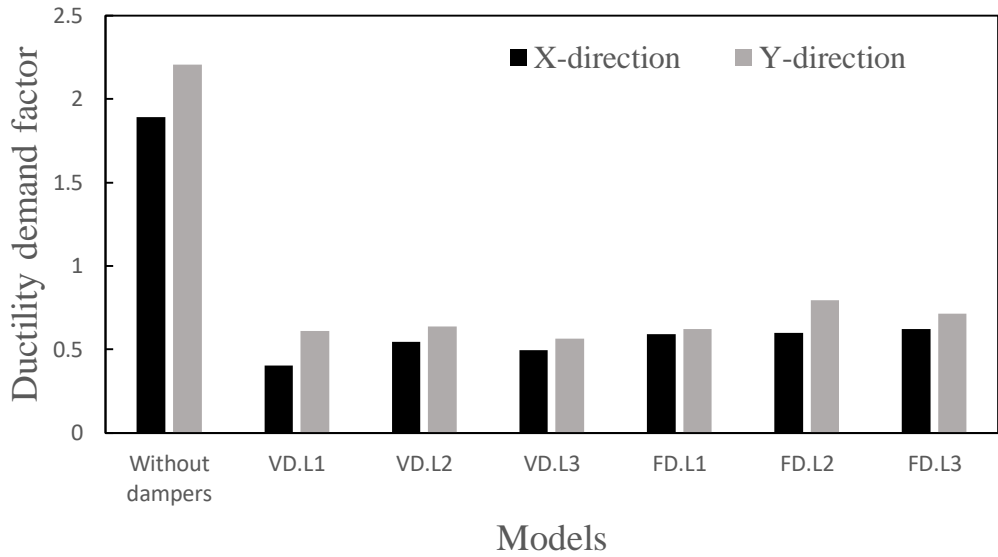


Figure 34: Ductility demand factor for 10-story steel building

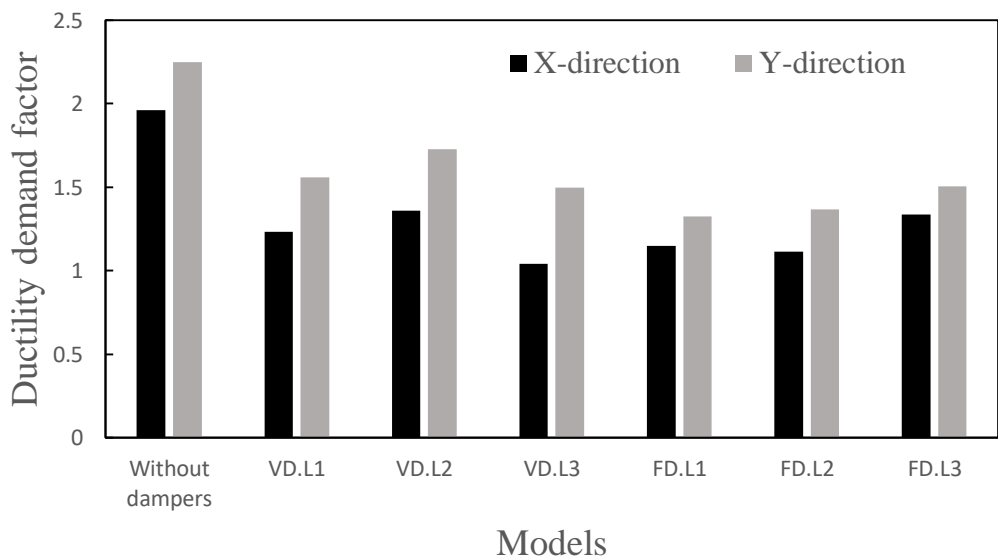


Figure 35: Ductility demand factor for 20-story steel building

#### 4.2.5 Pushover Capacity Curves

The pushover capacity curves are calculated for all models with and without dissipation devices. Figure 36 to Figure 38 illustrate the comparison of the curves of each structural system. It is clear that for the five story models the MRF had the highest displacement value and the lowest base shear comparing to the models with dampers,

while the greatest base shear is scored by VD.L1 and the least displacement is governed by VD.L2. However, in some points the values of displacement and base shear are having the same value and that is due to the mechanism of these devices during the process of pushing the models to the target displacement. Ultimately, for the ten story and the twenty story structures VD.L2 is having the minimum displacement and largest base shear. In addition, the behavior of the pushover curves in all circumstances is linear at the beginning which can be linked to the fact that the models are at the elastic stage which resulted in a linear elastic slop. But at the point when base shear exceeded beams and columns also the viscous and friction dampers in the structure yield to change the slop of the curves.

The target displacement values are calculated in accordance with FEMA 356 as shown in Table 8 until Table 10. Moreover, the target displacement value is increasing when number of story is getting higher and VD.L2 is having the lowest value of target displacement. Ultimately, the development of plastic hinges is dramatically influenced by the implementation of the damping devices where moment resistant frame has the highest number of plastic hinges. In contrast the addition of viscous dampers at the corner of the buildings prevented the formation of collapse prevention hinges. This is valid for all the analyzed cases.

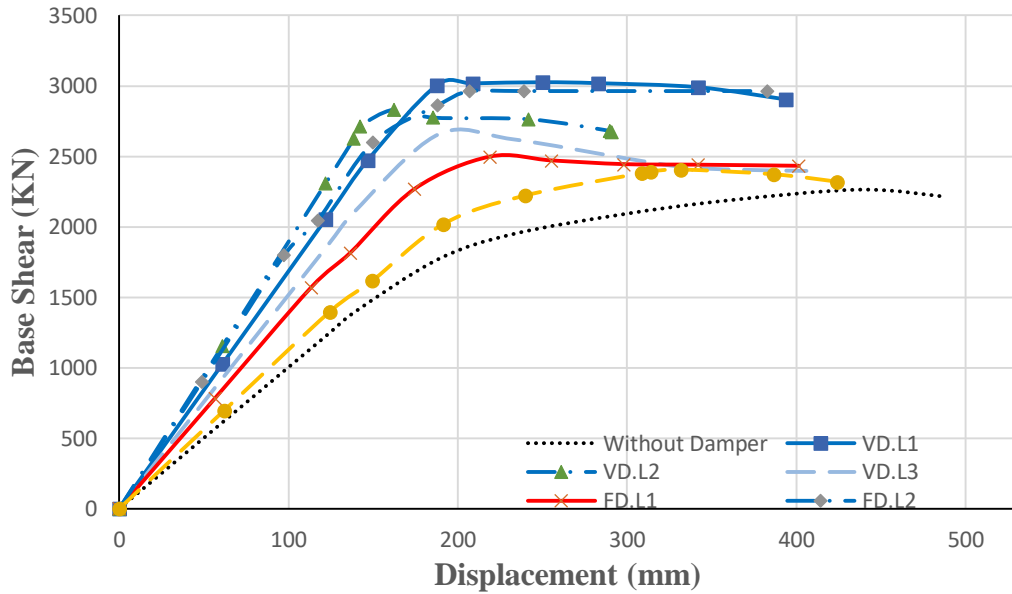


Figure 36: Capacity curves for 5-story steel building

Table 8: Target displacements obtained and number of hinges of 5-story steel building.

Modal Name	Target Displacement (mm)	Base shear (kN)	CP	LS	IO
Without dampers	487.861	2212.55	73	32	85
VD.L1	394.03	2903.14	0	7	26
VD.L2	291.08	2673.18	0	2	19
VD.L3	406.1	2395.04	2	21	40
FD.L1	401.64	2431.29	0	16	31
FD.L2	383.18	2964.42	0	6	29
FD.L3	424.27	2319.66	6	20	56

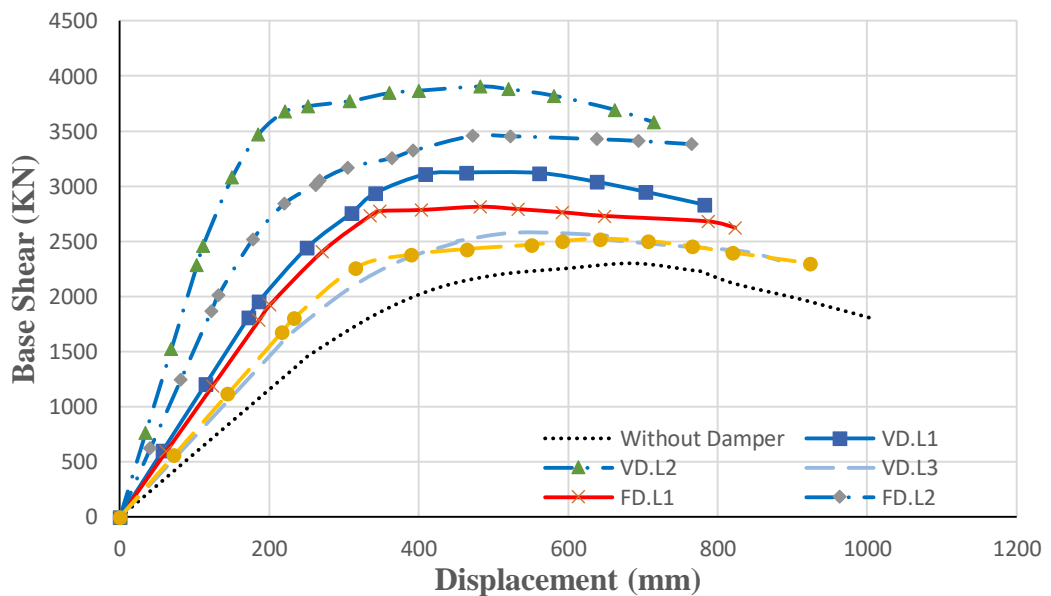


Figure 37: Capacity curves for 10-story steel building

Table 9: Target displacements obtained and number of hinges of 10-story steel building.

Modal Name	Target Displacement (mm)	Base shear (kN)	CP	LS	IO
Without dampers	1003.66	1806.38	160	60	115
VD.L1	782.64	2831.67	0	19	43
VD.L2	714.34	3582.5	0	5	31
VD.L3	881.47	2328.97	7	28	65
FD.L1	823.94	2623.31	0	22	51
FD.L2	765.32	3382.37	0	11	47
FD.L3	923.68	2298.17	14	26	91

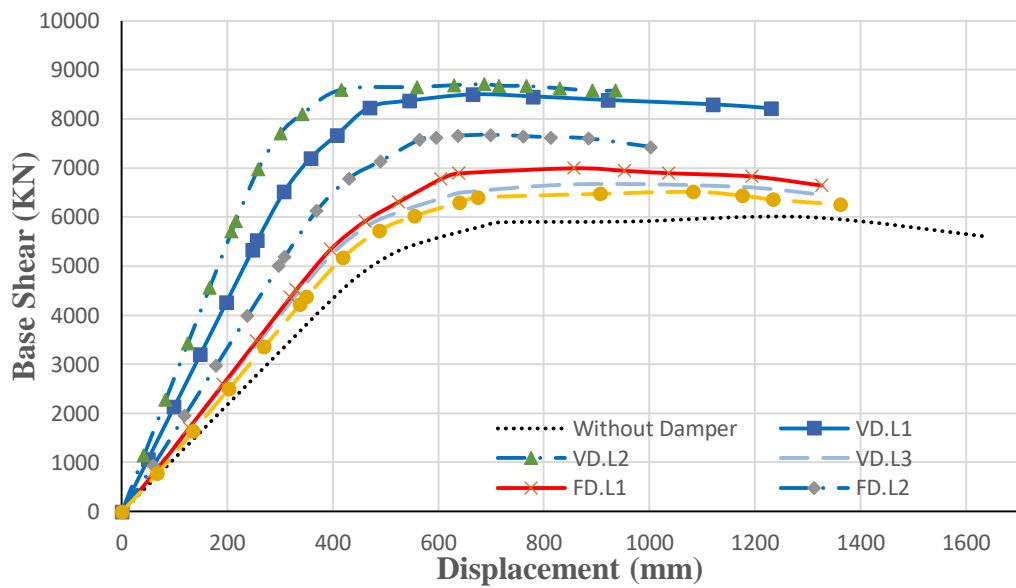


Figure 38: Capacity curves for 20-story steel building

Table 10: Target displacements obtained and number of hinges of 20-story steel building.

Modal Name	Target Displacement (mm)	Base shear (kN)	CP	LS	IO
Without dampers	1632.99	5612.36	239	90	172
VD.L1	1231.15	8214.63	4	25	65
VD.L2	936.31	8574.81	0	18	47
VD.L3	1321.66	6465.29	23	43	98
FD.L1	1326.9	6646.98	12	33	77
FD.L2	1003.18	7425.86	2	21	71
FD.L3	1362.64	6257.66	42	40	136



### **4.3 Time History Analysis Results**

This section of the research provides and discuss the results that have been obtained by using non-linear time history analysis.

#### **4.3.1 Base Shear**

The results of the analysis of all models show the base shear values in both X and Y directions when energy dissipation devices are placed in different locations in steel buildings compared to the models without dampers. In general, the base shear value decreased significantly for the models with viscous and friction dampers in both directions. However, the optimum reduction is observed for the models having the viscous dampers at the outer corner frames (L2). Also, when dampers are located at the frames between outer corner and outer mid-frames (L1) decreased the base shear magnitudes more than the outer mid-frame location (L3). On the other hand, viscous dampers gave less values of base shear than the friction dampers at all locations as shown in figure 39, figure 40 and figure 41. Also, an example of the nonlinear dynamic results (base shear Vs time) of 5 story steel building with friction dampers is illustrated by figure 42 and figure 43 in both directions respectively.

This improvement in the behavior of the steel buildings can be linked to the fact that dampers dissipate the delivered energy imposed by the seismic activity.

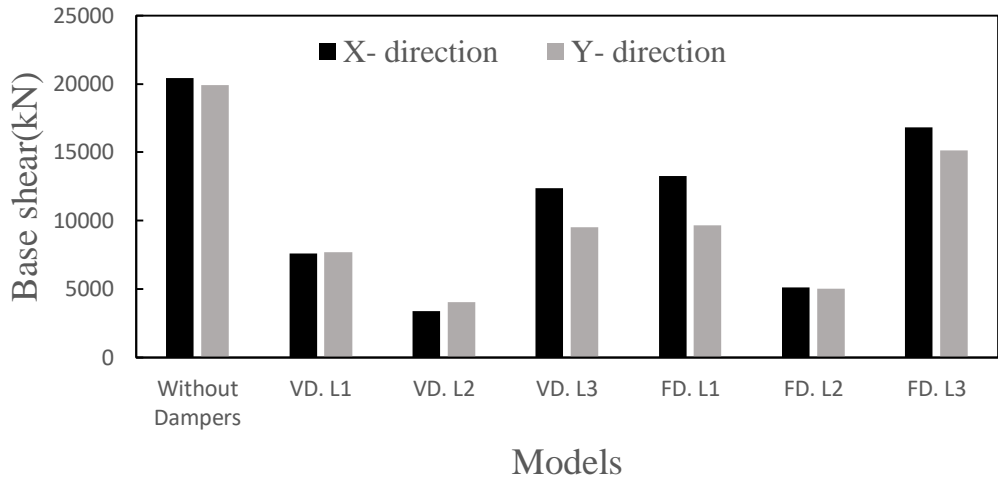


Figure 39: Base shear in X and Y directions for 5-story steel building

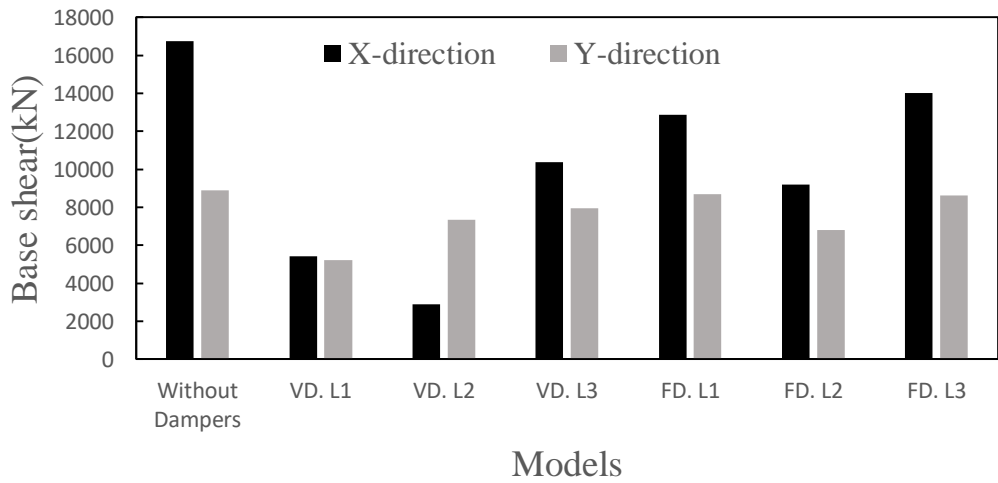


Figure 40: Base shear in X and Y directions for 10-story steel building

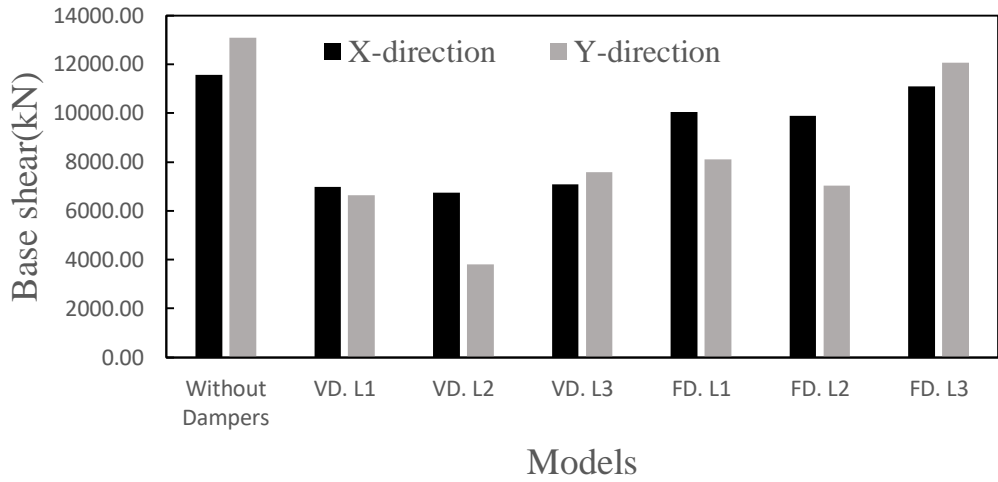


Figure 41: Base shear in X and Y directions for 20-story steel building

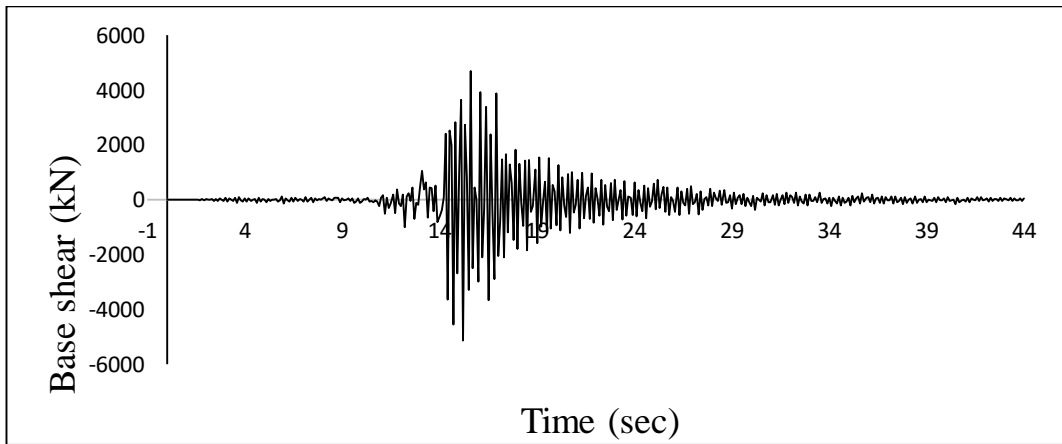


Figure 42: Base shear in X directions for 5-story steel building (FD.L2)

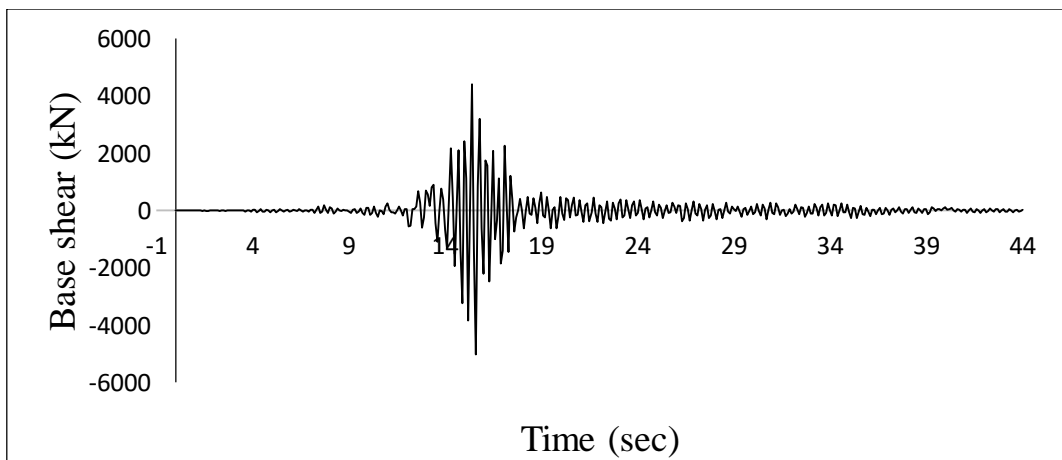


Figure 43: Base shear in Y directions for 5-story steel building (FD.L2)

Table 11: Reduction percentage of base shear force compared to the resisting moment frame.

Model Name	5-Story		10-Story		20-Story	
	(%) X	(%) Y	(%) X	(%) Y	(%) X	(%) Y
VD. L1	62.73	61.5	67.61	41.32	39.63	49.24
VD. L2	83.36	79.85	82.83	17.46	41.69	70.9
VD. L3	39.42	52.37	38.03	10.86	38.65	42.1
FD. L1	35.08	51.5	23.07	2.34	13.03	38.19
FD. L2	74.9	74.73	45.12	23.72	14.41	46.29
FD. L3	17.65	24.16	16.42	3.02	4.13	7.93

#### 4.3.2 Top Story Displacement

The time history analysis method of the steel structures provides that the models with energy dissipation devices have less roof displacement compared with moment resistant frame models since its ductility is high. On the other hand, the least displacement is resulted in the models that include viscous dampers at its outer corner frames (L2) which show that this location of viscous dampers provides the highest lateral stiffness to the structure. However, the reduction of displacement is more for the models having dampers at L1 than L3 as shown in Figure 44, Figure 45 and Figure 46. Also, an example of the nonlinear dynamic results (displacement Vs time) of 5 story steel building with viscous dampers is illustrated by figure 47 and figure 48 in both directions respectively.

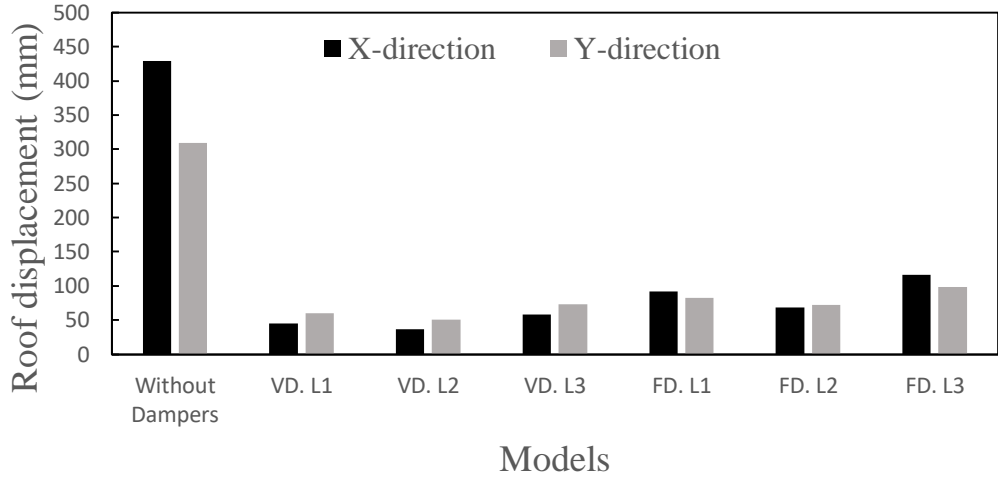


Figure 44: Roof displacement in X and Y directions for 5-story steel building

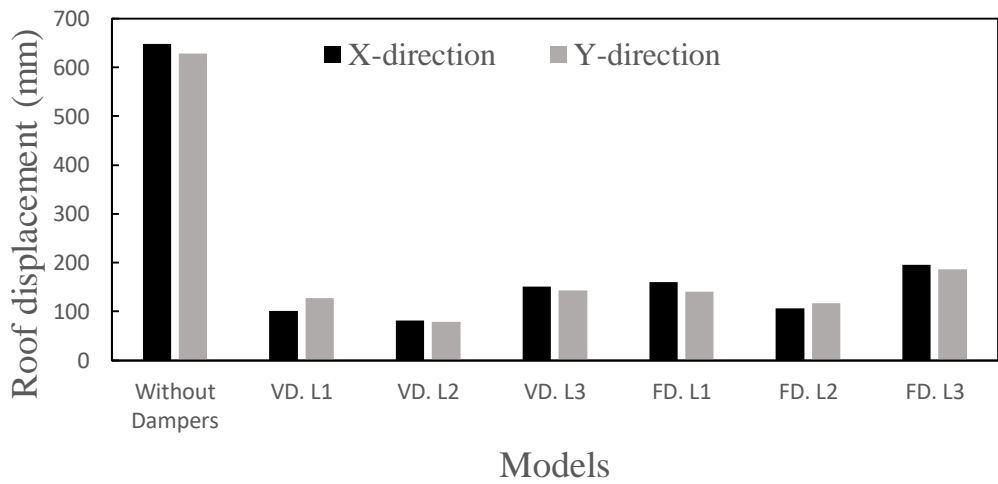


Figure 45: Roof displacement in X and Y directions for 10-story steel building

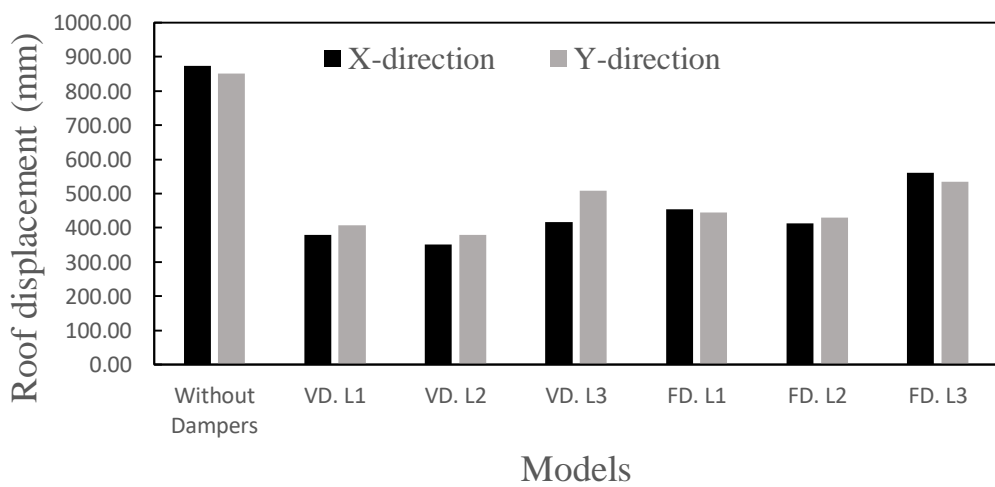


Figure 46: Roof displacement in X and Y directions for 20-story steel building

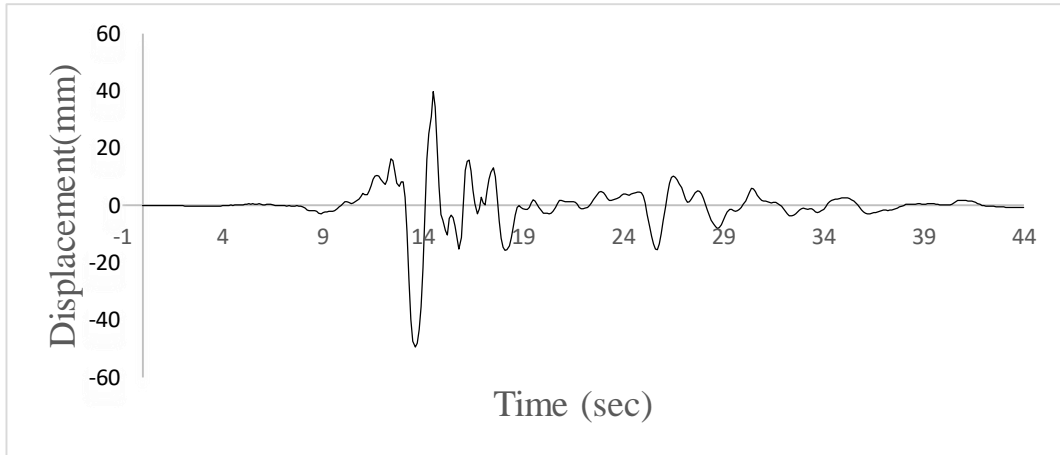


Figure 47: Displacement in X direction for 5-story steel building (VD.L2)

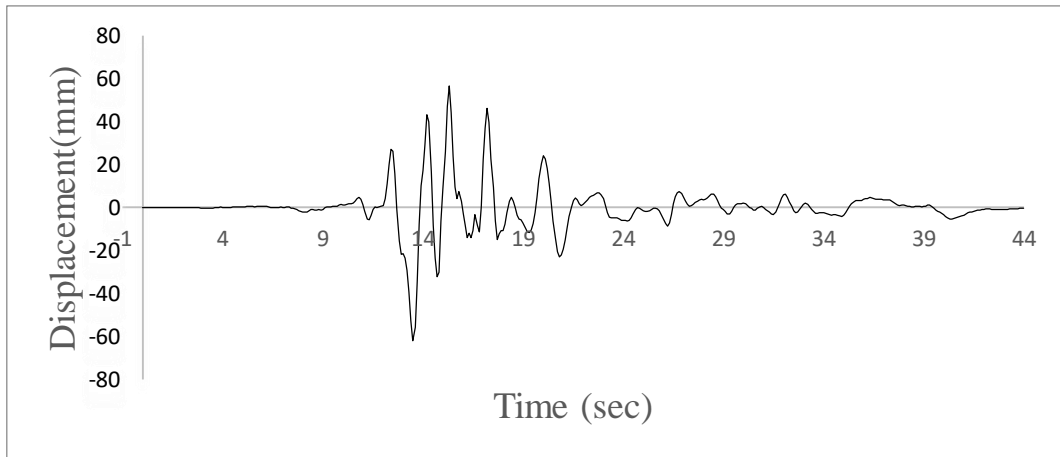


Figure 48: Displacement in Y direction for 5-story steel building (VD.L2)

Table 12: Reduction percentage of roof displacement compared to the resisting moment frame.

Model Name	5-Story		10-Story		20-Story	
	(%) X	(%) Y	(%) X	(%) Y	(%) X	(%) Y
VD. L1	89.46	80.53	84.37	79.72	73.42	68.19
VD. L2	91.46	83.68	88.37	87.37	77.52	72.5
VD. L3	86.53	76.39	76.68	77.21	67.73	52.6
FD. L1	78.61	73.46	75.19	77.72	63.62	62.28
FD. L2	83.95	76.67	83.56	81.29	68.46	64.75
FD. L3	72.92	68.19	69.75	70.32	46.49	48.48

### 4.3.3 Story Drift

The inconsistency of story drift ratio is clearly discovered by the results of the analyzed models. Also, multi curvature plots are shown by the moment resistant frames since the cross-sections of columns differs along the elevation of the structures at the design process. However, the least value of the story drift ratio is occurring at the top story of each model. This can be linked to the fact that lateral story forces are lower near the roof than the base of the structural system. In addition, the support fixities are leading the story drift to be low at the base. Ultimately, VD.L2 system showed the lowest value of inter story drift among all modeled systems. This is observed from all cases which have been analyzed. This can be obviously found in figures between Figure 49 until Figure 54.

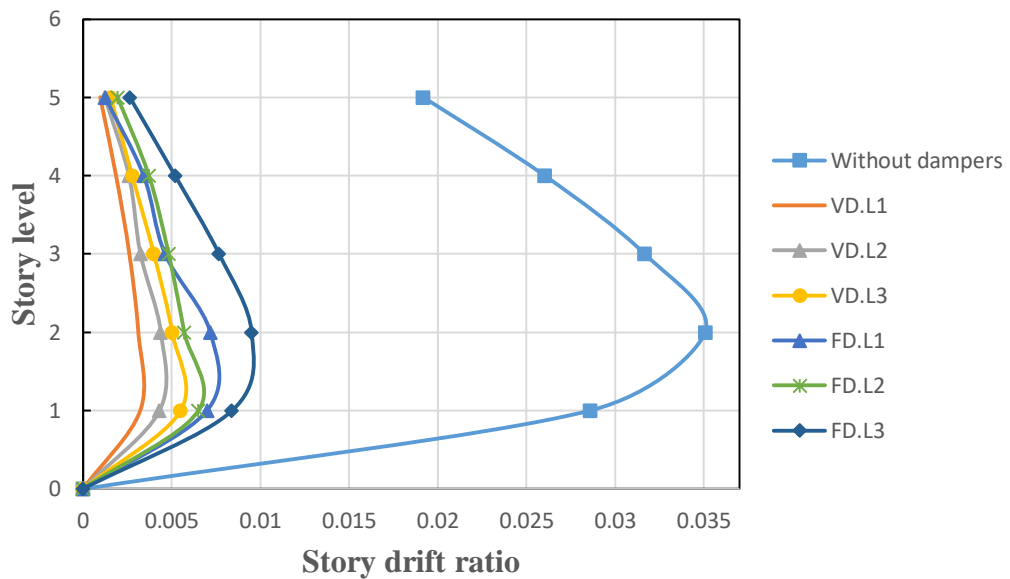


Figure 49: Story drift in X direction for 5-story steel building

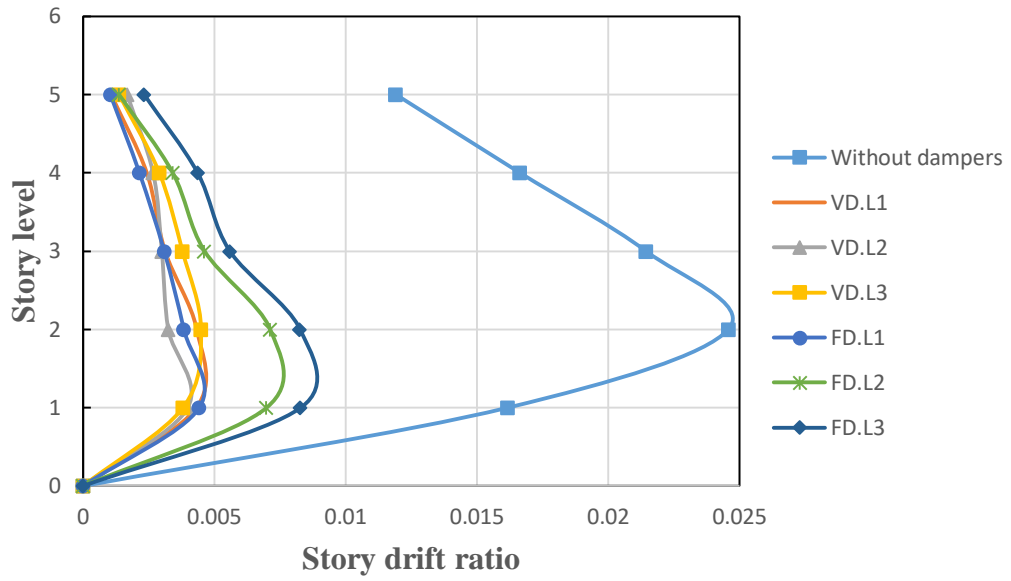


Figure 50: Story drift in Y direction for 5-story steel building

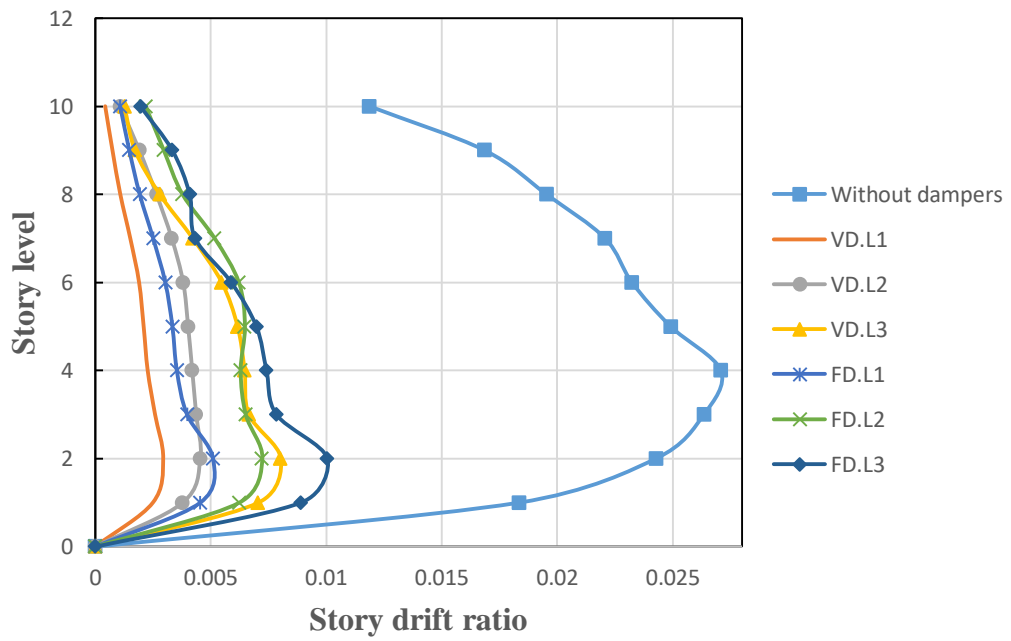


Figure 51: Story drift in X direction for 10-story steel building



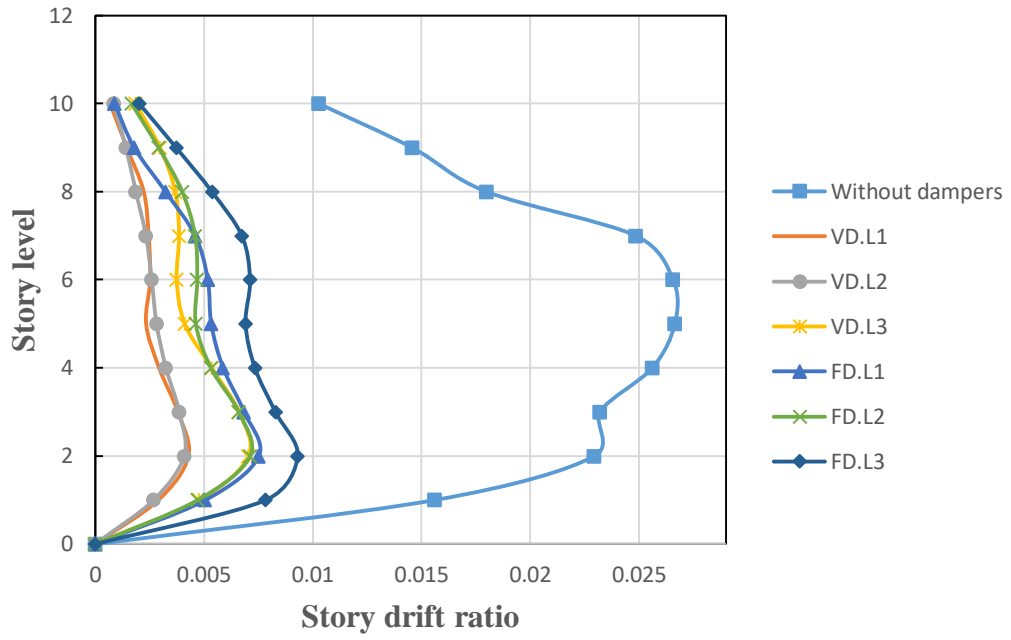


Figure 52: Story drift in Y direction for 10-story steel building

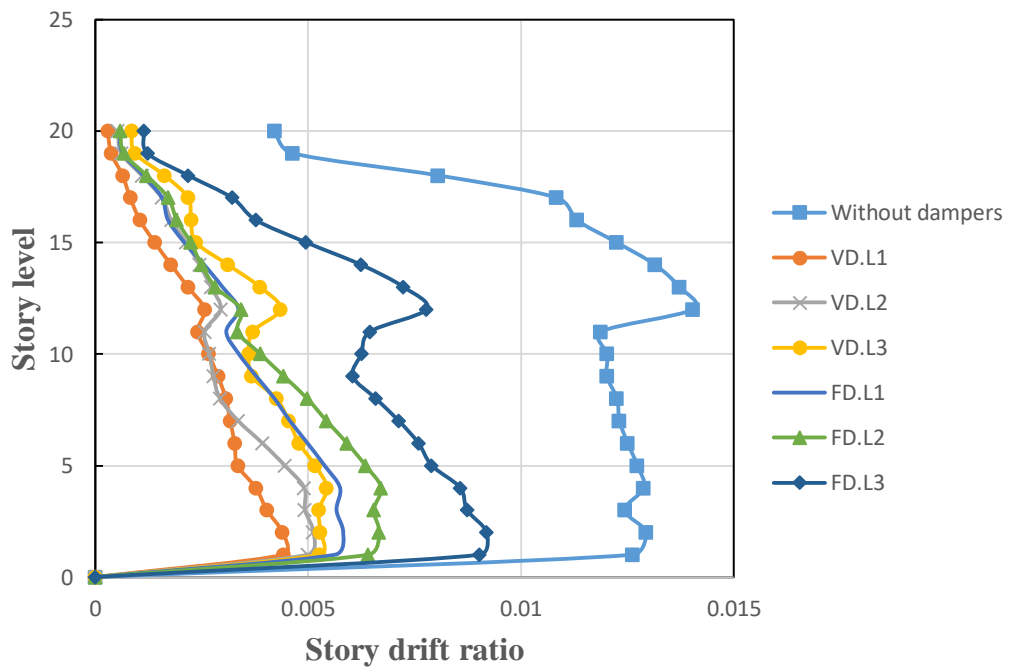


Figure 53: Story drift in X direction for 20-story steel building

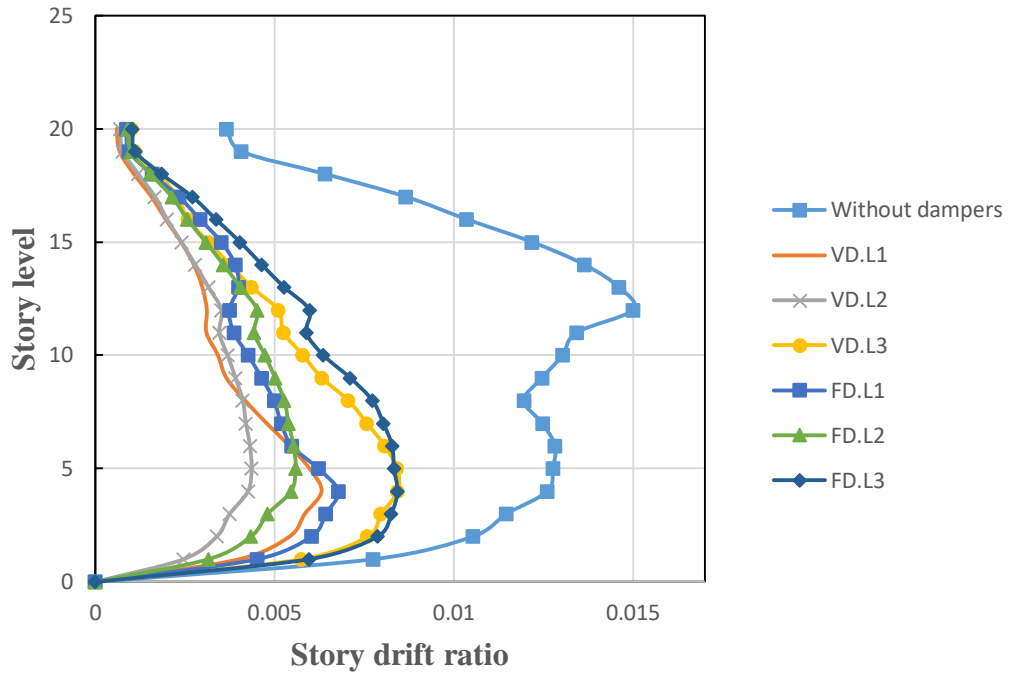


Figure 54: Story drift in Y direction for 20-story steel building

#### 4.3.4 Performance Level

The building performance is evaluated in accordance with ASCE41-17 from the nonlinear time history analysis where the maximum results obtained from three different records are used to calculate the demand capacity ratio. The calculation is done using ETABS2017 package which can perform performance check automatically. An example of the obtained result for the 5 story building is presented in Figures 55-60. Results indicate that moment resistant frame has the least performance where it yields collapse prevention performance for 5,10 and 20 story. On the other hand, viscous dampers at the corner of the building resulted in the best performance where it yields immediate occupancy for the 5 and 10 story and life safety for the 20 story building. This can be linked to the low number of plastic hinges developed upon the implementation of the viscous damping devices. The summary of the building performance is presented in Table 13.

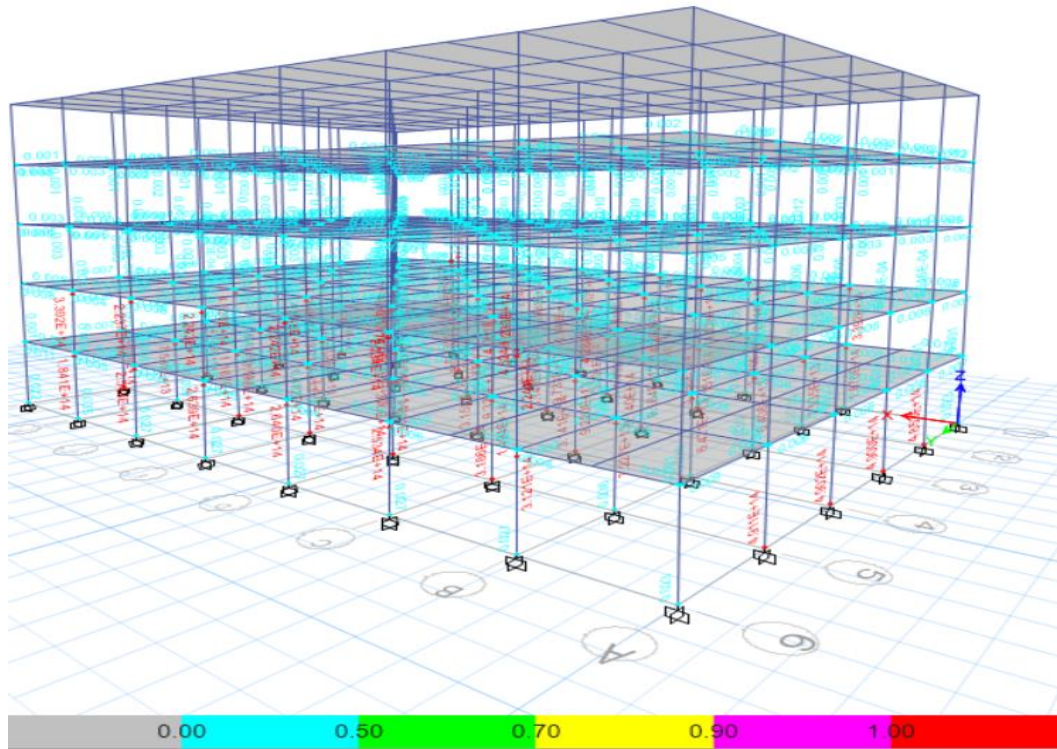


Figure 55: Performance check of MRF for 5-story steel building

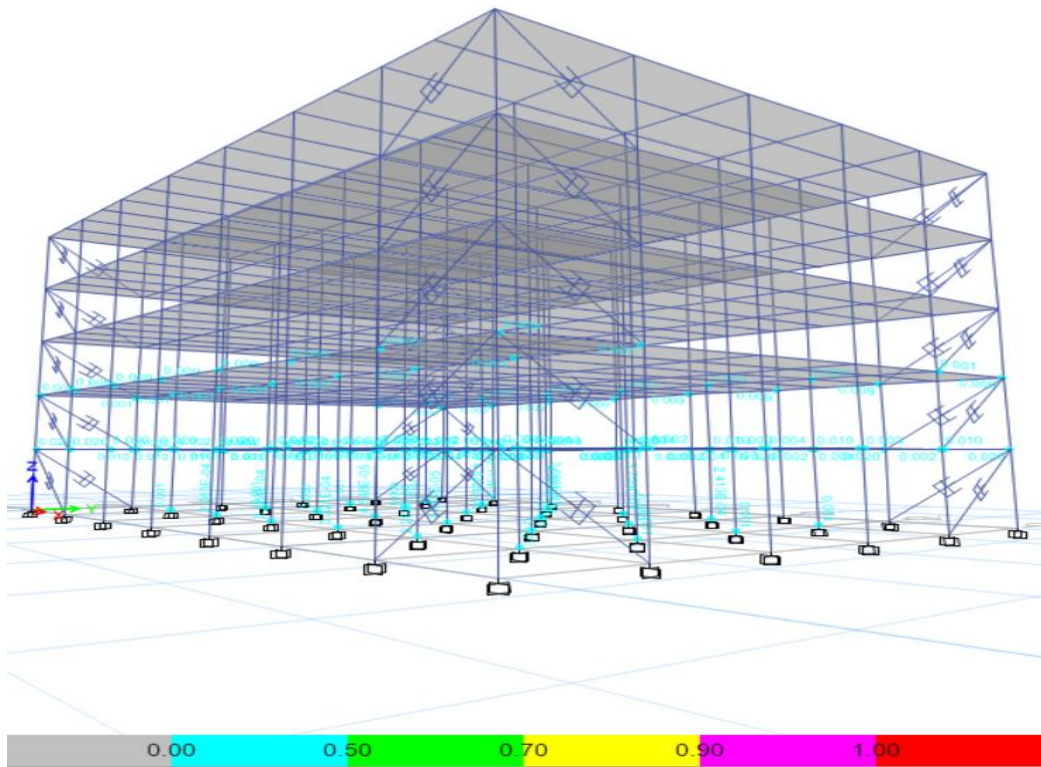


Figure 56: Performance check of VD.L2 for 5-story steel building

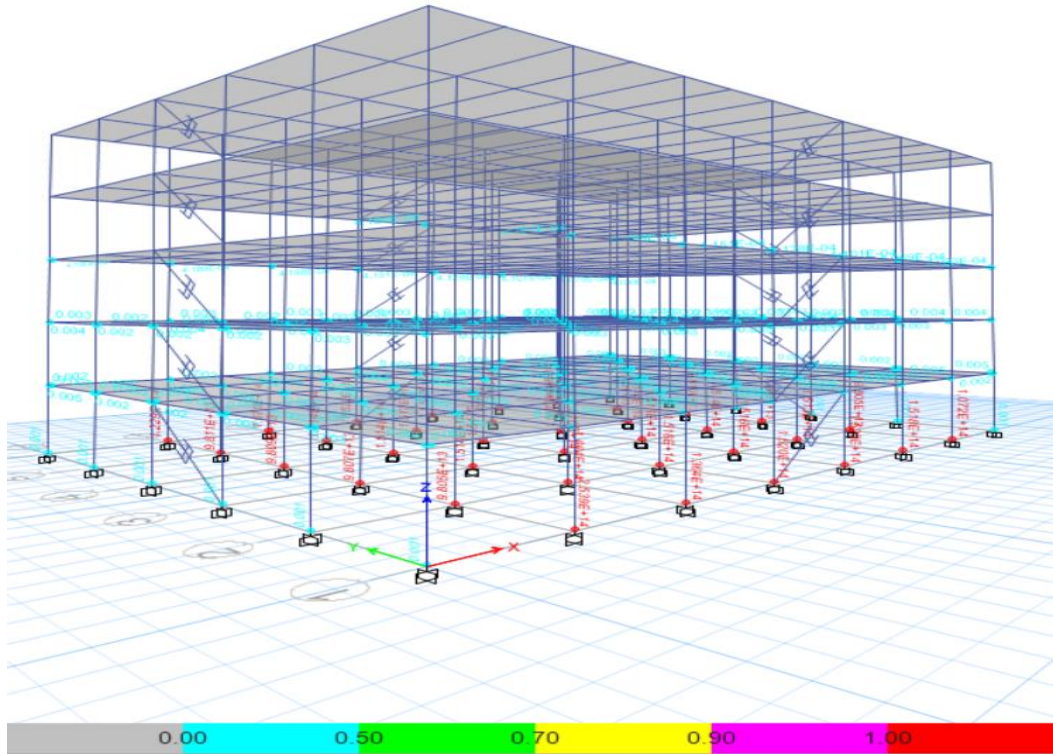


Figure 57: Performance check of VD.L3 for 5-story steel building

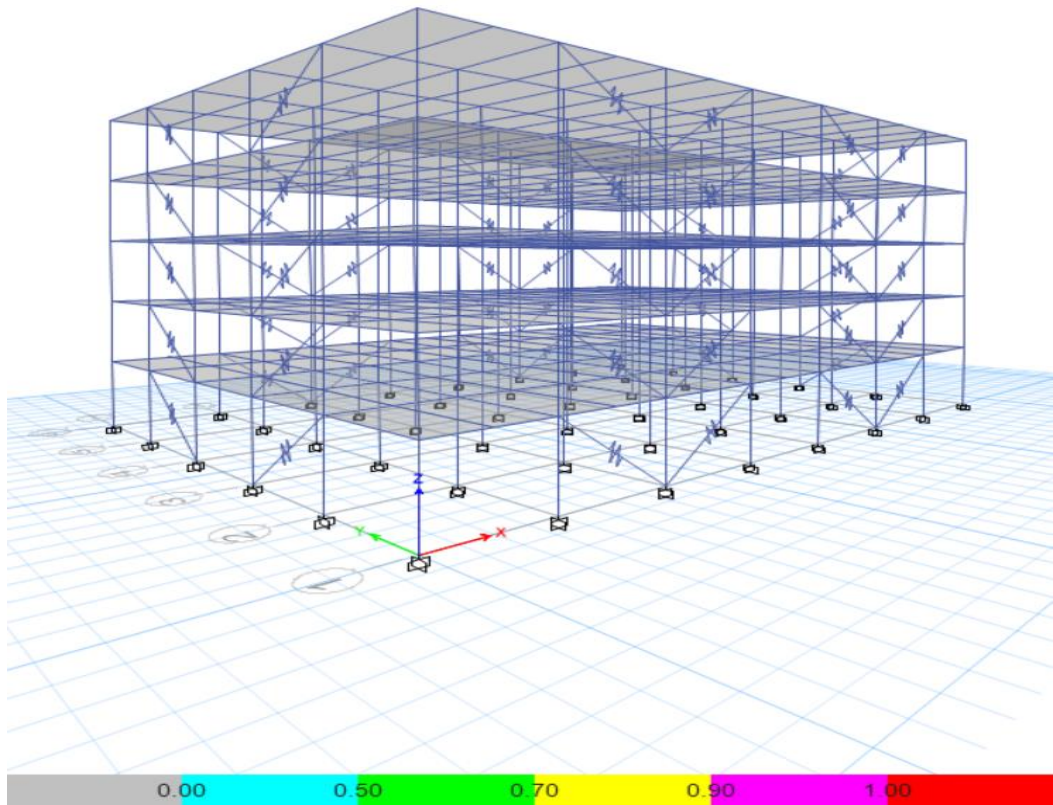


Figure 58: Performance check of FD.L1 for 5-story steel building



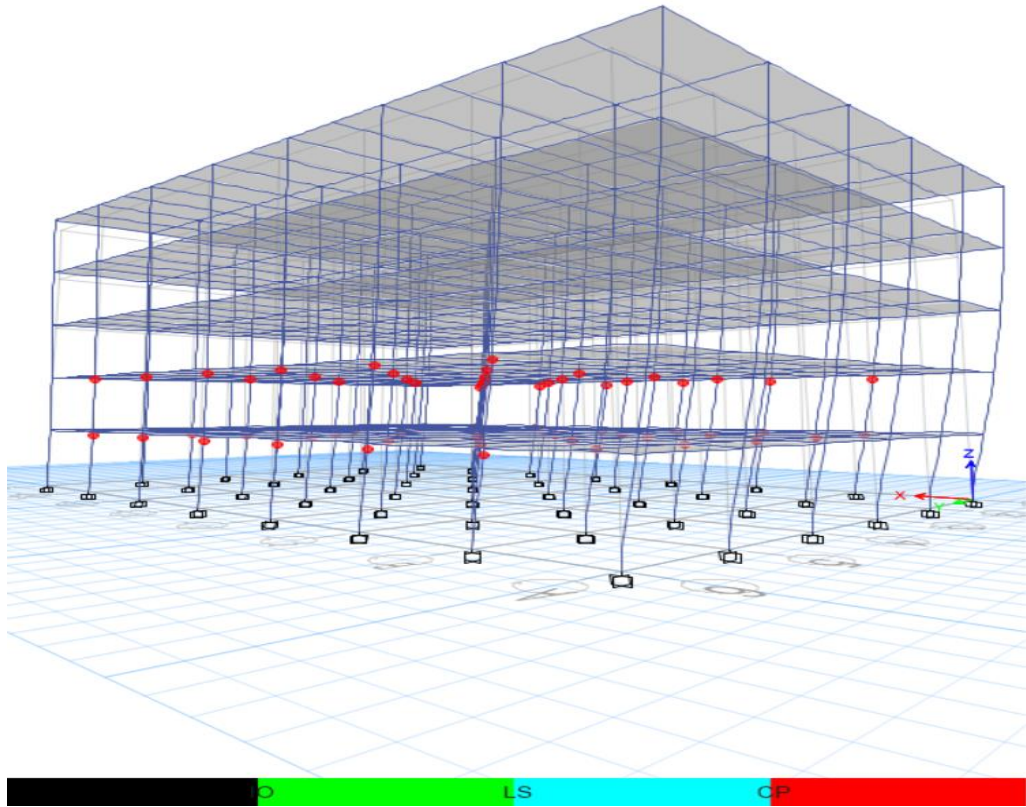


Figure 59: Collapse stage of plastic hinges of MRF 5-story steel building

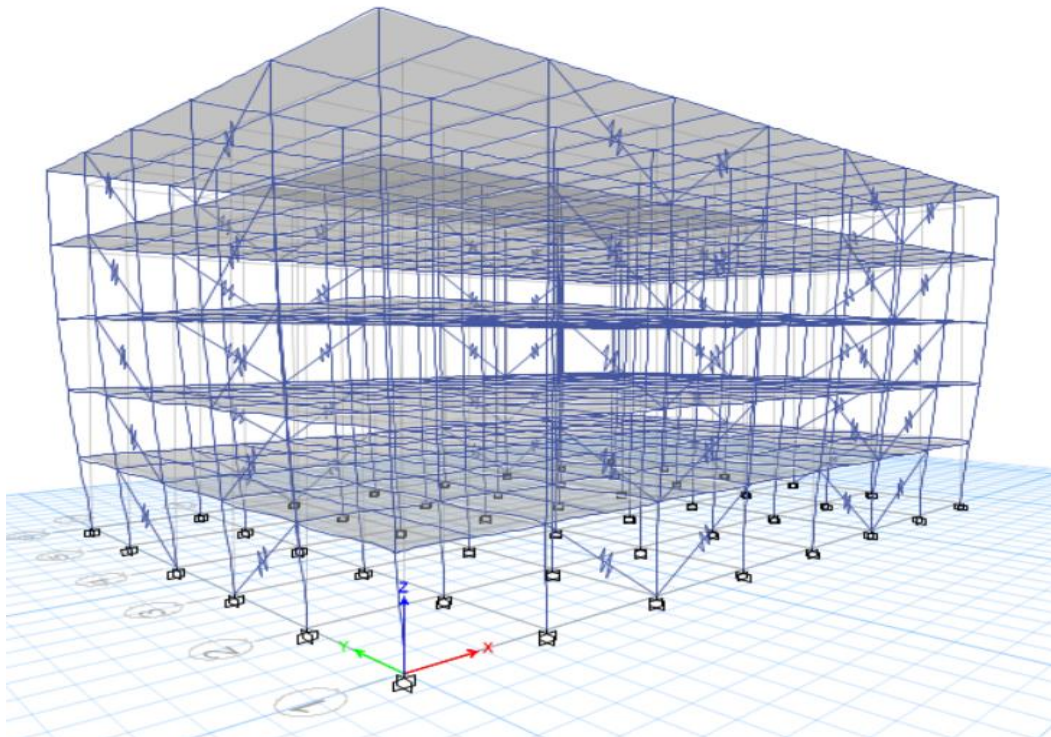


Figure 60: immediate occupancy stage of plastic hinges of FD.L1 5-story steel building

Table 13: Performance level of all modals (ETABS 2017)

Modal Name	5-Story	10-Story	20-Story
Without damper	collapse prevention	collapse prevention	collapse prevention
VD.L1	immediate occupancy	life safety	life safety
VD.L2	immediate occupancy	immediate occupancy	life safety
VD.L3	collapse prevention	collapse prevention	collapse prevention
FD.L1	immediate occupancy	life safety	life safety
FD.L2	immediate occupancy	life safety	life safety
FD.L3	collapse prevention	collapse prevention	collapse prevention

#### 4.3.5 Energy Component

During earthquake, portion of the seismic activity is transmitted to the structure causing increase in the kinetic and potential energy. Usually this energy is dissipated in the form of heat. However, under sever excitation part of the energy is transmitted through the hysteretic action (unrecoverable deformations of the structural elements). The nonlinear time history analysis indicates that structure unequipped with damping devices has very high kinetic and strain (potential) energy compared with the other systems. In addition, the energy absorbed by the moment resistant frame systems is mainly dissipated through the strain and hysteretic actions. Unlike the other system where dampers dissipate most of the delivered energy through the non-linear viscous damping and non-linear hysteretic damping. It is worth to mention that viscous dampers placed at the outer corner of the building (VDL2) has higher kinetic energy rather than potential energy which can be linked to the fact that these systems showed the least strain (displacement) compared with the other systems under the considered

ground motion records. This can be clearly observed in all analyzed cases throughout the Figures 61-63.

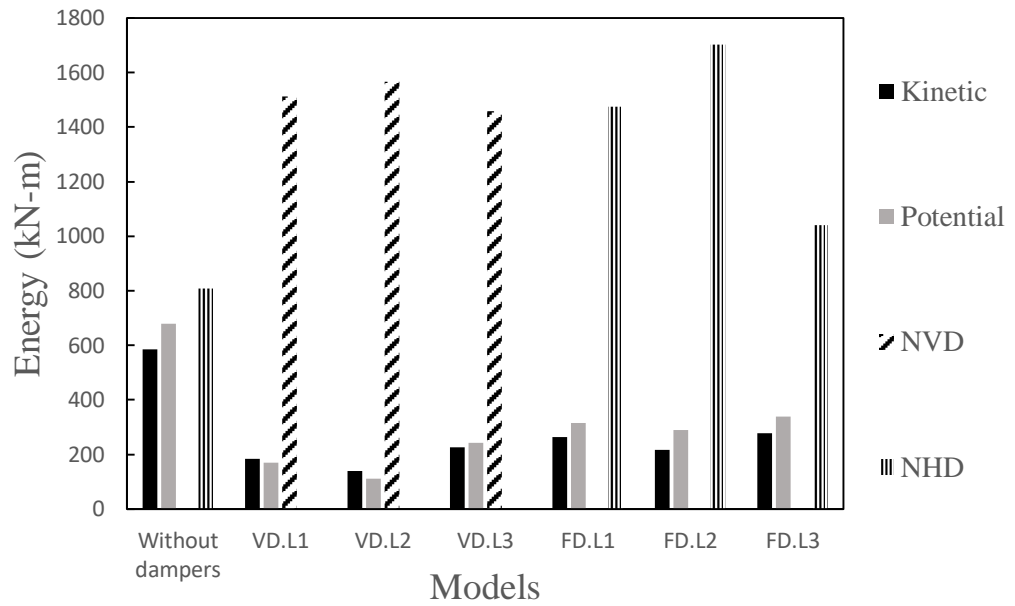


Figure 61: Energy component for 5-story steel building

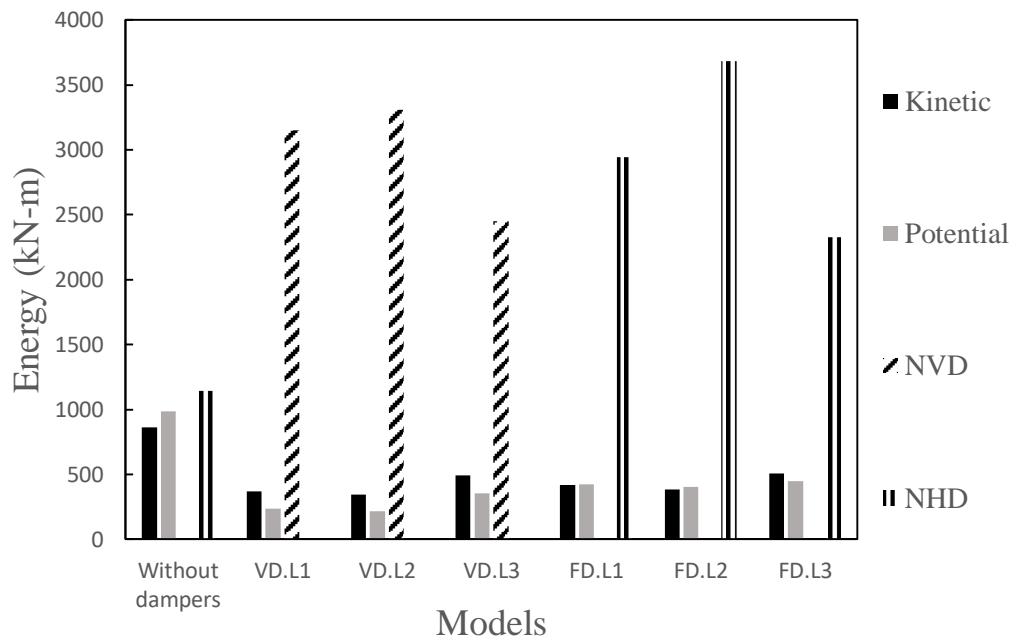


Figure 62: Energy component for 10-story steel building

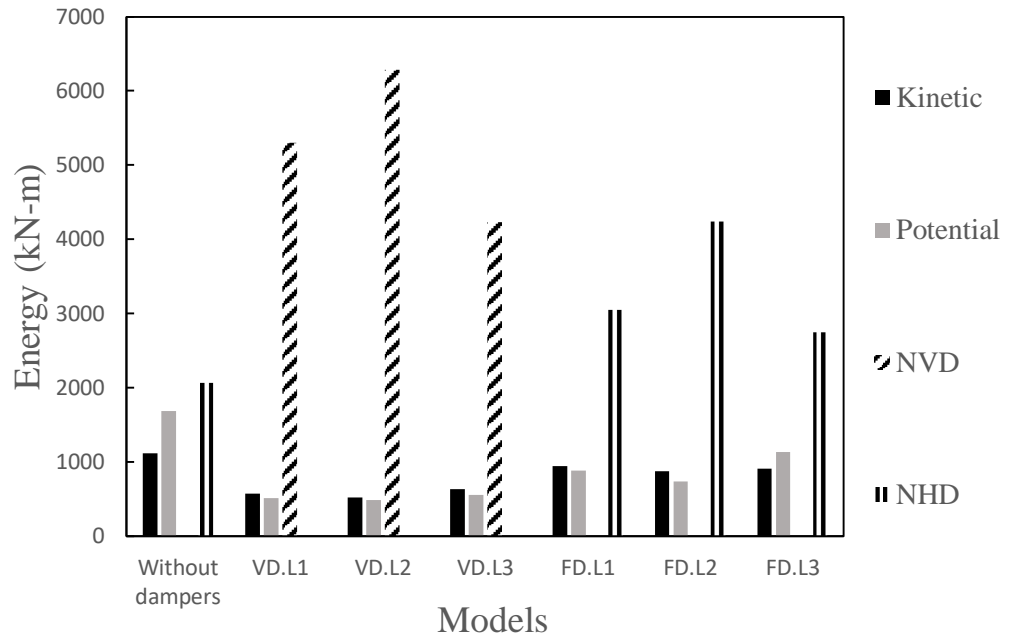


Figure 63: Energy component for 20-story steel building



## Chapter 5

# CONCLUSION AND RECOMMENDATIONS FOR FUTURE STUDIES

### 5.1 Conclusion

The aim of this research is to evaluate the behavior of steel framed building equipped with energy dissipating devices including both viscous and friction dampers. Where steel framed structure with different story number (5, 10 and 20) is analyzed through nonlinear pushover and time history analysis. The optimum location of the damper is also investigated. The obtained result of both nonlinear static pushover analysis and the nonlinear time history are summarized as follow;

- Initial lateral stiffness is highly influenced by the addition of dampers where initial lateral stiffness increased significantly. The best performance is observed for the viscous damper placed at the outer corners of the structure.
- The yield strength of buildings equipped with viscous damper is significantly greater than the other system.
- Ductility of the moment resistant frame is reduced upon the implementation of damping devices. Since damping devices have lower displacement compared with the moment resistant frames.
- The base shear results obtained by the nonlinear time history indicates a tremendous loss of the base shear for the models equipped with viscous and friction dampers along both orthogonal directions where the maximum

reduction is 83.36% compared to the moment resisting frame. The optimum reduction is observed for the models having the viscous dampers at the outer corner frames (L2).

- The implementation of energy dissipation devices dramatically reduced both of story displacement and drift especially building equipped with viscous dampers at the outer corners frames and most reduction value is 91.46% compared to the moment resisting frame.
- The seismic performance of the structure significantly enhanced upon the addition of damping devices especially viscous dampers placed at the outer corner of the structure, where the performance is altered from collapse prevention to immediate occupancy level.
- The energy delivered to the structure is mainly observed and dissipated by the equipped damping devices. Unlike the moment resistant frame where most of it is transmitted energy is dissipated through strain and hysteric actions.

## **5.2 Recommendations for Future Studies**

- Experimental model to validate the analysis results would add to the value of this research.
- Only one plan geometry is studied where different plans may result in different behavior.
- Irregularities along both plan and elevation is not studied.
- Trying combination of both viscous and friction dampers is not presented.
- The Site class parameter in calculating the earthquake force and spectra is fixed within this research. Hence, studies on the alteration of soil classes may yield a different outcome.

## REFERENCES

- Applied Technology Council (1996). "Seismic Evaluation and Retrofit of Reinforced Concrete Buildings", Report ATC 40 / SSC 96-01, Palo Alto.
- ASCE-41-17. (2017). ASCE Standard, ASCE/SEI, 41-17: Seismic Evaluation and Retrofit of Existing Buildings. Reston, VA: American Society of Civil Engineers.
- ASCE (2000). "FEMA 356 Prestandard and Commentary for the Seismic Rehabilitation of Buildings", ASCE for the Federal Emergency Management Agency, Washington, D.C., November 2000.
- Becker, J., & Gaul, L. (2007). Semi-active control of adaptive friction dampers for structural vibration control. In 25th IMAC (Vol. 78, p. 86).
- Constantinou, M. C., Soong, T. T., & Dargush, G. F. (1998). Passive energy dissipation systems for structural design and retrofit.
- CSI Analysis Reference Manual. (2013). CSI Analysis Reference Manual for SAP2000®, ETABS®, SAFE® and CSiBridge®
- CEN (European Committee for Standardization). (2005). Design of steel structures . Part 1-1: General rules and rules for buildings. EN 1993-1-1: 2005: E, incorporating corrigendum February 2006.

- Constantinou, M. C., and Symans, M. D. (1992). "Experimental investigation of seismic response of structures with supplemental fluid viscous dampers." National Center for Earthquake Engineering Research Rep. No. NCEER-92-0032, State Univ. of New York at Buffalo, Buffalo, N.Y
- Dehghan, M. J., & Soleymannejad, M. (2015). Improving Seismic Performance of Concrete Buildings with Special Moment Frames Using Viscous Damper. *International Journal of Modern Engineering Research*, 5(7).
- Dimopoulos, A. I., Tzimas, A. S., Karavasilis, T. L., & Vamvatsikos, D. (2016). Probabilistic economic seismic loss estimation in steel buildings using post-tensioned moment-resisting frames and viscous dampers. *Earthquake Engineering & Structural Dynamics*, 45(11), 1725-1741.
- Fridley, K. J. *Structural Engineering Handbook* Ed. Chen Wai-Fah Boca Raton: CRC Press LLC, 1999.
- Hakimi, B. E., Rahnavard, A., & Honarbaksh, T. (2004, August). Seismic design of structures using friction damper bracings. In 13th world conference on earthquake engineering, Vancouver.
- Hamidia, M., Filiatrault, A., & Aref, A. (2014). Seismic Collapse Capacity-Based Evaluation and Design of Frame Buildings with Viscous Dampers Using Pushover Analysis. *Journal of Structural Engineering*, 141(6), 04014153.

- Inel, M., & Ozmen, H. B. (2006). Effects of plastic hinge properties in nonlinear analysis of reinforced concrete buildings. *Engineering structures*, 28(11), 1494-1502.
- Jung, S. N., Nagaraj, V. T., & Chopra, I. (2001). Refined structural dynamics model for composite rotor blades. *AIAA journal*, 39(2), 339-348.
- Lee, D. and D. P. Taylor-2001. "Viscous Damper Development and Future Trends". *The Structural Design of Tall Buildings*. Vol. 10, No. 5, pp. 311-320.
- Kim, J., Lee, J., & Kang, H. (2016). Seismic retrofit of special truss moment frames using viscous dampers. *Journal of Constructional Steel Research*, 123, 53-67.
- Kang, J. D., & Mori, Y. (2017). Simplified estimation method of inelastic seismic demands of buildings with seesaw system using fluid viscous dampers. *Engineering Structures*, 138, 120-130.
- Miyamoto, H. K., Gilani, A. S., & Wada, A. (2012). The Effectiveness of Viscous Dampers for Structures Subjected to Large Earthquakes. In *Proceedings of the 15th World Congress on Earthquake Engineering*.
- Mualla, I. H., & Belev, B. (2002). Performance of steel frames with a new friction damper device under earthquake excitation. *Engineering Structures*, 24(3), 365-371.

Miyamoto, H. K., Gilani, A. S., Wada, A., & Ariyaratana, C. (2011). Identifying the collapse hazard of steel special moment-frame buildings with viscous dampers using the FEMA P695 methodology. *Earthquake Spectra*, 27(4), 1147-1168.

Pacific Earthquake Engineering Research Center. (n.d.). Retrieved from <https://peer.berkeley.edu/>

Pinho, R. (2007). An adaptive capacity spectrum method for assessment of bridges subjected to earthquake action. *Bulletin of Earthquake Engineering*, 5(3), 377-390.

Ribakov, Y. (2004). Semi-active predictive control of non-linear structures with controlled stiffness devices and friction dampers. *The Structural Design of Tall and Special Buildings*, 13(2), 165-178.

Ras, A., & Boumechra, N. (2016). Seismic energy dissipation study of linear fluid viscous dampers in steel structure design. *Alexandria Engineering Journal*, 55(3), 2821-2832.

Reinhorn, A. M., Li, C., and Constantinou, M. C. 1995. "Experimental and analytical investigation of seismic retrofit of structures with supplemental damping. Part1: Fluid viscous damping devices." National Center for Earthquake Engineering Research Rep. No. NCEER95-0001, State Univ. of New York at Buffalo, Buffalo, N.Y.

Saghafi, M. H., Movehedin, S. A. E., & Golafshar, A. (2016). Application of Viscous Dampers in Seismic Rehabilitation of Steel Moment Resisting Frames. In MATEC Web of Conferences (Vol. 67, p. 03054). EDP Sciences.

Seleemah, A. A., and Constantinou, M. C. (1997). "Investigation of seismic response of buildings with linear and nonlinear fluid viscous dampers." National Center for Earthquake Engineering Research Rep. No. NCEER-97-0004, State Univ. of New York at Buffalo, Buffalo, N.Y.

Seneviratna, G. D. P. K., & Krawinkler, H. (1996). Modifications of seismic demands for MDOF systems. In Proceedings of 11th World Conference on Earthquake Engineering, Acapulco, Mexico.

Turkey Ministry of Interior Disaster and Emergency Management Authority. (n.d.). Homepage - AFAD Republic of Turkey Ministry of Interior Disaster and Emergency Management Authority. Retrieved from <https://www.afad.gov.tr/en/4298/Homepage>

Turkish Earthquake Code.TEC. Regulations on Structures Constructed in Disaster Regions, Ministry of Public Works and Settlement, Ankara, 2018.

Turkish design load code. TS-498; Design Loads For Buildings, TSE, Ankara, 1987.  
Turkish design load code

Tokuda, Y., & Taga, K. (2008, January). A case of structural design in which viscous dampers are used to enhance earthquake resisting performance of building . In 14th World Conference on Earthquake

Tzimas, A. S., Kamaris, G. S., Karavasilis, T. L., & Galasso, C. (2016). Collapse risk and residual drift performance of steel buildings using post-tensioned MRFs and viscous dampers in near-fault regions. *Bulletin of Earthquake Engineering*, 14(6), 1643-1662.

Whittle, J. K., Williams, M. S., Karavasilis, T. L., & Blakeborough, A. (2012). A comparison of viscous damper placement methods for improving seismic building design. *Journal of Earthquake Engineering*, 16(4), 540-560.

Wang, S., & Mahin, S. A. (2017). Seismic retrofit of a high-rise steel moment-resisting frame using fluid viscous dampers. *The Structural Design of Tall and Special Buildings*, 26(10), e1367.

Zhou, Y., & Li, H. (2014). Analysis of a high-rise steel structure with viscous damped outriggers. *The Structural Design of Tall and Special Buildings*, 23(13), 963-979.



## **APPENDICES**

## Appendix A: Properties of Slab Deck and Materials

Table 1.1: Tensile strength and yield strength of steel grades.

Steel Grade	Tensile Strength (MPa)	Yield Strength (MPa)
S235	510	235
S275	530	275
S355	630	355

Table 1.2: Material properties.

Property	S275	C25/30
Mass / unit volume	7850 kg/m <sup>3</sup>	2550 kg/m <sup>3</sup>
Weight / unit volume	77 kN/m <sup>3</sup>	25 kN/m <sup>3</sup>
Poisson's ratio	0.3	0.2
Shear Modulus	80770 N/mm <sup>2</sup>	13000 N/mm <sup>2</sup>
Modulus of Elasticity	210000 N/mm <sup>2</sup>	31000 N/mm <sup>2</sup>

Table 1.3: Properties of slab deck (70/915).

Slab depth	70 mm
Rip width top	210 mm
Rip width bottom	104 mm
Rip depth	60 mm
Rip spacing	305 mm
Unit weight of the deck	0.11 kN/m <sup>2</sup>
Shear thickness of the deck	1.2 mm
Shear stud tensile strength	400 N/mm <sup>2</sup>
Shear stud diameter	19 mm
Shear stud height	150 mm

## Appendix B: Properties of Response Spectrum



# Türkiye Deprem Tehlike Haritaları İnteraktif Web Uygulaması

## Kullanıcı Girdileri

Rapor Başlığı:	duzce	
Deprem Yer Hareketi Düzeyi	DD-1	50 yılda aşılma olasılığı %2 (tekrarlanma periyodu 2475 yıl) olan deprem yer hareketi düzeyi
Yerel Zemin Sınıfı	ZB	Az ayrışmış, orta sağlam kayalar
Enlem:	40.835299°	
Boylam	31.180848°	

## Çıktılar

$S_s = 2.380$        $S_1 = 0.645$        $PGA=0.933$        $PGV=60.469$

$S_s$  : Kısa periyot harita spektral ivme katsayısı [boyutsuz]

$S_1$  : 1.0 saniye periyot için harita spektral ivme katsayısı [boyutsuz]

$PGA$  : En büyük yer ivmesi [g]

$PGV$  : En büyük yer hızı [cm/sn]

Figure 2.1: Properties of response spectrum for 2% accuracy

# Türkiye Deprem Tehlike Haritaları İnteraktif Web Uygulaması

## Kullanıcı Girdileri

---

Rapor Başlığı:	duzce	
Deprem Yer Hareketi Düzeyi	DD-2	50 yılda aşılma olasılığı %10 (tekrarlanma periyodu 475 yıl) olan deprem yer hareketi düzeyi
Yerel Zemin Sınıfı	ZB	Az ayrılmış, orta sağlam kayalar
Enlem:	40.835299°	
Boylam	31.180848°	

## Çıktılar

---

$S_5 = 1.344$        $S_1 = 0.365$        $PGA = 0.552$        $PGV = 35.460$

$S_5$  : Kısa periyot harita spektral ivme katsayısı [boyutsuz]

$S_1$  : 1.0 saniye periyot için harita spektral ivme katsayısı [boyutsuz]

$PGA$  : En büyük yer ivmesi [g]

$PGV$  : En büyük yer hızı [cm/sn]

Figure 2.2: Properties of response spectrum for 10% accuracy

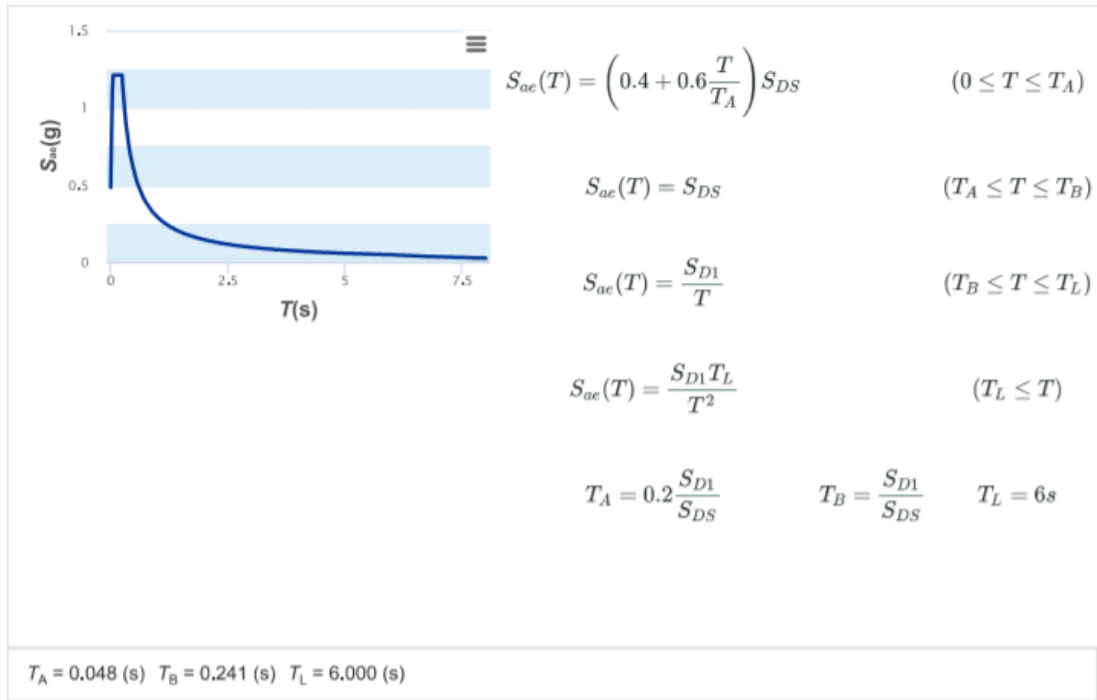


Figure 2.3: Horizontal elastic design spectrum

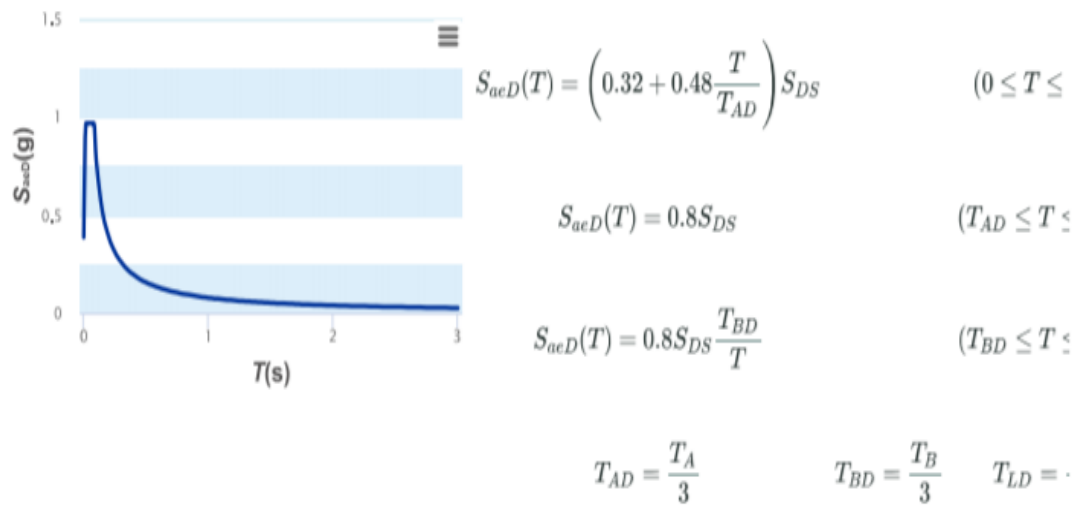


Figure 2.4: Vertical elastic design spectrum

## Appendix C: Ground Motion Records and Spectral Matching

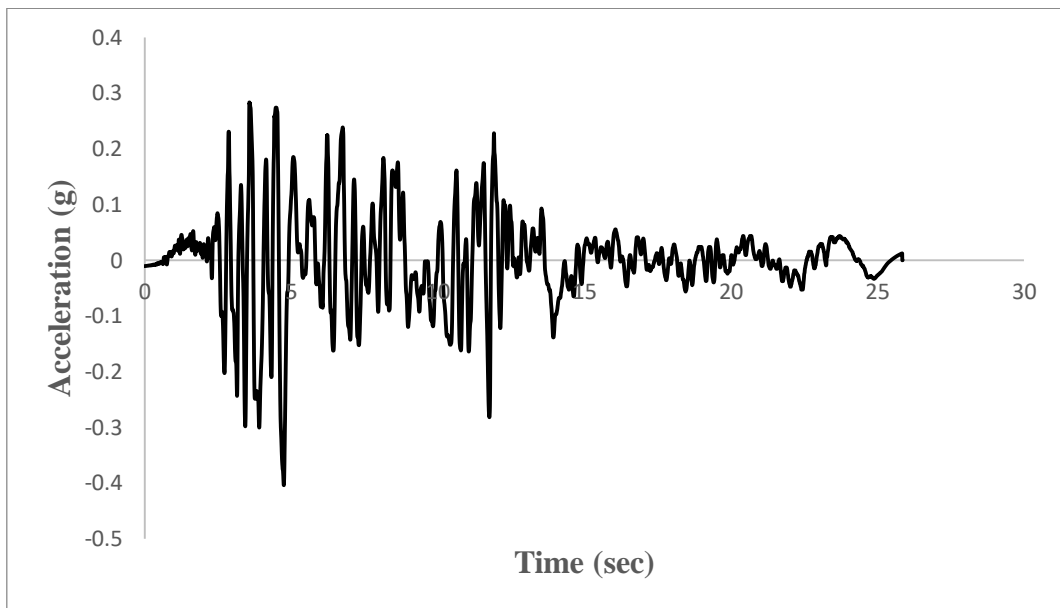


Figure 3.1: Ground motion record of Duzce (180 X)

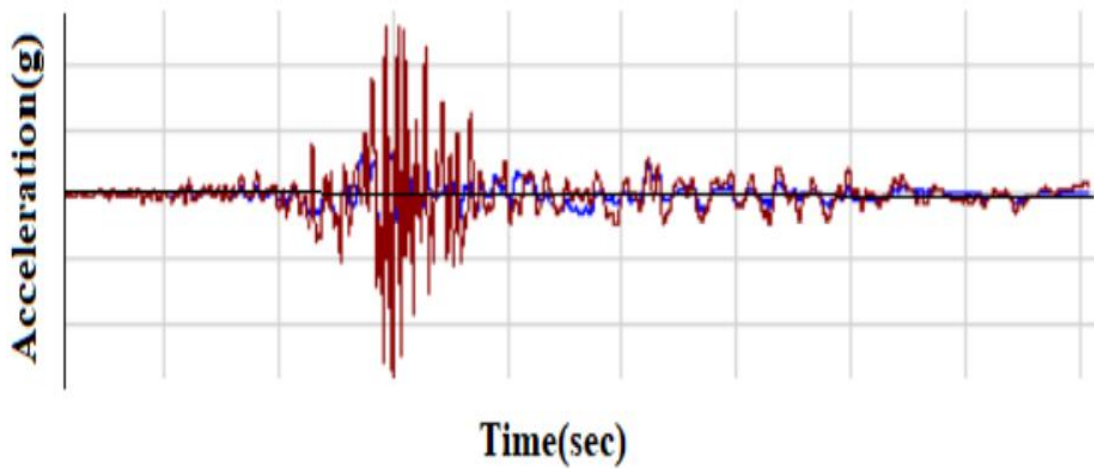


Figure 3.2: Spectral matching of Duzce (180 X) in time domain

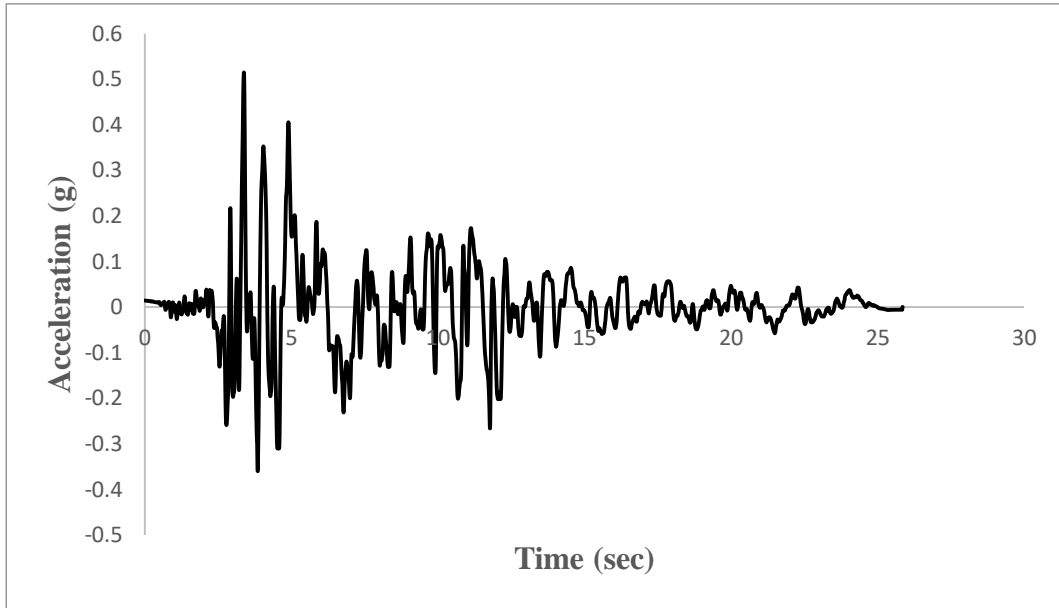


Figure 3.3: Ground motion record of Duzce (270 Y)

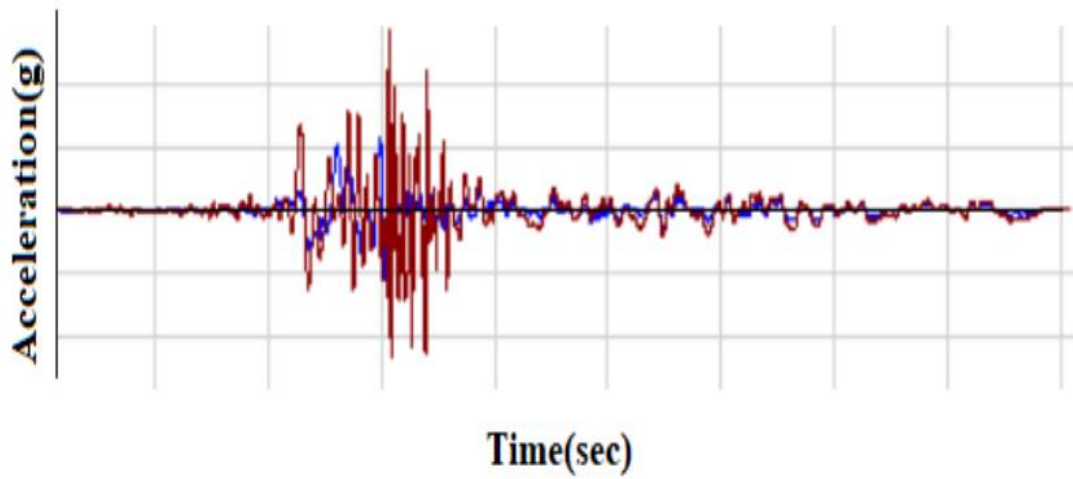


Figure 3.4: Spectral matching of Duzce (270 Y) in time domain

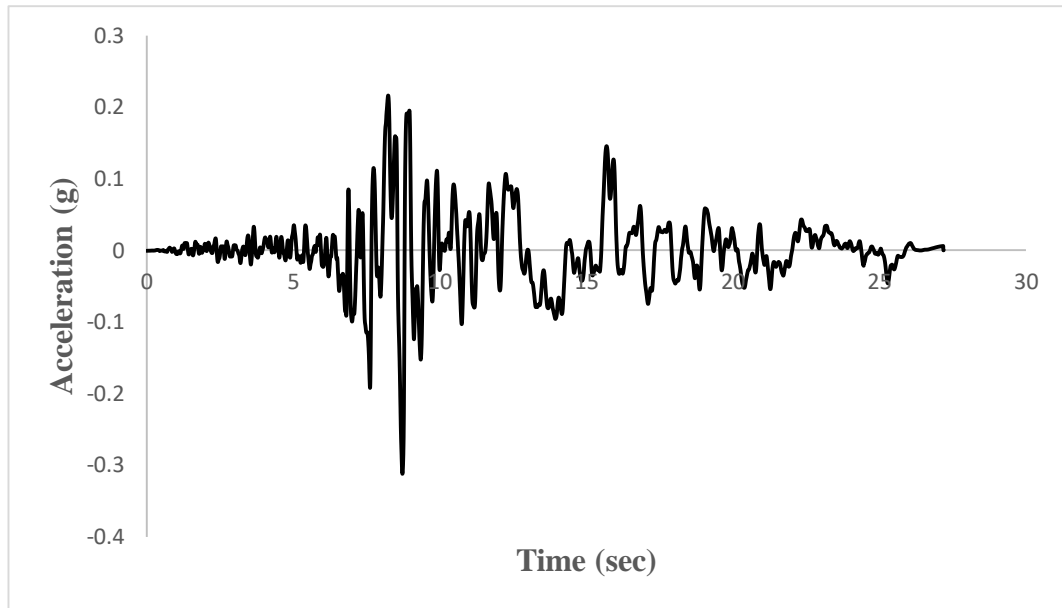


Figure 3.5: Ground motion record of Kocaeli (180 X)

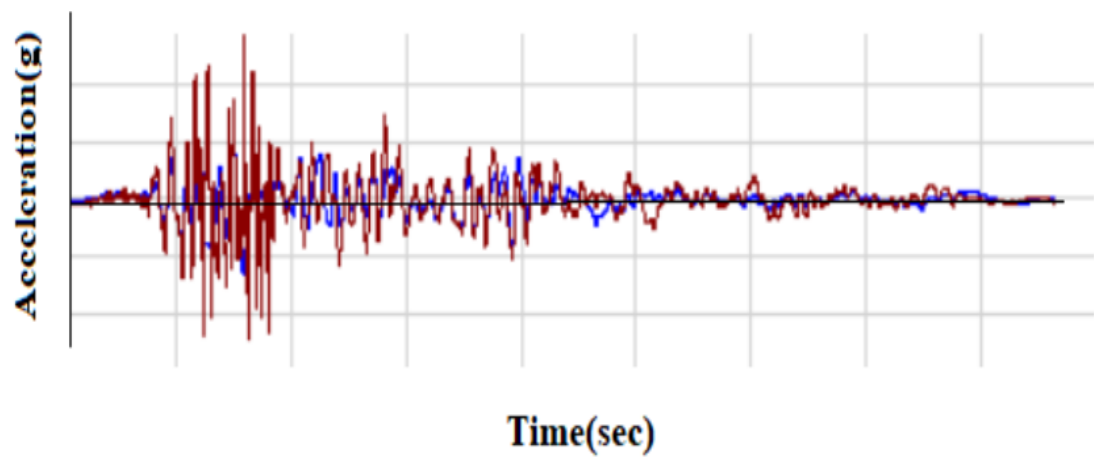


Figure 3.6: Spectral matching of Kocaeli (180 X) in time domain



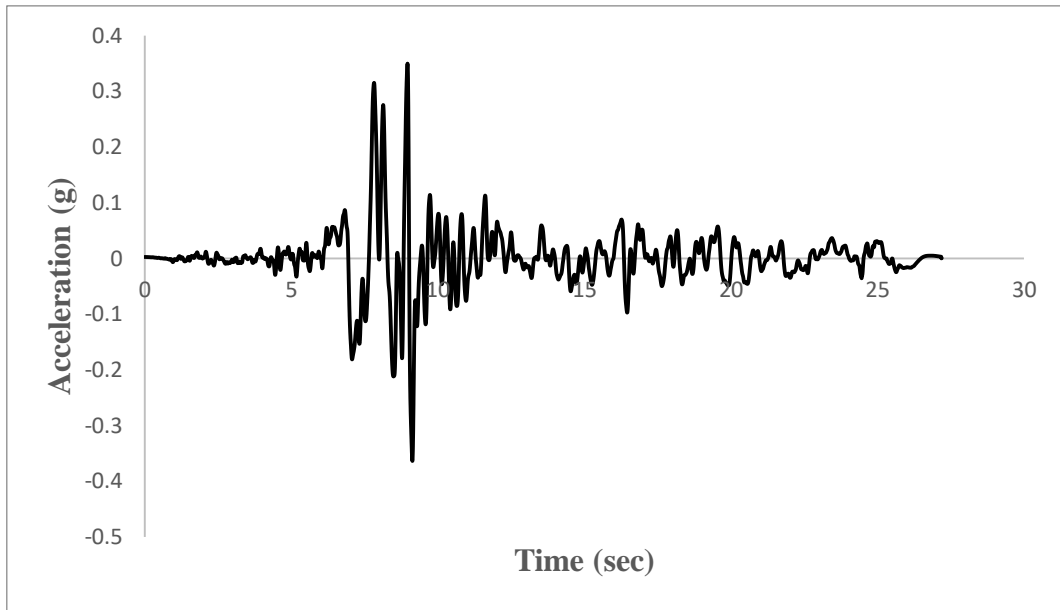


Figure 3.7: Ground motion record of Kocaeli (270 Y)

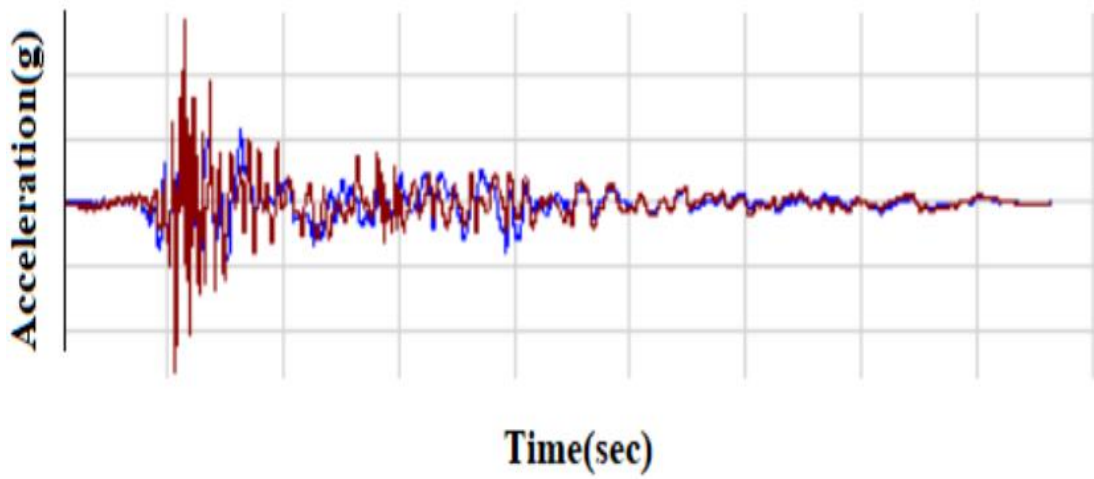


Figure 3.8: Spectral matching of Kocaeli (270 Y) in time domain

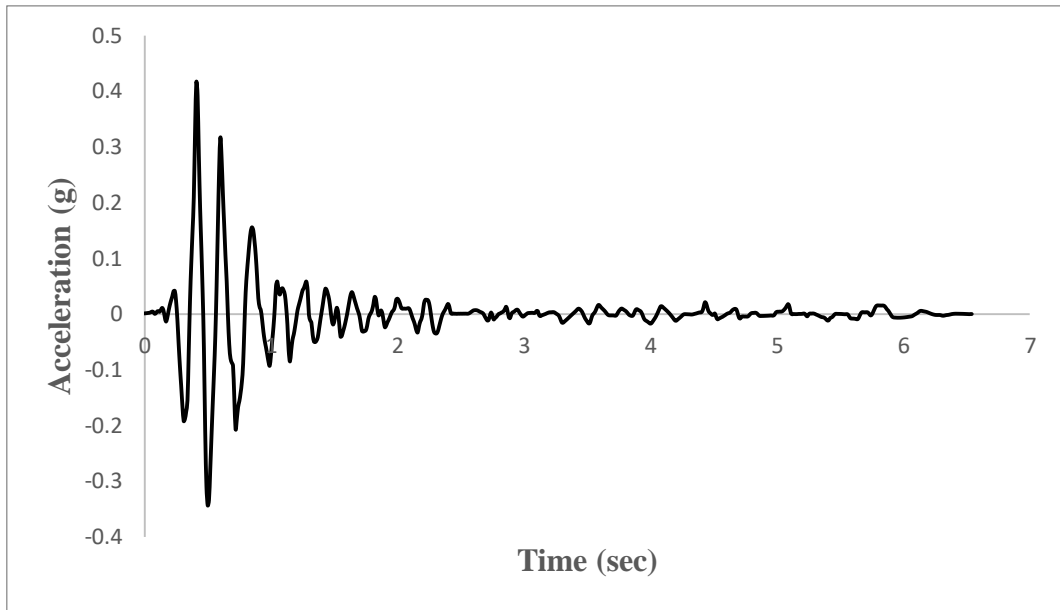


Figure 3.9: Ground motion record of Izmir (180 X)

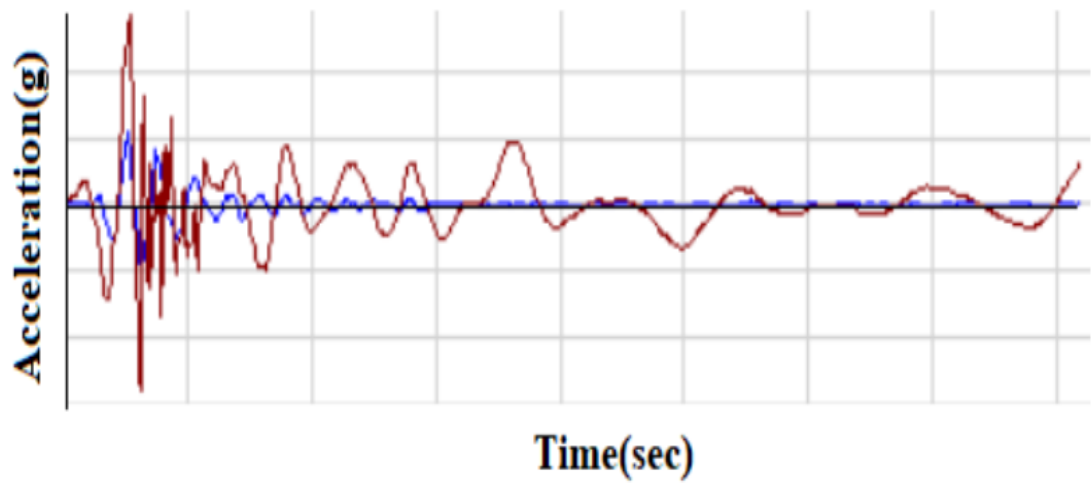


Figure 3.10: Spectral matching of Izmir (180 X) in time domain

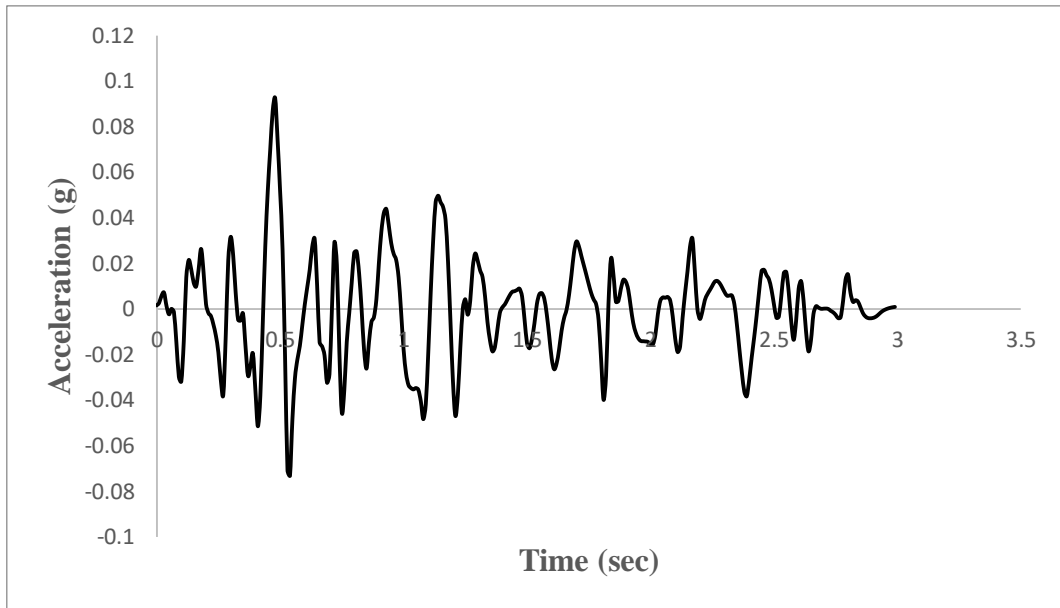


Figure 3.11: Ground motion record of Izmir (270 Y)

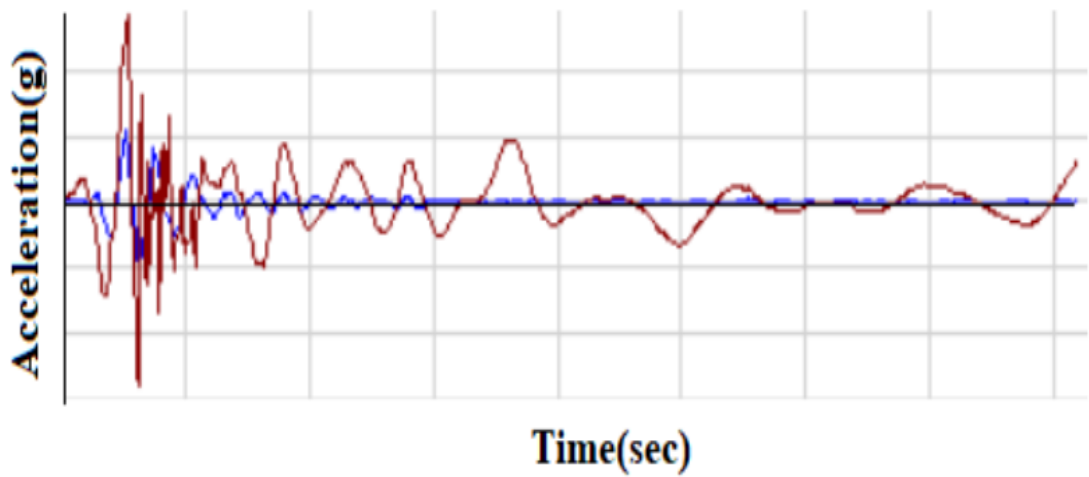


Figure 3.12: Spectral matching of Izmir (270 Y) in time domain